In Vitro Pharmacological Screening of Thiazolidinedione-Derivatives on Diabetes and Alzheimer's Potential Therapeutic Targets

A thesis submitted in fulfilment of the

requirements for the degree of

Master of Science (Pharmacy)

at

Rhodes University

by

Charles Arineitwe

March 2022

Acknowledgements

First and foremost, I would like to express my gratitude to Rhodes University for according me the opportunity to attain university education through financial leeway which has facilitated my continual registration and enrolment for this master's degree, and all the support extended to me. In a special way, I would like to thank Dr Sizwe Mabizela, the vice chancellor of Rhodes University; for standing in as my surety when I was on the verge of financial exclusion. Your support has been key in all the higher education I have obtained thus far, and I will remain indebted to you. I am especially grateful to the National Research Foundation (NRF) for extending a grant to me through my supervisor. Your financial support was a great relief and is thus highly appreciated.

I am especially grateful to my supervisor, Dr Ntethelelo Sibiya for the special role played in moulding me into a better drug research student. I have obtained numerous understandings from your guidance, encouragement, expertise, constructive criticism and patience. In addition, I am very grateful to Dr N Sibiya for ensuring that I received the financial support through his NRF research grant. Words are insufficient to express how thankful I am. I will always be indebted to you, and I pray that may the good Lord and your ancestors continue to bless you abundantly.

In a special way, I want to extend my gratitude to my co-supervisor Prof. Setshaba D. Khanye for providing the compounds used in this study. Furthermore, your expertise, guidance, and motivation has been of inspiration and has been of substantial importance in this research journey. In accordance, I would also like to thank Dr Ogunyemi Olajide Oderinlo for allowing me to do this study using the compounds you synthesized. You are highly appreciated.

I am thankful to my lab partner, Ms Chiamaka Onyekwuluje for the role she has played in this course of study. Those insightful discussions we have had, and the lab assistance accorded to me whenever a need arose, have been essential in my course of study. Your role is greatly appreciated. I would also like to extend my appreciation to Ms Amanda Zuma for all the technical support you have provided to our pharmacology lab (T21) and making sure that we receive all the supplies required. Thank you.

I would like to extend my thanks to the Faculty of Pharmacy for the platform and resources that have been provided to me which have aided the successful completion of study. To the Division of Pharmacology, headed by Prof Mamza Mothibe, and through our supervisor Dr N. Sibiya who has ensured that our labs are at least equipped with the basic instruments for use in our study analysis. Your strive for a conducive and effective research environment is highly appreciated. Further acknowledgment goes to the Department of Biotechnology, Division of Pharmaceutical Chemistry for granting us access to use the equipment in their labs.

Finally, “everyone needs a house to live in, but a supportive family is what builds a home”, my parents and siblings have been the pillar of my strength, and encouragement throughout my studies. Mukama agume alyomukumu weitu tulikulaba omuntsyi omu.

Abstract

Introduction

There is an increased prevalence of diabetes and other non-communicable diseases in Sub-Saharan Africa and globally. In South Africa, the prevalence of type 2 Diabetes mellitus is currently estimated at 9.0% in people aged 30 and older and is expected to increase. Diabetes-related complications result in acute alterations in the mental state due to poor metabolic control as well as greater rates of decline in cognitive functioning with age, higher prevalence of depression and increased risk of Alzheimer's disease. Alzheimer's disease is the most common form of dementia in older adults and possibly contributes to 60 - 70% of cases. Alzheimer's disease remains incurable, its progression inevitable with the currently available symptomatic therapies being palliative while the treatment of diabetes relies on insulin preparations and other glucose-lowering agents.

Current treatment options have numerous side effects such as hypoglycaemia, diarrhoea, weight gain and abnormal liver function. This has geared the investigation of new generations of small molecules which exhibit improved efficacy and safety profiles. On this basis, several studies have shown that thiazolidinediones and their corresponding derivatives exhibit a broad spectrum of biological activities including anti-inflammatory, and antioxidant activities. Furthermore, recent evidence from experimental, epidemiological, and clinical studies highlight the utility of antioxidants for treating diabetes and its complications. Interestingly, there is increasing evidence that links diabetes and Alzheimer's disease due to their pathophysiology and suppressing glycaemia has been shown to be beneficial in Alzheimer's disease treatment. Accordingly, the aim of this study, was to evaluate the anti-diabetic and anti-Alzheimer's properties of four novel synthesized thiazolidinedione-derivatives owing to their antioxidant properties.

Methods

The aim of this study was achieved through performing ferric reducing antioxidant power activity, 2,2'-Diphenyl-1-Picry Hydrazyl radical scavenging activity, α-amylase inhibition, α-glucosidase inhibition, aldose reductase inhibition, protein tyrosine phosphatase-1B inhibition, dipeptidyl peptidase-4 inhibition, acetylcholinesterase inhibition, matrix metalloproteinase-1 inhibition, and β-amyloid aggregation inhibition assays. In addition, peroxisome proliferator-activated receptor-γ activation was performed through docking studies. To establish

physicochemical properties of TZD derivatives investigated, further in-silico studies were done using SwissADME tools.

Results

To this end, *in-vitro* and in-silico studies were successfully performed. In-silico ADME profiling predicted these derivatives to be drug-like with moderate to good solubility in the GI and not blood-brain barrier permeable. Furthermore, docking of these molecules against PPARγ predicted a similar mode of action to that of thiazolidinediones using Rosiglitazone as the standard drug with **TZDD2** and **TZDD4** forming equivalent conformations to that of Rosiglitazone in the same binding site and **TZDD3** having an equivalent LBE to that of Rosiglitazone (-8.84 and -8.63kcal/mol respectively). *In-vitro* evaluation predicted a moderate antioxidant activity with **TZDD2** and **3** exhibiting the highest FRAP activity and DPPH radical scavenging activity. Furthermore, enzymatic inhibition assays showed a relative inhibition activity with **TZDD3** exhibited > 100% inhibition in concentrations ≥ 30 µg/mL and **TZDD1**, **2** and **4** exhibited ≥ 50% inhibition activity in all the concentrations (10, 20, 30, 40 and 50 µg/mL) in the α-amylase inhibition assay. Similarly, in the α-glucosidase inhibition assay, all the four derivatives exhibited a concentration dependent activity with **TZDD3** showing the most activity. All the four derivatives exhibited ≥ 30% inhibition in the aldose reductase inhibition assay except **TZDD1** at 10 µg/mL. **TZDD4** exhibited a concentration dependent inhibition activity in the protein tyrosine phosphatase-1B inhibition assay. Interestingly, TZDD3 showed a decreasing inhibition activity as its concentration increased from 10 µg/mL through to 50 µg/mL. In the dipeptidyl peptidase–4 inhibition assay, **TZDD2** and **TZDD4** exhibited ≥ 20% inhibition activity across all the concentrations and in the acetylcholinesterase assay, **TZDD1**, **3** and **4** exhibited ≥ 25% across all the concentrations. Interestingly, in the matrix metalloproteinase-1 inhibition assay, some of these derivatives exhibited partial activation activity and partial inhibition with **TZDD1** showing activation in concentrations 10 and 20 µg/mL and inhibition in concentrations 30, 40 and 50 µg/mL. **TZDD4** showed activation in all the concentrations. In the β-amyloid aggregation assay, all the four derivatives showed inhibition activity ≥ 10% except **TZDD1** at 50 µg/mL.

Conclusions

Diabetes mellitus and Alzheimer's disease are a type of pathology of global concern, and several researchers worldwide have strived to search for novel therapeutic treatments and prevention for diabetes as well as Alzheimer's disease. Recent studies provide a direct link

between diabetes mellitus and Alzheimer's disease, and the need to find novel drugs that can mitigate these two is of increasing interest. In our search for antidiabetic and anti-Alzheimer's activity, TZD derivatives (**TZDD1, TZDD2, TZDD3** and **TZDD4**) exhibited good antioxidant activity, anti-hyperglycaemic activity and a relatively promising anti-Alzheimer's activity. This was observed from the *in vitro* evaluation performed which included α – amylase, α – glucosidase, aldose reductase, PTP1B, DPP4, amyloid β aggregation, and AChE inhibition assays. Furthermore, docking of the derivatives against PPARγ predicted a similar molecular interaction to that of thiazolidinediones using Rosiglitazone as the standard drug. Furthermore, in silico ADME profiling predicted the derivatives to have moderate to good solubility in the GI (good GI bioavailability), and also exhibited excellent drug likeness. However, they are predicted not permeate the BBB. Further in silico studies and *in vivo* should be conducted to establish toxicities, as well as drug delivery to the brain for effective therapeutic effect against Alzheimer's disease.

Key words

In-vitro screening, thiazolidinedione-derivatives, Diabetes mellitus, Alzheimer's disease

List of Abbreviations

a.a	amino acids
Abs	absorbance
ACh	Acetylcholine
AChE	Acetylcholinesterase
AD	Alzheimer's disease
ADL	activity of daily living
ARIs	aldose reductase inhibitors
ATP	adenosine triphosphate
BBB	blood-brain barrier
BBM	brush border membrane
BChE	butylcholinesterase
C	Carbon
cAMP	cyclic adenosine monophosphate
CNS	central nervous system
CPT	Carnitine palmitoyl transferase
CYP450	Cytochrome P450
Da	Daltons
DM	diabetes mellitus
DPP-4	dipeptidyl peptidase-4
EIC	estimated inhibition constant
FDA	Food & Drug Administration
GI	gastrointestinal
GIP	glucose-dependent insulinotropic polypeptide
GLP-1	glucagon-like peptide-1
GLUT4	glucose transporter type 4
HBA_{1c}	glycosylated haemoglobin
HLA	human leukocytes antigen
IC_{50}	50% inhibition concentration
IRS-1	insulin receptor substrate-1
K^+	potassium ion
LBE	low binding energies
LMICs	low- and middle-income countries

min	minute
mL	milliliter
mM	millimolar
MW	Molecular weight
Na^+	sodium ion
NADPH	adenine dinucleotide phosphatase
NCDs	non-communicable diseases
nm	nanometers
NMDA	N-methyl-D-aspartate
OH	hydroxyl / hydroxide
PDH	pyruvate dehydrogenase kinase
pH	potential of Hydrogen
PI3K	phosphoinositide 3-kinase
PPARγ	peroxisome proliferator-activated receptor-γ
PTP-1B	protein tyrosine phosphatase-1B
PTPases	protein tyrosine phosphatases
RMSD	root-mean square deviations
ROS	reactive oxygen species
SGLT1	sodium-glucose cotransporter 1
TPSA	total polar surface area
TZD	thiazolidinediones
TZDD	thiazolidinedione derivatives

Table of Contents

CHAPTER ONE: LITERATURE REVIEW

1.1. Background

There has been an increased prevalence of diabetes mellitus (DM) and other non-communicable diseases (NCDs) in Sub-Saharan Africa and globally due to population aging and increasing urbanisation [1–6]. Urbanisation mainly because it results in rising unhealthy lifestyle risk factors such as unhealthy diet, dietary patterns, and lack of physical activity that largely contribute to increase in rates of chronic diseases [3-4, 7-8]. This has contributed to NCDs being the leading cause of mortality globally, in Low- and Middle-Income Countries (LMICs) [9]. DM is an important cause of global morbidity and mortality, and current estimates are that there are approximately 11.3% of deaths of which almost half of these deaths are in people below the age of 60 [10-12].

In South Africa, the prevalence of type 2 diabetes mellitus (T2DM) is currently estimated at approximately 9.0% in people aged 30 and older and is expected to increase [13-15]. This imposes a significant financial burden on the public healthcare system as DM requires continuous clinical care and management [5, 16-17]. DM has also been linked with lower expression of neuronal growth factors, decreased brain volume and higher occurrence of all types of dementia [18-19]. Due to the high metabolic demand for energy in the brain, small perturbations in glucose metabolism can noticeably impact cognitive performance.

Diabetes complications extending to the central nervous system result in a range of alterations in brain function [18]. The main factors contributing to cognitive impairment include aging, oxidative stress, insulin resistance and chronic inflammation amongst others. Diabetes-related complications result in acute alterations in the mental state due to poor metabolic control as well as greater rates of decline in cognitive functioning with age, higher prevalence of depression and increased risk of Alzheimer's disease (AD) [18].

AD is the leading cause of dementia in the whole world and dementia is a growing public health concern globally even though little is known about the prevalence of dementia or its impacts in persons over the age of 60 living in LMICs in Africa including South Africa [20, 21]. Current estimates are that there is approximately 44 million people with dementia worldwide with 60% of these living in LMICs [21]. Although dementia mainly affects older people, it is not a normal part of ageing. AD is the most common form of dementia in older adults and possibly contributes to 60 - 70% of cases [22]. At present, both DM and AD lack precise diagnostic

approaches for early intervention and effective cure. Further, the currently available diagnostic tools for AD screening are insufficiently sensitive and robust for preventive measures [23]. Although several drugs are used for the treatment of both these diseases, none of these drugs offers complete remission of the disease, merely symptomatic relief. Moreover, these drugs have limited efficacy because of diminished potency [23]. This, therefore, is an attempt to find more potent and orally safe drugs with less toxicity, improved hypoglycaemic activity, established anti-Alzheimer's activity and least side effects. Accordingly, in this study we directed our efforts in *in vitro* screening of novel thiazolidinediones (see **Figure 1.2)** for their potential activity against DM and AD therapeutic targets.

1.2. Diabetes Mellitus

DM is a metabolic disorder that results from a defect in insulin secretion, insulin action, or both. Insulin deficiency in turn leads to chronic hyperglycaemia with disturbances of carbohydrate, fat, and protein metabolism [4]. DM is also a risk factor for blindness, vascular brain diseases, renal failure, and limb amputations [4, 15, 24-25]. The glucose uptake by the insulin dependent cells of the body in a diabetic individual is abnormally low and is indicated by abnormally high blood glucose concentrations especially after a period of consuming a carbohydrate-rich meal [24, 26-27]. DM has been categorised as Type 1, 2 and gestational diabetes.

Type 1 DM results due to progressive destruction of insulin-producing β-cells by CD4+ and CD8+ T cells and macrophages infiltrating the islets [28]. Although, the aetiology of type 1 is believed to have a major genetic component, studies on the risk of developing type 1 suggest that environmental factors may be important aetiological determinants [27]. Evidence of an autoimmune aetiology is found in about 95% of these cases and is classified as type 1A, and the remaining 5% lacks defined markers of autoimmunity and therefore are classified as type 1B, also termed idiopathic [29]. Type 1 is observed in approximately 10% of patients with DM [30].

Type 1 is a complex polygenic disorder. It cannot be classified strictly by dominant, recessive, or intermediate inheritance, making identification of diseases susceptibility or resistant gene difficult [31-32]. The lifetime of type 1 risk for a number of the general population is often quoted as 0.4%. Eighty-five percent of cases of type 1 occur in individuals with no family history of the disease. Differences in risk also depend on which parent has DM. The risk increases to 1 – 2% if the mother has DM and intriguingly to 3 – 7% if the father has DM [33-34]. The sibling

risk is 6% [35]. Monozygotic twins have a concordance rate of 30 to 50%, whereas dizygotic twins have a concordance rate of 6 to 10% [33].

Disease susceptibility is highly associated with inheritance of the Human Leukocyte Antigen (HLA) alleles DR3 and DR4 as well as the associated alleles DQ2 and DQ8. More than 9% of patients with type 1 express either DR3DQ2 or DR4DQ8. Heterozygous genotypes DR3/DR4 are most common in children diagnosed with type 1 prior to the age of 5 (50%) [31]. Individuals with the HLA haplotype DRB1*Q302-DQA1*0301, especially when combined with DRB*10201-DQA1*0501 are highly susceptible to type 1. On the other hand, HLA class II haplotypes such as DR2DQ6 confer dominant protection [36]. Individuals with the haplotype DRB1*0602-DQA1*0102 rarely develop type 1 [37]. Candidate genes studies also identified the insulin gene as the second most important genetic susceptibility factor [38]. Whole genome screen has indicated that there are at least 15 other loci associated with type 1 [39-40]. To date, no single gene is either necessary or sufficient to predict the development of type 1. Although type 1 diabetes is likely a polygenic disorder, epidemiological pattern suggests that environmental factors are involved [41].

T2DM is a complex heterogeneous group of metabolic disorders including hyperglycaemia and impaired insulin action and/or insulin secretion [27]. Current theories of type 2 include a defect in insulin-mediated glucose uptake in skeletal muscle, a dysfunction of the pancreatic β- cells, a disruption of secretory function of adipocytes, and an impaired insulin action in the liver or skeletal muscle [42]. The aetiology of human T2DM is multifactorial with genetic background and environmental factors of the modern world which favour the development of obesity. Several findings indicate that genetics is an important contributing factor. It has been estimated that 30 – 70% of type 2 risk can be attributed to genetics [43]. The lifetime risk of type 2 is about 7% in a general population, about 40% in offspring of one parent with type 2, and about 70% if both parents have type 2 [44].

Patterns of inheritance suggest that type 2 is both polygenic and heterogeneous [45]. Genetic research effort has led to the identification of at least 27 type 2 diabetes susceptibility genes [46] and most recent genome-wide association studies have identified 20 common genetic variants associated with type 2 [47]. Since skeletal muscle accounts for ~ 75% of whole-body insulin-stimulated glucose uptake, defects in this tissue play a major role in glucose homeostasis in patients with T2DM [48].

1.2.1. Glucose Homeostasis

Glucose homeostasis is a tightly regulated process which involves mainly the gut, pancreas, liver, skeletal muscles and adipose tissues

The role of the gut

The digestion and absorption of nutrients trigger enteroendocrine cells located in the epithelium of the stomach, small intestines, and large intestines to secrete multiple gut hormones that act on distal targets. This is termed the "incretin effect" and suggests that signals from the gut are important in the hormonal regulation of glucose uptake [27]. Incretin hormones have several important biological effects, such as, release of insulin, inhibition of glucagon, maintenance of β-cells mass and maintaining satiety [49]. Several incretin hormones have been characterised, which include Glucagon-Like Peptide-1 (GLP-1) and Glucose-Dependent Insulinotropic Polypeptide (GIP). Both GLP-1 and GIP stimulate glucose-dependent insulin secretion. Plasma concentrations of most gut hormones rise quickly within minutes of nutrient uptake and fall rapidly thereafter mainly due to being cleared by the kidney and enzymatically inactivated by dipeptidyl peptidase (DPP-4) [49]. This therefore poses a possible target for therapeutic treatment of hyperglycaemia.

GIP exerts its actions through the GIP receptor (GIPR), a member of the 7–transmembrane domain, heterotrimeric G protein–coupled glucagon receptor superfamily [50, 51]. GIPR is widely expressed in the pancreas, stomach, small intestine, adipose tissue, adrenal cortex, lung, pituitary gland, heart, testis, vascular endothelium, bone, and brain [50, 52]. GIP is expressed predominantly in the stomach and the K cells of the proximal small intestine and fat is a potent stimulus for GIP secretion in humans. The dominant action of GIP is the stimulation of glucose-dependent insulin secretion. This effect is mediated through elevation of intracellular cAMP concentration and inhibition of ATP-sensitive K^+ channels, which together induces insulin exocytosis from the β cells [53]. GIP also promotes insulin biosynthesis and exhibits growth factor–like activity for β cells *in vitro* through activation of cAMP/protein kinase A–dependent, MAPK-dependent, and PI3K-dependent pathways [54, 55]. GIP contains an alanine at position 2 and is a substrate for enzymatic inactivation by dipeptidyl peptidase-4 (DPP4), an aminopeptidase that cleaves dipeptides from the amino terminus of proteins containing alanine or proline at position 2 [56]. The inhibition of DPP-4 prolongs the half-life of this GIP thus resulting in better glycaemic regulation in diabetics.

Similarly, GLP-1 is also rapidly inactivated by the DPP-4 enzyme, which results in a short circulating half-life of the active form of GLP-1 (< 2 min) [57]. Two strategies have been used to overcome this obstacle as a treatment of diabetes. One is to use GLP-1 receptor agonists that have a prolonged half-life due to reduced degradation by DPP-4. These GLP-1 mimetics include exenatide and liraglutide. Another strategy is to inhibit the enzyme DPP-4, which prolongs the half-life of endogenously released active GLP-1 [57]. This identifies a target site for DPP4 inhibitors and thus in this study we explored novel thiazolidinedione-derivatives for potential inhibition of DPP-4.

In the intestines and duodenum, the pancreatic α-amylase enzyme, which is a digestive enzyme, is located in the brush border membrane (BBM). This enzyme exerts its enzymatic effect by cleaving the α-1,4 glycosidic bonds in starch and glycogen to produce maltose and oligosaccharides. The final glucose product is then carried into the enterocytes by Na^+/glucose co-transporter 1 (SGLT1) at the BBM. It also has regulatory functions such as (1) enhancement of α-glucosidase activity, sucrase-isomaltase, (2) regulation of sodium-dependent glucose uptake, and (3) localization of pancreatic α-amylase in the small intestine. The enzyme α-glucosidase is present in the chorion of the mucous membrane of the small intestine. It is essential for the digestion and absorption of carbohydrates, in which polysaccharides are broken down into monosaccharides [58, 59].

Pancreatic α-amylase is synthesized by pancreatic acinar cells and secreted into the duodenum as a major component of pancreatic fluid. α-Amylase catalyses the initial step of starch hydrolysis for glucose production and is therefore, a key enzyme in energy acquisition. As such, α-amylase is a putative drug target for the treatment of T2DM; its inhibitors reduce the plasma glucose concentrations which is desired in the management of diabetes [60].

Mammalian pancreatic α-amylase binds specifically to glycoprotein *N*-glycans in the brush-border membrane to activate starch digestion, whereas it significantly inhibits glucose uptake by SGLT1 at high concentrations [60]. This results in the functional regulation of glucose assimilation by *N*-glycan-specific interaction of pancreatic α-amylase with glycoproteins of duodenal brush border membrane. This protects enterocytes against a sudden increase in glucose concentration and restores glucose uptake by gradual internalization, which homeostatically controls the postprandial blood glucose concentrations. This provides significant targets into the control of blood glucose concentrations during the absorption stage

in the intestine by inhibiting the enzymes α-amylase and α-glucosidase. Therefore, in this study, we also explored the activity of our TZD derivatives on these therapeutic targets.

Role of skeletal muscle and adipose tissue

Insulin stimulates glucose uptake in skeletal muscle and adipose cells primarily by recruiting GLUT4 from an intracellular storage pool to the plasma membrane. When insulin binds to its receptor, it activates the receptor tyrosine kinase activity by autophosphorylation. This causes tyrosyl-phosphorylation of IRS-1. The IRS-1 in turn activates PI3-kinase [61]. This IRS-1-PI3-kinase interaction is the signal transduction pathway for insulin-induced GLUT4 redistribution (**Figure 1.1)**. Protein kinase B/Akt is also an essential component in this pathway. The insulin activity is regulated by the protein-tyrosine phosphatases (PTPases) that dephosphorylates the active (auto-phosphorylated) form of the insulin receptor and attenuating its tyrosine kinase activity [62]. PTPases can also modulate post-receptor signalling by catalysing the dephosphorylation of cellular substrates of the insulin receptor kinase. This reversible tyrosine phosphorylation event in insulin action in liver and skeletal muscle may be involved in the regulation of insulin action [62]. Therefore, inhibiting the action of PTPases could provide a therapeutic target for hyperglycaemia treatment. In this study, we therefore explored the inhibitory properties of our TZD derivatives on the PTPases.

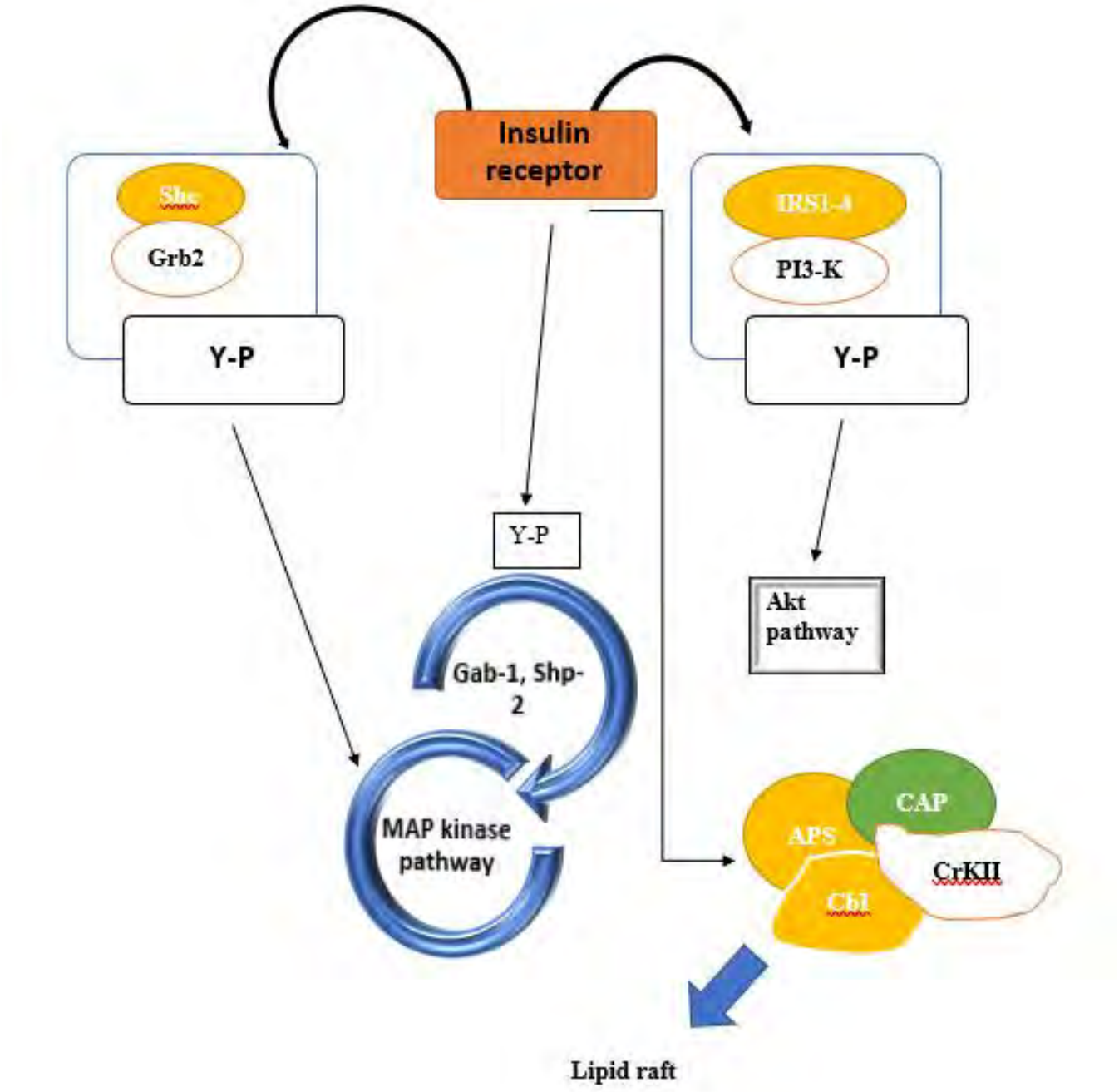

Figure 1.1: Insulin signalling, the insulin receptor is a tyrosine kinase that undergoes autophosphorylation upon binding of insulin, resulting in increased kinase activity against intracellular substrates. Several substrates have been identified, including the insulin receptor substrate proteins (IRS1–IRS4), Shc, Gab-1, Cbl and APS. Upon tyrosine phosphorylation (Y-P), each of these substrates interacts with a series of signalling proteins containing Src-homology 2 (SH2) domains, leading to initiation of different signalling pathways. Each of these pathways plays a separate role in the different cellular effects of insulin. (Adapted from: https://www.ncbi.nlm.nih.gov/books/NBK378978/)

1.2.2. Diabetes Pathophysiology

Peripheral insulin resistance coupled with progressive β-cell failure and decreased availability of insulin, amylin, and GLP-1 contribute to the clinical picture of hyperglycaemia in diabetes [63]. Abnormal gastric emptying is common in both type 1 and type 2 [64]. The rate of gastric emptying is a key determinant of postprandial glucose concentrations. If gastric emptying is accelerated, then the presentation of meal-derived glucose to the circulation is poorly timed with insulin delivery. In individuals with diabetes, the absence or delayed secretion of insulin further exacerbates postprandial hyperglycaemia [65].

Hyperglycaemia generates reactive oxygen species (ROS), which in turn cause damage to the cells in many ways [66]. Damage to the cells ultimately results in secondary complications in DM. Oxidative stress plays a pivotal role in cellular injury from hyperglycaemia. High blood glucose concentrations can stimulate free radical production [67-71]. Weak defence system of the body becomes unable to counteract the enhanced ROS generation. This results in a condition of imbalance between ROS and their protection which leads to increased oxidative stress [69].

A certain amount of oxidative stress/ ROS is necessary for the normal metabolic processes since ROS play various regulatory roles in cells. ROS are produced by neutrophils and macrophages during the process of respiratory burst in order to eliminate antigens [67]. They also serve as stimulating signals of several genes which encode transcription factors, differentiation, and development. In addition, they stimulate cell-cell adhesion, cell signalling, are involved in vaso-regulation, fibroblast proliferation and increased expression of antioxidant enzymes [72].

However, uncontrolled production of ROS is deleterious. Due to increase in oxidative stress, the metabolic abnormalities of diabetes result into mitochondrial superoxide overproduction in endothelial cells of both large and small vessels, as well as in the myocardium [67]. Oxidative stress is a mediator of insulin resistance, which leads to glucose intolerance and the onset of DM. This favours the development of atherosclerotic complications and contributes to the rise in various micro- and macrovascular problems [68-71]. Oxidative stress is central in pathophysiology of diabetes, hence molecules with antioxidant properties are fundamentally important in the management of DM. Therefore, in this study, we also screened thiazolidinedione-derivatives *in vitro* for their antioxidant properties as one of the possible targets to consider for antidiabetic properties.

Hyperglycaemia induces tissue damage through multiple mechanisms. These mechanisms include:

(i) increased flux of glucose and other sugars through the polyol pathway [73]. The polyol pathway is a two-step metabolic pathway in which glucose is reduced to sorbitol, and subsequently converted to fructose. Aldose reductase plays an important role in the development of diabetes complications since it is the initial enzyme in the intracellular polyol pathway. This pathway converts glucose into sorbitol. High glucose concentrations increase its flux through the polyol pathway, which causes sorbitol accumulation in cells. The conversion of glucose into sorbitol is a NADPH consuming reaction, and the NADPH consumed up in this reaction will no longer regenerate reduced Glutathione which is an important defence mechanism against ROS leading to increased OS [73]. Furthermore, high glucose levels can stimulate free radical production and reactive oxygen species formation. Osmotic stress from sorbitol accumulation has been postulated as an underlying mechanism in the development of diabetic microvascular complications, including diabetic retinopathy. Inhibition of aldose reductase, the first and rate-limiting enzyme in this pathway, reproducibly prevents diabetic retinopathy. Hence, aldose reductase inhibition is one of the possible targets we explored with our TZD derivatives.

(ii) High concentrations of glucose promote non-enzymatic formation of advanced glycosylated end products (AGEs). The increased intracellular formation of AGEs and increased expression of the receptor for AGEs and its activation of ligands, and

(iii) activation of protein kinase C isoforms, and over activity of the hexosamine pathway [74-75]. Atherosclerosis and cardiomyopathy in type 2 diabetes are caused in part by insulin resistance that is specific to a pathway, which increases mitochondrial ROS production from free fatty acids, and by inactivation of anti-atherosclerosis enzymes by ROS [76]. Various studies indicate that the inhibition of AGEs formation could be a novel therapeutic target for preventing vascular complications in diabetes [77-78]. Currently, there are novel compounds whose mechanism of action is inhibition of AGEs and these include guanidines such as aminoguanidine and metformin [78]. Advancing further, we have therefore, screened these thiazolidinedione derivatives *in vitro* for their AGEs inhibition properties as a possible target site for their antidiabetic properties.

Diabetics differ significantly in their sensitivity to ROS. Inflammatory damage that characterises type 1 diabetes is mediated at least in part through islet ROS, and in type 2 diabetes, the high nutrient flux and consequent ROS production appear to mediate loss of β-cell function [79]. In insulin-sensitive tissues including the skeletal muscle, liver and heart, high fatty-acid flux leads to oxidative damage, whereas non-insulin-sensitive tissues including the eye, kidney, and nervous system are exposed to both high circulating glucose and fatty acid concentrations and, consequently, ROS-induced diabetic complications [75]. Removal of/limiting the generation of ROS is a potential mechanism of action for both antidiabetic and anti-Alzheimer's disease therapeutic compounds that exhibit antioxidant activities. These antioxidants can regulate the amount of these radicals in the body which provides potential therapeutic effects for these diseases [80]. If no treatment is achieved, these diseases can progress into various complications.

1.2.3. Diabetic Complications

Diabetes is a major cause of morbidity, mortality, and economic cost to the society. People with diabetes show the risk of the development of acute metabolic complications such as diabetic ketoacidosis, hyperglycaemic hyperosmolar non-ketotic coma, and hypoglycaemia [81-82]. In addition to this, diabetics are also at risk of experiencing chronic complications such as coronary heart diseases, retinopathy, nephropathy and neuropathy and gangrene [83]. The injurious effects of hyperglycaemia are divided into macrovascular complications (coronary artery disease, peripheral arterial disease, and stroke) and microvascular complications (diabetic nephropathy, neuropathy, and retinopathy). The risk of developing diabetic microvascular complications depends on both the duration and the severity of hyperglycaemia [84]. In diabetic nephropathy, the patients are characterised by microalbuminuria. The pathological changes to the kidney include increased glomerular basement membrane thickness, microaneurysm formation, and mesangial nodule formation. The underlying mechanism of injury may also involve some or all the same mechanisms as in diabetic retinopathy. The precise nature of injury to the peripheral nerves leading to neuropathy is related to mechanisms such as polyol accumulation, injury from AGEs, and oxidative stress [85].

The central pathological mechanism in macrovascular disease is the process of atherosclerosis, which leads to the narrowing of arterial walls throughout the body. Atherosclerosis is thought to result from chronic inflammation and injury to the arterial wall in the peripheral or coronary

vascular system. In response to endothelial injury and inflammation, oxidised lipids from LDL particles accumulate in the endothelial wall of arteries. Angiotensin II may promote the oxidation of such particles. Monocytes then infiltrate the arterial wall and differentiate into macrophages, which accumulate oxidised lipids to form foam cells. Once formed, the foam cells stimulate macrophage proliferation and attraction of T-lymphocytes which in turn induce smooth muscle proliferation in the arterial walls and collagen accumulation. The net result of the process is the formation of a lipid-rich atherosclerotic lesion with a fibrous cap. Rupture of this lesion leads to acute vascular infarction [84-87]. Impaired nitric oxide generation and increased free radical formation in platelets, as well as altered calcium regulation, may promote platelet aggregation. Elevated levels of plasminogen activator inhibitor type 1 may also impair fibrinolysis in patients with diabetes. The combination of increased coagulability and impaired fibrinolysis likely further increases the risk of vascular occlusion and cardiovascular events. Furthermore, the increased ROS are precursors for AD as elaborated later in the text. Currently, there are various treatments directed at the management of DM.

1.3. Current Treatments of Diabetes Mellitus

The goal of therapy in type 1 DM is to maintain blood glucose concentration as close to normal as possible and to avoid wide glycaemic fluctuations. For type 2 DM, the goal of the treatment is to maintain blood glucose concentration within normal limits and to prevent the development of long-term complications. The administration of insulin preparations or other glucose-lowering agents can reduce morbidity and mortality associated with diabetes [24]. A person with type 1 DM must rely on exogenous insulin to control hyperglycaemia, avoid ketoacidosis, and maintain acceptable levels of glycosylated haemoglobin (HbA_{1c}). HbA_{1c} is glycated haemoglobin which is a measure of average blood glucose over a period of 3 months in a person, that is used for diagnosis of diabetes. An HbA_{1c} value of 6.5 % is recommended as the diagnostic cut point for diabetes. Weight reduction, exercise, and dietary modification decrease insulin resistance and correct hyperglycaemia in some patients with type 2 DM. However, most patients require pharmacological intervention with oral glucose-lowering agents. As the disease progresses, β-cell function declines and insulin therapy are often needed to achieve satisfactory glucose concentration [88]. **Table 1.1** summarises the current treatments of diabetes mellitus and are discussed here below.

Table 1.1: Summary of available anti-hyperglycaemic agents and their major side effects

Anti-hyperglycemic agents	**Mechanism of action**	**Major side effects**	**References**
Insulin	Facilitates glucose disposal in target tissues	hypoglycemia weight gain lipodystrophy	89, 90
Sulphonlyureas	Stimulate insulin secretion	hypoglycemia hyperinsulinemia weight gain	96
Glinides	Stimulate insulin secretion	hypoglycemia Drug-drug interactions with CYP3A4 inhibitors	98
Biguanides	Permissive action to insulin	lactic acidosis Gastrointestinal effects Anaemia	24, 99
TZDs	Sensitizes insulin receptors to insulin	cardiac adverse effects due to electrolyte imbalance and fluid retention	24
Amylin and incretion mimetics	Enhances insulin secretion after a meal	Gastrointestinal effects Risk of increased fluid and electrolyte	24
Alpha glucosidase inhibitors	Delays intestinal carbohydrate	Risk of increased fluid and electrolyte loss flatulence, diarrhoea, and abdominal cramping	100
DPP4 inhibitors	Blocks DDP-4 enzyme, thus increasing incretins availability	hypoglycemia in kidney dysfunction Nasopharyngitis Headache	93
SGLT 2 inhibitors	Blocks SGLT 2 in the proximal convoluted tubule,	hypotension due to enhanced loss of fluid	103

	thus promoting glucose excretion	female genital mycotic infections	
Neprilysin inhibitors	Insulinotropic effects of GLP-1	potential accumulation of amyloid in islets and beta cell apoptosis and brain over time	105-112

1.3.1. Insulin

Insulin therapy is administered clinically to all patients with type 1 diabetes, and maybe used in some patients with type diabetes. Insulin initiates its action by binding to a glycoprotein receptor on the surface of the cell. This receptor consists of an alpha-subunit, which binds the hormone, and a beta-subunit, which is an insulin-stimulated, tyrosine-specific protein kinase. Activation of this kinase is believed to generate a signal that eventually results in insulin's action on glucose, lipid, and protein metabolism [89]. The effect of insulin's mode of action facilitates entry of glucose into muscle, adipose and several other tissues. Insulin also stimulates the liver to store glucose in the form of glycogen. Through these mechanisms, insulin decreases the concentration of glucose in the blood stream [88-90]. Hypoglycaemia is the most serious and common adverse reaction to insulin. Other adverse reactions include weight gain, local injection site reactions, and lipodystrophy [89-90]. Lipodystrophy can be minimized by rotation of injection sites.

1.3.2. Amylin and Incretin Mimetics

Amylin is a hormone that is co-secreted with insulin from β cells following food intake. Amylin delays gastric emptying, decreases postprandial glucagon secretion, and improves satiety [24, 91]. Pramlintide is a synthetic amylin analog that is indicated as an adjunct to mealtime insulin therapy in patients with type 1 and type 2 DM. The incretin mimetics (Exenatide and liraglutide) are analogs of GLP-1 that exert their activity by acting as GLP-1 receptor agonists. These agents improve glucose- dependent insulin secretion, slow gastric emptying time, reduce food intake by enhancing satiety, decrease postprandial glucagon secretion, and promote β-cell proliferation [24]. Consequently, weight gain and postprandial hyperglycaemia are reduced, and HbA_{1c} levels decline. The major clinical side effects of these drug are gastrointestinal in nature including nausea and vomiting

1.3.3. Dipeptidyl peptidase-4 Inhibitors

DPP-4 inhibitors exert their effect by inhibiting the enzyme DPP-4 which is responsible for the inactivation of incretin hormones such as GLP-1 and GIP. This prolongs the activity of incretin hormones increasing insulin release in response to meals and reduces inappropriate secretion of glucagon [92]. DPP-4 inhibitors may be used as mono- therapy or in combination with sulphonylureas, metformin, thiazolidinediones (TZDs), or insulin. The registered novel compounds include alogliptin, linagliptin, saxagliptin, and sitagliptin. In general, DPP-4 inhibitors are well tolerated, with the most common adverse effects being nasopharyngitis and headache. Although infrequent, pancreatitis has occurred with use of all DPP-4 inhibitors. Strong inhibitors of CYP450 3A4/5, such as ritonavir, atazanavir, itraconazole, and clarithromycin, may increase levels of saxagliptin [93, 94]. Saxagliptin is metabolized by CYP3A4/5 to 5-hydroxy saxagliptin, its major pharmacologically active metabolite and therefore inhibiting CYP3A4/5 will reduce this metabolism resulting in increased concentrations of saxagliptin.

1.3.4. Sulphonylureas

These agents are classified as insulin secretagogues since they promote insulin release from the β cells of the pancreas [24]. The main mechanism of action includes stimulation of insulin release from the β cells of the pancreas. Sulphonylureas block ATP-sensitive K^+ channels, resulting in depolarization, Ca^{2+} influx, and insulin exocytosis [95]. In addition, sulphonylureas may reduce hepatic glucose production and increase peripheral insulin sensitivity. The sulphonylureas in current use are the second-generation drugs glyburide, glipizide, and glimepiride. The major adverse effects of the sulphonylureas are weight gain, hyperinsulinemia, and hypoglycaemia [96].

1.3.5. Glinides

The glinides stimulate insulin secretion by binding to a distinct site on the β cell, closing ATP-sensitive K^+ channels, and initiating a series of reactions that results in the release of insulin. In contrast to the sulphonylureas, the glinides have a rapid onset and a short duration of action [97]. Glinides have an overlapping mechanism of action to sulphonylureas. Glinides include repaglinide and nateglinide. Although glinides can cause hypoglycaemia and weight gain, the incidence is lower than that with sulphonylureas [98]. Glinides are substrates of CYP3A4 and

have drug-drug interactions where CYP3A4 inhibitors, such as itraconazole, fluconazole, erythromycin, and clarithromycin, may enhance the glucose-lowering effect of repaglinide, and drugs that induce CYP3A4, such as barbiturates, carbamazepine, and rifampicin, reduce the glucose-lowering effect.

1.3.6. Biguanides

Biguanides increase glucose uptake and use by target tissues, thereby decreasing insulin resistance [24]. The registered novel compound is Metformin and is classified as an insulin sensitizer. Metformin is clinically used as the first line of treatment for type 2 diabetes. The main mechanism of action of metformin is inhibition of hepatic gluconeogenesis. Metformin also slows intestinal absorption of sugars and improves peripheral glucose uptake and utilization. The adverse effects are largely gastrointestinal including diarrhoea, nausea and upset stomach [24]. Metformin is contraindicated in patients with an eGFR below 30 mL/minute/1.73 m^2 [99].

1.3.7. Thiazolidinediones

The TZDs are also insulin sensitizers and examples of this class are pioglitazone and rosiglitazone. Although insulin is required for their action, the TZDs do not promote its release from the β cells, so hyper- insulinemia is not a risk. The TZDs lower insulin resistance by acting as agonists for the peroxisome proliferator–activated receptor-γ (PPARγ), a nuclear hormone receptor expressed primarily in adipose tissue [24]. TZDs bind to the gamma form of the PPARγ. Regulation of glucose homeostasis, cellular differentiation, apoptosis, and inflammatory responses has been shown by activating PPARγ with TZDs. Activation of PPARγ regulates the transcription of several insulin responsive genes, resulting in increased insulin sensitivity in adipose tissue, liver, and skeletal muscle. Rosiglitazone is less utilized due to concerns regarding cardiac adverse effects including risks of developing oedema and congestive heart failure [24].

1.3.8. Alpha-Glucosidase Inhibitors

α-Glucosidase enzymes are in the intestinal brush border, and they break down carbohydrates into glucose and other simple sugars that can be absorbed. Acarbose and miglitol are the registered novel compounds and reversibly inhibit α-glucosidase enzymes hence delays intestinal carbohydrate digestion [100, 101]. Acarbose is poorly absorbed, hence it is metabolized

primarily by intestinal bacteria, and some of the metabolites are absorbed and excreted into the urine. The major side effects are flatulence, diarrhoea, and abdominal cramping [101, 102]. Adverse effects limit the use of these agents in clinical practice.

1.3.9. Sodium–Glucose Co-transporter 2 Inhibitors

The sodium–glucose co-transporter 2 (SGLT2) is responsible for re-absorbing filtered glucose in the tubular lumen of the kidney. By inhibiting SGLT2, these agents decrease reabsorption of glucose, increase urinary glucose excretion, and lower blood glucose. Inhibition of SGLT2 also decreases reabsorption of sodium and causes osmotic diuresis [103]. They include canagliflozin and dapagliflozin. The most common adverse effects with SGLT2 inhibitors are female genital mycotic infections such as vulvovaginal candidiasis, urinary tract infections, and urinary frequency [103]. Hypotension has also occurred, particularly in the elderly or patients on diuretics. Furthermore, diabetic ketoacidosis is significant in patients taking SGLT2 inhibitors [102, 104].

1.3.10. Neprilysin Inhibitors

Neprilysin degrades multiple peptides which have glucoregulatory properties. The glucose-lowering effect of neprilysin inhibition is through increased plasma levels of these substrates, including GLP–1, bradykinin and natriuretic peptides, atrial natriuretic peptide (ANP) and B–type natriuretic peptide (BNP) [105-109]. Neprilysin inhibition improves glucose homeostasis by increasing levels, and thereby the insulinotropic effects, of GLP–1 [105]. Plasma levels of bradykinin, which modulates glucose metabolism in peripheral tissues by increasing insulin sensitivity, another peptide degraded by neprilysin are increased by neprilysin inhibition [110]. In addition to their role in the cardiovascular system, natriuretic peptides exert metabolic effects. BNP has similar effects, wherein its administration has been shown to increase insulin sensitivity and decrease blood glucose levels [111]. Thus, raising circulating levels of natriuretic peptides with neprilysin inhibitors may protect against glucose intolerance and weight gain, in part by improving lipid mobilisation and oxidation [112]. Potential side effects include potential accumulation of amyloid in islets causing islets apoptosis, and brain over time.

1.3.11. Dopamine Receptor Antagonists

Dopamine agonist bromocriptine and the bile acid sequestrant colesevelam produce modest reductions in HbA_{1c} [113]. The mechanism of action of glucose lowering is unknown for both drugs. Although bromocriptine and colesevelam are indicated for the treatment of type 2 diabetes, their modest efficacy, adverse effects, and pill burden limit their use in clinical practice [114].

The combination of sulphonylurea and metformin (but not either one alone) has proved to significantly reduce both the incidence and relative risk for affective disorder in association with type 2 diabetes and it has been pointed out that pioglitazone (antihyperglycemic drug) also has antidepressant properties [18, 115]. The use of available therapeutic drugs coupled with nutraceutical adjuncts could represent a potential therapeutic strategy for the reduction of mental-health consequences and serve as a preventive measure for at-risk individuals [116]. An understanding of the mechanisms of diabetes-related cognitive impairment and the resulting behaviours of patients can help healthcare professionals implement treatments to significantly improve health status and quality of life of patients with diabetes [18].

1.4. Emerging Alternative Agents

Diabetes treatment options are increasingly expensive, not readily available and frequently have numerous side effects such as hypoglycaemia, diarrhoea, weight gain and abnormal liver function [117-119]. Current diabetes treatment is being directed at lowering circulating blood glucose and inhibiting postprandial hyperglycaemic spikes. Current strategies to treat diabetes include reducing insulin resistance using glitazones, supplementing endogenous insulin with exogenous insulin, increasing endogenous insulin production with sulfonylureas and meglitinides, reducing hepatic glucose production through biguanides, and limiting postprandial glucose absorption with alpha-glucosidase inhibitors.

New generations of small molecules are being investigated which exhibit improved efficacy and safety profiles. Promising biological targets are also emerging such as (i) insulin sensitizers including protein tyrosine phosphatase-1B (PTP-1B), (ii) inhibitors of gluconeogenesis like pyruvate dehydrogenase kinase (PDH) inhibitors, (iii) lipolysis inhibitors, (iv) fat oxidation including carnitine palmitoyl transferase (CPT) I and II inhibitors, and (v) energy expenditure

by means of beta 3-adrenoceptor agonists [120]. Also important are alternative routes of glucose disposal such as Na^+ -glucose co-transporter (SGLT) inhibitors, combination therapies, and the treatment of diabetic complications (e.g., retinopathy, nephropathy, and neuropathy).

From the pioneering discovery of pioglitazone, a new class of thiazolidinedione-based compounds have been developed to treat diabetic patients that can reverse the insulin resistance in T2DM [121]. Among various substituted benzyl-2,4-thiazolidinedione compounds, troglitazone, pioglitazone, and rosiglitazone, are potentially antidiabetic compounds that have been clinically examined [122-124]. The first marketed thiazolidinedione, troglitazone, was withdrawn because of the increased risk of hepatotoxicity [125-126]. The potent side effects include hepatotoxicity, weight gain, heart failure which are due to increased fluid retention. Furthermore, osteopenia, increased fracture risk, and the risk of bladder cancer were also linked to TZDs. Several meta-analyses identified a potential increased risk of myocardial infarction and death from cardiovascular causes with rosiglitazone [24].

These adverse effects limit the use of thiazolidinediones as safe drug candidates. However, many drugs have been approved from this class for the treatment of diabetes like rosiglitazone, pioglitazone, and many more. Though the marketed drugs show additive effect with other antihyperglycemic agents, they are also prone to show toxicity. For example, rosiglitazone shows hepatotoxicity [127]. Hence, there is a need to discover and explore more potent and orally safe thiazolidine 2,4-diones with less toxicity and possibly with multiple indications [117]. The identification of biologically active compounds needs to be interpreted in the light of the chemical and pharmacological effects such as that of the TZDs [25].

1.4.1. Thiazolidinedione-Derivatives

In 1953, Chien-Pen Lo *et al* synthesized a few 5-arylalkylidene-3-isobutyl-2,4-thiazolidinediones by isobutylation of 5- aryalkylidene-2,4-thiazolidinediones [128]. In 1979, P. Monforte *et al* synthesized 2,3-substituted 5-methyl-4-thiazolidinones and 3- substituted 5-methyl-2,4-thiazolidine-diones by reacting some carbodiimides with α-mercaptopropionic acid, in order to obtain potentially chemotherapeutic agents, no beneficial chemotherapeutic properties were identified [129]. In 1992, Sohda T *et al* conducted research on studies of anti-diabetic agents and synthesized a series of 5- [4-(2- or 4-azolylalkoxy) benzyl- or -

benzylidene]-2,4- thiazolidinediones which showed insulin sensitizing properties reducing plasma glucose concentrations [130].

In continuation of this research in 1999, Carol Koro *et al* worked on cancer risks in thiazolidinedione users compared to other anti-diabetic agents [131]. Results showed that TZDs have neutral chances of enhancing development of the cancers tested (colon, prostate, and breast), and that there is no evidence that TZDs are beneficial or harmful to the malignancies analysed. Similarly, many researchers are focusing on PPARs in order to understand the effects of TZDs. Banerjee *et al* concentrated on in silico designing and molecular docking studies of selected reported and proposed new compounds against PPAR-γ receptor for type-2-diabetes [132]. Higher antidiabetic activity in comparison to rosiglitazone was seen in piperine-derivatives containing benzothiazole moiety as shown by Kharbanda C *et al* [133]. These tiny ligands fit perfectly into the large pocket of the PPAR-domain, forming a stable complex in the ligand-binding pocket of PPAR-γ, with a high dock and exhibited their effect by enhancing PPAR-γ gene expression and there has been increased *in vitro* studies of these compounds.

1.4.1.1. Recent Work on Thiazolidinediones-derivatives

Rakowitz *et al* Synthesised many 5-benzyl-2,4-thiazolidinediones and evaluated them for anti-diabetic activity [134]. The insertion of an acetic acid chain on N-3 proved to be the most effective among the tested compounds. In addition, the presence of an additional aromatic ring on the 5-benzyl moiety was generally beneficial. Mohammad Iqbal *et al.* synthesised novel thiazolidinedione derivatives by incorporating thiazole, triazole and oxadiazole moieties [135]. These compounds were screened for their *in vivo* hypoglycaemic and hypolipidemic activities and showed insulin sensitizing properties. The incorporation of thio-ethyl-oxy linkage connecting to triazole and oxadiazole is showing more antidiabetic activity by significantly decreasing plasma glucose and tri-glyceride.

Bharat Raj Bhattarai *et al.* Synthesised Benzylidene-2,4- thiazolidinedione derivatives with dual substitutions on the phenyl ring in ortho & para positions of the thiazolidinedione group which act as PTP1B inhibitors and showed potent antidiabetic activity [136].

Maccari *et al.* reported new aldose reductase inhibitors (ARIs) through *in vitro* evaluation of a series of 5-arylidene-3-(3,3,3-trifluoro-2-oxopropyl)-2,4-thiazolidinediones as ARIs identified two new noncarboxylic acid containing 5-arylidene-2,4-thiazolidinedione derivatives that were found active against aldose reductase at low-micromolar doses [137].

Current literature reveals that TZD-derivatives are potential antidiabetic agents with various modes of action such as PPAR-γ activation, aldose reductase inhibition, protein tyrosine phosphate-1B inhibition, and insulin sensitization [138]. Therefore, it is paramount to evaluate TZD-derivatives as possible anti-diabetics with fewer side effects. In this study, we aimed at conducting *in vitro* screening of novel TZD-derivatives to establish their potential to inhibit α-amylase, α-glucosidase, aldose reductase, protein tyrosine phosphatase-1B and DPP4.

1.5. Alzheimer's Disease

AD represents a neurodegenerative disorder characterised by a progressive loss of neurons, cognition, and brain functions [139]. Loss of larger neurons of the superficial cortex is a consistent feature of AD, as synaptic alterations like reduction of pre-synaptic terminal density [140]. AD is characterised by dementia that typically starts with subtle and poorly recognized failure of memory and slowly becomes more severe, and eventually, incapacitating. The clinical diagnosis of AD is characterised by slow progressive dementia and gross cerebral cortical atrophy [80]. The age-related decline in neurotransmitter synthesis and signalling, coupled with reductions in synaptic density and plasticity (adaptability), and loss of as much as 50% of the length of myelinated axons make the brain increasingly less efficient with aging [18].

The pathological hallmarks of AD include high levels of oxidative stress, accumulation of intra-neuronal amyloid beta peptide, extracellular senile amyloid plaques, intra-neuronal and extra neuronal neurofibrillary tangles made of hyper-phosphorylated tau, loss of synapses, loss of neurons and neurotic degeneration and gliosis. Numerous studies have reported increased oxidative stress in T2DM patients compared with their healthy counterparts [141-144]. This pathology culminates in clinical signs predominantly associated with impaired cognitive processes which in part depends on acetylcholine.

1.5.1. Role of Acetylcholine

Acetylcholine (ACh) is a fast-acting, point-to-point neurotransmitter at the neuromuscular junction and in the autonomic ganglia; however, there are fewer demonstrations of similar actions in the brain. Instead, central cholinergic neurotransmission predominantly changes neuronal excitability, alters presynaptic release of neurotransmitters, and coordinates

the firing of groups of neurons. As a result, ACh appears to act as a neuromodulator in the brain, despite its role as the primary excitatory neurotransmitter in the periphery [145].

The definition of a neuromodulator is flexible but has evolved to describe any kind of neurotransmission that is not directly excitatory (mediated through ionotropic glutamate receptors) or inhibitory (mediated through ionotropic gamma-aminobutyric acid [GABA] receptors) [146-148]. Neuromodulation can be thought of as a change in the state of a neuron or group of neurons that alters its response to subsequent stimulation. Several models have been proposed to explain the actions of ACh in the central nervous system (CNS). Another model has suggested that ACh re-inforces neuronal loops and cortical dynamics during learning by enhancing the influence of feed-forward afferent inputs to the cortex carrying sensory information and decreasing excitatory feedback activity mediating retrieval [147]. ACh can also alter firing of neurons on a rapid time scale, as in fear-conditioning, when foot-shock results in direct cholinergic activation of interneurons in the auditory cortex that contribute to learning [148].

All these models are consistent with a primary role of ACh as a neuromodulator that changes the state of an ensemble of neurons in response to changing environmental conditions [147]. Cholinergic neurotransmission in the brain is primarily neuromodulatory and is categorically distinct from the actions of ACh at the neuromuscular junction. The role of ACh as a neuromodulator in the brain is to increase neurotransmitter release in response to other inputs, to promote burst firing, and/or suppress tonic firing, depending upon the system and the neuronal subtypes stimulated. Furthermore, ACh contributes to synaptic plasticity in many brain areas [147-148].

The actions of ACh released from both populations of cholinergic cells are mediated through pre- and postsynaptic receptors on a large variety of neuronal subtypes throughout the brain, and it should be noted that cholinergic inputs contribute to cortical and hippocampal function across phylogeny [149]. The pathogenesis of Alzheimer's disease (AD) has been linked to a deficiency of acetylcholine in the brain. This was based on observations that correlated cholinergic system abnormalities with intellectual impairment. It has been argued that acetylcholine dysfunction is not a primary pathological cause for AD but rather a consequence of the disease. Thus, in addition to cholinergic dysfunction, a role for β-amyloid deposition, oxidative stress and inflammation have been investigated in the aetiology of AD, and currently, trials are underway to test disease-modifying agents [150-153].

Nevertheless, attempts at correcting acetylcholine deficiency in the brain of affected individuals produced the first licensed medication for the symptomatic treatment of AD in the form of acetylcholinesterase inhibitors (AChEIs) [154]. The symptomatic efficacy of AChEIs is attained through their augmentation of acetylcholine-mediated neuron-to-neuron transmission. However, there is evidence that AChEIs may slow disease progression and hippocampal atrophy and may have disease-modifying effects [155]. AChE inhibition, therefore, is a possible target for developing new drug compounds hence we screened for AChE inhibition properties of these compounds. In addition, symptomatic improvement in AD patients is not restricted to agents that enhance acetylcholine function in the brain, as is the case for memantine which acts on another neurotransmitter. Thus, in our study, the focus was on exploration of the antioxidant effects of thiazolidinedione derivatives as a possible chemotype for the therapeutic treatment of AD.

In cell cultures and animal studies, as well as in human epidemiological surveys, agents known to dampen down inflammation such as vitamin antioxidants, herbal extracts with antioxidant properties (e.g., *Gingko Biloba*) and long-term use of non-steroidal anti-inflammatory drugs (NSAIDs) have shown some protective effect against AD pathology [156]. Hence, it may be reasonable to consider that the efficacy of AChEIs is, at least in part, because of the anti-inflammatory effects. However, for an anti-inflammatory mechanism of action to be confirmed for AChEIs, two essential requirements are to be satisfied [155].

They are the following: (i) direct link between the cholinergic system and inflammation (i.e., a direct role for acetylcholine in attenuating inflammation) and (ii) data showing clear effect of AChEIs on inflammatory mediators of toxicity and inflammatory processes. A link between the cholinergic system and inflammation has been established through the discovery of an anti-inflammatory role for a stimulated vagus nerve. In an animal model of toxaemia, acetylcholine suppressed proinflammatory cytokine release from peripheral tissue-activated macrophages [54, 155-156]. This resulted from the action of acetylcholine on specific nicotinic receptors expressed on these cells.

Hence, this ‘cholinergic anti-inflammatory pathway’ provides a physiological mechanism linking acetylcholine with inhibition of inflammation. Pre-incubation of rat cells with tacrine and donepezil protected them from the effect of hydrogen peroxide, and significantly produced an increase in catalase and glutathione peroxidase antioxidants. Free radicals are known to

directly damage cells and appear to be involved in reciprocal induction of other mediators of toxicity in AD such as β-amyloid which if we can inhibit its aggregation, we reduce the inflammation. Hence, we screened for the β-amyloid aggregation inhibition of these compounds. This would be an alternative to the existing therapeutic treatments for AD.

1.6. Current Treatments of Alzheimer's Disease

AD remains incurable and its progression is inevitable with the currently available symptomatic therapies being palliative [139]. Clinical treatment of this disease relies mostly on enhancing cholinergic function by stimulation of cholinergic receptors or prolonging the availability of ACh released into the neuronal synaptic cleft by use of agents which restore or improve the levels of acetylcholine. Inhibition of acetylcholinesterase (AChE) and butyl cholinesterase (BChE), enzymes which breakdown acetylcholine, are considered as promising strategies for the treatment of AD [157]. The potential pharmacologic therapies for AD can be broadly divided into two categories:

(i) symptomatic approaches based on enhancement of neurotransmitter systems and

(ii) neuroprotective strategies using antioxidants such as vitamin E (α-tocopherol) and selegiline. Antioxidants are molecules that scavenge free radicals and ROS, that may induce oxidative stress, and consequently, cellular damages [158-159]. Antioxidants are known to have anti-cancer, anti-diabetic, and anti-aging effects [140]. Antioxidants would be helpful in treating AD, because the ROS generated in AD pathogenesis causes neuronal damage which increases risks in morbidity and mortality [160]. Many AD patients also are prescribed antipsychotics or antidepressants to manage psychiatric and behavioural symptoms, but with an apparently increased risk of mortality [161].

1.6.1. Acetylcholinesterase Inhibitors

The most effective medications for AD to date are the AChE inhibitors, which reduce the enzymatic degradation of the neurotransmitter Ach, deficient in the AD brain, and thus enhance the cholinergic system. The three AChE inhibitors approved by the Food and Drug Administration (FDA) for treatment of AD, donepezil, galantamine and rivastigmine, have been demonstrated to improve cognition, function in activity of daily living (ADL) and behaviour in patients with AD in double-blind, placebo-controlled trials [139, 162]. Although

AChEI can alleviate the symptoms and delay the progression of AD, AChEIs cannot cure the disease [163]. Also, patients taking AChEIs have presented higher discontinuation due to adverse events. The most common side effects are nausea, diarrhoea, insomnia, muscle cramps, vomiting and fatigue, denoting an important issue on anti-AChE therapy [164]. Therefore, there is a need to search for novel compounds which can be investigated for their effective complete remediation and with less severe adverse events.

1.6.2. N-methyl-D-aspartate Receptor Antagonist
Memantine

Memantine is an *N*-methyl-D-aspartate (NMDA) receptor antagonist also approved for use in AD [165], and works by antagonizing glutamate at the NMDA receptor, potentially improving signal transmission, and by preventing excess calcium from rushing into the neurons with glutamate stimulation and may therefore protect against toxic damage to cholinergic neurons. Memantine in combination with the AChE inhibitors (donepezil, galantamine, or rivastigmine) significantly slows deterioration in both cognitive function and ADLs compared to patients treated with AChE inhibitors alone [166]. Treating other underlying chronic conditions such as diabetes can also result in improved palliative response for AD due to reduced complications extending to the nervous system [18]. Numerous studies have established potential links between DM and AD, supporting the hypothesis that DM is linked with an increased risk of AD, and that suppressing glycaemia have a beneficial impact on prevention of AD [167-173].

The TZD derivatives being investigated in this study are:

1. (E)-5-(2,4,6-trimethoxybenzylidene)-3-(2-oxo-2-(4-phenylpiperazin-1-yl)ethyl)thiazolidine-2,4-dione
2. (E)-5-((2,5-dimethyl-1-phenyl-1H-pyrrol-3-yl)methylene)-3-(2-oxo-2-(24yrrolidine-1-yl)ethyl)thiazolidine-2,4-dione
3. 2-((E)-5-((2,5-dimethyl-1-phenyl-1H-pyrrol-3-yl)methylene)-2,4-dioxothiazolidin-3-yl)acetic acid
4. (2Z,5E)-5-((2,5-dimethyl-1-phenyl-1H-pyrrol-3-yl)methylene)-2-(phenylimino)thiazolidin-4-one

For simplicity, these TZD derivatives have been named; 1- TZDD1, 2 - TZDD2, 3 - TZDD3 and 4 - TZDD4.

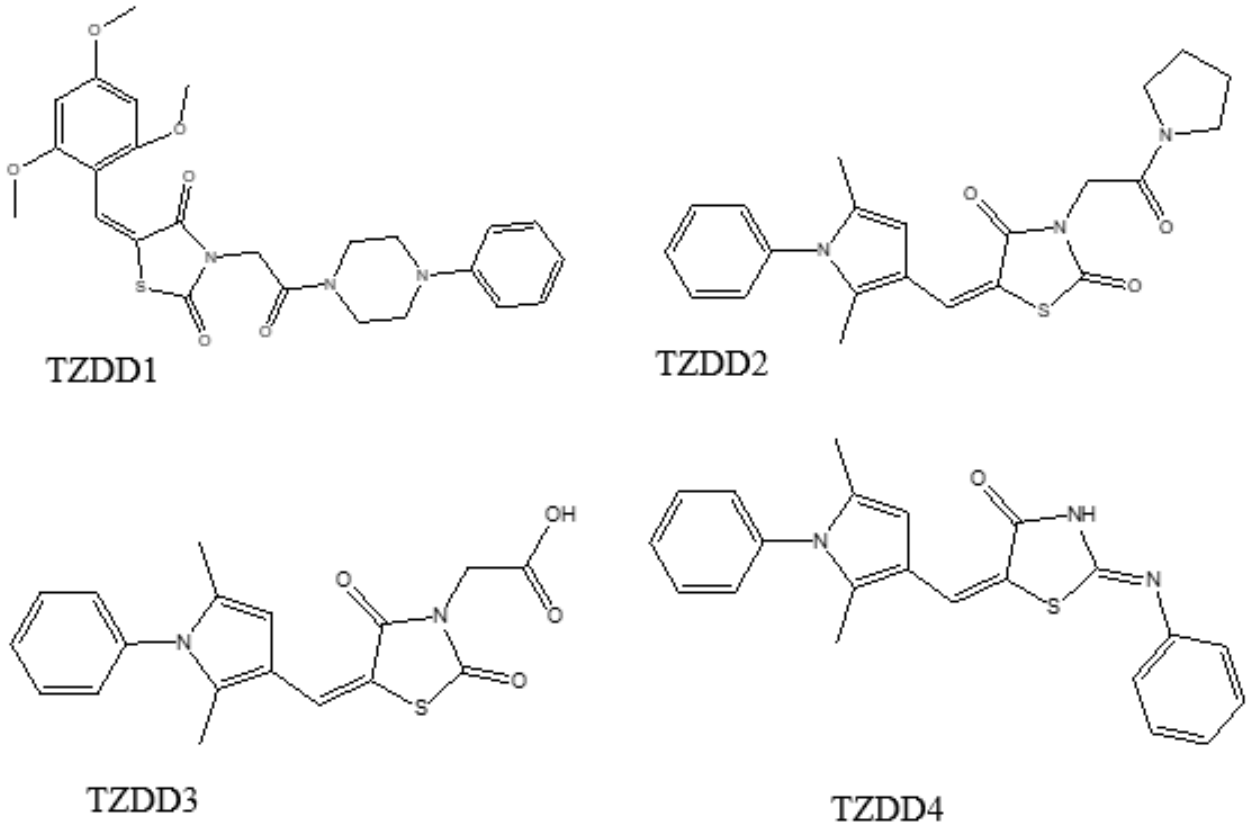

Figure 1.2. Chemical structures of the thiazolidinedione derivatives.

These TZD derivatives were synthesized through the pharmacophore hybridisation strategy based on two known pharmacophoric units, the *N*-arylpyrrole and thiazolidinedione (TZD) [174]. This was based on the fact that a significant number of compounds containing these structural scaffolds are known to exert biological activity, and earlier studies have shown that TZD-derived hybrids with *N*-functionalized side chain on the *N*-3 nitrogen TZD ring displayed improved efficacy and that such modifications exhibited low toxicity towards primary cultured non-malignant human hepatocytes [174, 175]. One report notes that incorporation of *N*-heterocyclic structures, such as; pyrrolidinyl, piperidinyl, morpholinyl and thiomorpholinyl groups into a molecule resulted in compounds with enhanced metabolic stability and increased antimalarial activity [176]. In addition, a large number of clinically approved drugs are having *N*-heterocyclic ring as a subunit of their chemical structures and mefloquine (antimalarial) and levofloxacin (antitubercular) are two representative examples of drugs with *N*-heterocyclic ring [177, 178]. On the basis of the above observations, the new thiazolidinedione-derivatives were

synthesised by exploring the use of *N*-heterocyclic amines as an appendant on the *N*-3 of the TZD scaffold, and further, in this study, we investigated their anti-diabetic and anti-Alzheimer's disease.

1.7. Justification of the study

Diabetes mellitus and Alzheimer's disease are of global concern. Furthermore, T2DM has been identified as a main risk factor for the onset and progression of AD [173]. Impaired glucose metabolism, insulin resistance, and mitochondrial dysfunction are pathologies common to both T2DM, and AD [173, 179]. This has led several researchers worldwide to strive and search for novel treatment therapies for diabetes as well as Alzheimer's disease. However, to date, there is no therapy able to induce management and treatment of both diseases as current therapies aim at management of one and in some instances are only palliative. This continues to promote polypharmacy because of co-morbidities in patients. In this line, the discovery of new therapies is undoubtedly an important goal, to provide better and more efficient treatment for both diabetes and Alzheimer's disease patients.

TZDs, of which have an established mode of action as PPAR-γ agonists and used clinically as insulin sanitizers for DM treatment, have also shown to inhibit neuroinflammation, facilitate amyloid-*β* plaque clearance, enhance mitochondrial function, improve synaptic plasticity, and, more recently, attenuate tau hyperphosphorylation in several studies [180-187]. Furthermore, some studies have reported TZD derivatives to have improved antidiabetic activity and others with various antidiabetic targets [130, 134, 136-138]. Based on the above, we targeted the screening of TZD derivatives against diabetes and Alzheimer's disease potential therapeutic targets.

1.8. Aims and objectives

The aim of this research study was to determine the anti-diabetic and anti-Alzheimer's properties of newly synthesised thiazolidinedione-derivatives (TZD derivatives). This was achieved through the implementation of the following objectives:

i. Absorption, distribution, metabolism, and excretion (ADME) profiling of the four TZD derivatives to predict safety and efficacy profiles.
ii. *In vitro* screening of these compounds to establish their antioxidant activity using the following assays:
    a) Ferric Reducing Antioxidant Power

b) 2,2'-Diphenyl-1-Picry Hydrazyl radical scavenging activity

iii. *In vitro* screening of these compounds to establish their antidiabetic activity using the following assays:

a) Alpha amylase inhibition since this enzyme converts carbohydrates to oligosaccharides by cleaving glycosidic linkages of α-D-(1,4), which are further broken down by α-glucosidase

b) Alpha glucosidase inhibition as this enzyme converts the oligosaccharides to monosaccharide glucose which increases postprandial glucose concentrations. Therefore, inhibiting the activities of both α-amylase and α-glucosidase will delay the increase in blood glucose concentration, hence controlling hyperglycaemia

c) Aldose Reductase inhibition, Aldose Reductase is responsible for catalysing the conversion of glucose to galactitol in the polyol pathway, which is the alternate metabolism pathway for small quantities of non-phosphorylated glucose. The polyol pathway plays an important role in the aetiology of diabetic complications and therefore inhibiting aldose reductase may provide potential treatment for long-term diabetic complications

d) Protein Tyrosine Phosphatase–1B inhibition, protein tyrosine phosphatase-1B catalyses the de-phosphorylation of activated insulin receptor, hence downregulating insulin signalling. Inhibiting this enzyme has potential to treat T2DM

e) Dipeptidyl peptidase-4 inhibition since this enzyme cleaves glucagon like peptide-1, an incretin hormone that plays an important role in glucose homeostasis, and reduces its biological activity by shortening its half-life. Inhibiting DPP-4 therefore provides potential for glycaemic control

iv. In silico determination of peroxisome proliferator-activated receptor-γ activation PPAR-γ is a master regulator of adipogenesis, which binds compounds such as synthetic antidiabetic thiazolidinediones that activates the trans activating function of PPAR-γ causing a powerful adipogenic response. Binding and activation of PPAR-γ by these TZD derivatives would indicate that the mode of action of TZDs have been retained.

v. *In vitro* screening of these compounds to establish their anti-Alzheimer's properties, using the following assays:

a) Acetylcholinesterase inhibition as this enzyme is responsible for hydrolysing acetylcholine, a naturally occurring neurotransmitter and neuromodulator, whose

deficiency is linked to the pathogenesis of AD. Inhibiting this enzyme may prolong the lifespan of acetylcholine hence controlling AD

b) Matrix metalloproteinase-1 inhibition as this enzyme is responsible for altered extracellular matrix remodelling which is associated with vascular complications in type 1 diabetes. Inhibiting this enzyme may control these diabetic complications
c) β-amyloid aggregation inhibition as accumulation of these plaques is a hallmark in AD physiopathology.

CHAPTER TWO: MATERIALS AND METHODS

2.1. Chemicals and Equipment

α-Amylase, α-glucosidase, human recombinant aldose reductase, protein tyrosine phosphatase-1B (PTP1B) (human recombinant), DL-glyceraldehyde, β-mercaptoethanol, β-nicotinamide adenine dinucleotide phosphate (NADPH), quercetin, acarbose, *p*-nitrophenyl phosphate (*p*NPP), ethylenediaminetetraacetic acid (EDTA), acetylcholinesterase (AChE), acetylthiocholine iodide (AChI), 5,5′-dithiobis [2-nitrobenzoic acid] (DTNB), bovine serum albumin (BSA), D-(+)-glucose, dithiothreitol (DTT), thioflavin T (ThT), potassium ferricyanide, trichloroacetic acid (Tris-HCl), and iron (III) chloride were purchased from Sigma-Aldrich Chemical Corporation (Johannesburg, South Africa). All other chemicals were of analytical grade and were used with no further purification.

SpectraMax M3 multi-mode microplate reader (100 – 240V~3.5A 50 – 60Hz; manufactured in China, designed in California, USA), UV-VIS Spectrophotometer (UVmini-1240)(AC 220 – 240 ~50/60Hz 160VA; SHIMADZU CORPORATION, made in Chine), Ivymen microplate reader (2100-C)(110V – 220V – 50/60Hz 120W T3.15AL 250V; Ivymen Optic Systems), Incubator (FSOH4)(220/240V 50Hz, 0.5kW; Labcon (pty) ltd 15 Aschenberg street Chamdor Krugersdorp Transvaal), BV1000 vortex mixer(230VAC 50Hz, 0.75amps; Benchmark Scientific Inc. PO BOX 709, Edison, NJ 08818, USA; made in Taiwan), and Hotplate stirrer (H3760-HSE)(230V, 60Hz; (Lasec Laboratories) Benchmark Scientific Inc. PO BOX 709, Edison, NJ 08818, USA).

2.2. Synthesis and Characterization of Compounds

The synthesis and characterisation of thiazolidinedione derivatives were performed by the Drug Discovery and Pharmaceutical Chemistry Group (Division of Pharmaceutical Chemistry, Rhodes University) under the supervision of Prof. S.D. Khanye [178]. The TZD derivatives were synthesized through the pharmacophore hybridisation strategy based on two known pharmacophoric units, the *N*-arylpyrrole and TZD [178, 174]. The *N*-heterocyclic amines were used as an appendant on the *N*-3 of the TZD scaffold. The target compounds were achieved via two synthetic routes; namely route **A** and **B**. Route **A** utilized the well-known Knoevenagel condensation of the respective arylpyrrole carbaldehydes and the active methylene containing TZD intermediates to generate the target hybrid compounds.

The starting point for the arylpyrrole carbaldehyde common to both routes was accessed via Paal-Knorr condensation of appropriate anilines with 2,5-hexanedione. Our adopted procedure followed a neat method that was recently reported by Willianson *et al*., with only slight modifications to obtain compounds in moderate to good yields [175] The last step in the synthesis of common arylpyrrole carbaldehydes, achieved via the Vilsmeier-Haack reaction using phosphorus oxychloride ($POCl_3$), and the excess $POCl_3$ was neutralized with 30% NaOH to adjust the pH, and thus, precipitating the desired products in pure form (based on NMR) for subsequent use without the need for further purification [176].

2.2.1. Synthesis of the target hybrid compounds via route A

2.2.1.(a) Synthesis of the active methylene containing TZD intermediates

The TZD intermediates bearing the active methylene were obtained in two steps synthetic reaction. The first step involves *N*-acylation reaction of appropriate commercialy available cyclic secondary amines with chloroacetyl chloride in the presence of trimethylamine to give rise to the respective chloroacetyl amides. The second step is the SN2 reaction of chloroacetyl amides with TZD, under basic conditions to give the desired active methylene bearing TZD intermediates in moderate yields [177].

2.2.1. (b)Knoevenagel condensation to arrive at the target hybrids

The last step in obtaining the desired hybrid compounds through route **A** involves Knoevenagel condensation of *N*-arylpyrrole carbaldehyde with an active methylene containing TZD intermediates to give the desired target compounds [178]. Having successfully synthesized the required aldehydes and the active methylene containing TZD intermediates, the Knoevenagel condensation was achieved in moderate to good yields (70 – 91%) by reacting equimolar amount of each of the appropriate starting materials at 60 □C for 5 – 16 h in ethanol and using piperidine as a base [178]. The structures of all the synthesized hybrid compounds were established by combination of spectroscopic methods i.e., IR, ^{1}H NMR, ^{13}C NMR, and high-resolution mass spectrometry (HRMS).

2.2.2. Synthesis of the target hybrid compounds through route B

To resolve the challenges faced in route **A**, route **B** of the retrosynthetic analysis was followed. With the arylpyrrole carbaldehyde intermediates in hand, the TZD acetic acid, to be condensed with, was prepared via an efficient two steps synthetic protocol. Following the successful synthesis of the key acid intermediates, the next and last step of the reaction scheme is the transformation of these acid intermediates into carboxamides. The synthesis was achieved by a standard one-pot carbodiimide-promoted amide formation, using EDC.HCl as a coupling

reagent, whose function is to activate the carboxylic acid by forming the *o*-acyliourea intermediate [177]. Structural characterization of all these target hybrids were carried out using a combination of all the spectroscopic techniques, which were in agreement with the proposed structures.

The synthesis of the rhodanine analogues of the key TZD acid intermediates was performed and the synthesis commenced with the preparation of rhodanine acetic acid, which was achieved through one-pot cyclisation of dithiocarbamate of aminoacetic acid prepared by the reaction of carbon disulfide with equimolar amount of cooled-solution of 2-aminoacetic acid and sodium hydroxide. Subsequent reaction of intermediate with sodium chloroacetate and refluxing with hydrochloric acid resulted in the rhodanine ring formation. Finally, the Knoevenagel condensation of the rhodanine acetic acid with selected arylpyrrole carbaldehyde. The structures were characterized using both ^{1}H and ^{13}C-NMR spectroscopy [178]. The selected TZD derivatives synthesised and investigated in this study were those in **Figure 1.2**.

2.3. Bioavailability (ADME) Profiling

In order to predict the pharmacokinetics of these compounds, *in silico* tools were used to determine the absorption, distribution, metabolism and excretion (ADME) profiles. *In silico* methods include early computer software programs and current advanced computer methods with modern computer analytics used for compartmental modelling of pharmacokinetic data. In this study, SwissADME tool (http://www.swissadme.ch/index.php) was used to generate the Boiled-egg model (**Figures B1 – B4, in the appendix**) [188]. The BOILED-Egg model (*Brain Or IntestinaL EstimateD permeation* predictive model) delivers a rapid, easily reproducible, and yet statistically unprecedented robust method to predict the passive gastrointestinal absorption and brain access of small molecules useful for drug discovery and development. On the BOILED-Egg, the coordinates of respective ellipses and an Excel file including the Cartesian coordinates of both ellipses' trace is provided. For up to 100 molecules, the WLOGP and tPSA, and the corresponding points can be mapped onto the BOILED-Egg.

This method discriminates between well-absorbed and poorly absorbed molecules based on their lipophilicity and polarity, which is described by the *n*-octanol/water partition coefficient (log *P*) and the polar surface area (PSA). It also provides a clear picture of how far a molecular structure is from the ideal physicochemical region for good absorption. As lipophilicity and polarity are often inversely correlated properties, the sometimes-tricky chemical modifications simultaneously impacting log *P* and PSA are efficiently supported by the model. This

prediction tool merely depicts the dispersion of properties related to good absorption and can be used as the model for gastrointestinal passive absorption, and the prediction for brain access by passive diffusion. SwissADME was used to determine the physiochemical properties, water solubility, pharmacokinetics, drug likeness, lipophilicity and medicinal chemistry of the compounds and compared with Rosiglitazone as the standard control [188]. Briefly, the TZD derivatives (**TZDD1**, **TZDD2**, **TZDD3** and **TZDD4**) were prepared using ChemDraw-AcdLabs software to generate the .dxt format and Openbabel-2.4.1 software was used to generate the .pbd formats. The .pdb formats were then added onto the SwissADME software and the BOILED-Egg generated using the in-built methods of SwissADME software.

2.4. Preparation of Compounds for *In vitro* Testing

0.01g of each compound was weighed out using the Precisa analytical balance and dissolved in DMSO (1 mL) and made up to volume to 10mL with distilled water to make the stock solutions (concentration: 1000µg/mL). These stock solutions were diluted further and used to make the desired concentrations (10, 20, 30 40 and 50µg/mL) using $C_1V_1 = C_2V_2$ formula. For every assay, the desired concentrations were freshly prepared using distilled water.

2.5. Antioxidant Activity

2.5.1. Determination of Ferric Reducing Antioxidant Power

The ferric reducing antioxidant power was determined using the method described by Benzie and Strain, with minor modifications [189]. In this method, the determination of antioxidant activity is based on electron transfer due to the reduction of Fe^{3+} to Fe^{2+}. When the reduction of Fe^{3+} to Fe^{2+} occurs in the presence of 2,4,6-trypyridyl-s-triazine, the reaction is accompanied by the formation of a violet-blue complex of Fe^{2+} and these changes are evaluated using spectrophotometer at the wavelength of 593 nm. the FRAP assay is therefore based on an electron transfer mechanism with formation of a radical. This assay was used since it is simple to use and very inexpensive.

$$Fe(TPTZ)_2^{3+} + \text{antioxidant compound} \rightarrow Fe(TPTZ)_2^{2+} + \text{radical} + H^+$$

To perform this assay, a 2.5 mL of a 0.2 M phosphate buffer (pH 6.6) was added to 400 µL of the test compound solutions of different concentrations (10, 20, 30, 40 and 50 µg/mL), with a subsequent addition of 2.5 mL of 1 % potassium ferricyanide. The mixture was incubated at

50 ºC for 20 min. The reaction was then stopped by adding 2.5 mL of 10 % w/v trichloroacetic acid solution, and the mixture was allowed to cool at room temperature (24 ºC). A 500 µL of iron (III) chloride (0.1 %) was added and absorbance measured at 593 nm. Ascorbic acid (10, 20, 30, 40, 50 µg/mL) was used as the positive control. The absolute control contained all the assay reagents except the investigated compounds. The assay was done in 6 replicates. The absorbances values were used to determine the mass of Iron (II) formed (µM) per gram of dry mass by extrapolating from the standard curve (**figure D1, attached in the appendix**) generated by plotting Iron (II) and it's absorbances at increasing concentrations (0, 100, 200, 300, 400, 500, 600, 700, 800, 900 and 1000 µM).

2.5.2. 2,2-Diphenyl 1-picryl hydrazyl Radical Scavenging Assay

The 2,2-diphenyl 1-picryl hydrazyl (DPPH) radical scavenging activity was determined using the method described by Kwon *et al.* with some modifications [190]. This assay is based on the scavenging of the DPPH by the antioxidant. In its radical form, DPPH shows an active absorption band at λmax 515-517 nm, and after reaction of the antioxidant with DPPH, the DPPH accept the hydrogen donor, and the solution loses its colour from purple to pale yellow. Ascorbic acid was used in this assay because it is considered an effective antioxidant as it has scavenging effects against O_2^-, H_2O_2, OH, $^1O_2$ and reactive NO_2.

The commercially available DPPH was dissolved in ethanol to make 0.1 mM. 1 mL of this solution was added to 2 mL of the test compounds (10, 20, 30, 40 and 50 µg/mL). The mixture was then vortexed for 10 seconds and allowed to stand at room temperature (24 ºC) for 30 min. Absorbance values were then read at wavelengths of 517nm. Ascorbic acid was used as the positive control (10, 20, 30, 40 and 50 µg/mL). The absolute controls contained all the reagents used except the compounds being investigated. The assay was done in 6 replicates. The percentage radical scavenging activity was calculated using the following:
$[1 - (Abs_{sample}/Abs_{control})] \times 100\%$, where Abs is the absorbance measured.

2.6. Antidiabetic Assays

2.6.1. α-Amylase Inhibition Assay

The α-amylase inhibitory activity was determined by the method described by the Worthington Enzyme Manual with slight modifications [191]. In this method, the α-amylase activity is

measured using a colorimetric method with 3,5-dinitrosalicylic acid (DNS) reagent. The dietary starch is digested by α-amylase to maltose, which is measured by the reduction of DNS.

Starch + H2O $\xrightarrow{\alpha\text{-Amylase}}$ Maltose (reducing agent)

Maltose reduces the pale-yellow alkaline DNS to orange red.

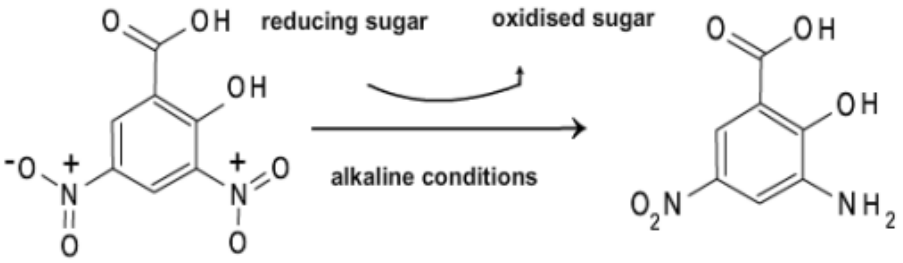

3,5-dinitrosalicylic acid 3-amino-5-nitrosalicylic acid

This intensity change in colour is proportional to the concentration of maltose present in the sample and is measured using a spectrophotometer at the absorbance of 540nm wavelength. Wavelength is set to 540 nm because it is the region where orange-red colour absorbs.

Briefly, a 500 µL of TZD-derivatives (10, 20, 30, 40 and 50 µg/mL) and 500 µL of 0.02 M sodium phosphate buffer (pH 6.9 with 0.006 M NaCl) containing α-amylase solution (1.0 IU/mL) was incubated at 37 ºC for 10 min. After preincubation, 1% starch solution (500 µL) was added to 0.02 M sodium phosphate buffer (pH 6.9 with 0.006 M NaCl). The reaction mixture was then incubated at 37 ºC for 10 min. The reaction was stopped by adding DNS (1.0 mL) colour reagent. The test tubes were then incubated in a boiling water bath for 5 min and cooled to room temperature. The reaction mixture was then diluted by adding distilled water (2 mL), and absorbance values measured at 540 nm. Acarbose (10, 20, 30, 40 and 50 µg/mL) was used as the positive control and the absolute control contained all the reagents used except the inhibitor compounds.

Acarbose was used as a positive control since it is a registered antidiabetic for treatment of T2DM whose mode of mechanism is by inhibiting α-amylase and α-glucosidase. Acarbose is a complex oligosaccharide that competitively and reversibly inhibits α-glucosidase and α-amylase, hence controlling postprandial glycaemia due to delayed enzymatic digestion of

carbohydrates. The sodium phosphate buffer was used as the blank. The experiment was done in triplicates and the he α-amylase inhibitory activity was calculated according to the equation: Inhibition (%) = $((A_{control} - A_{sample})/A_{control}) \times 100\%$, where $A_{control}$ was the absorbance of the control (without the inhibitor); A_{sample} was the absorbance in the presence of TZD-derivatives.

2.6.2. α-Glucosidase Inhibition Assay

The α-glucosidase inhibitory activity was determined using the Worthington Enzyme Manual with slight modification [192]. Under conditions of pH = 6.8; T = 37 °C), α -glucosidase catalyses the conversion of 4-nitrophenyl-α-D-glucopyranoside (PNPG) to α-D-glucopyranoside and p-nitrophenol (PNP). The yellow colour of PNP is measured spectrophotometrically at 405 nm.
PNPG + α-glucosidase → α-D-glucopyranoside + PNP (yellow)

To perform this assay, 70 µL of TZD-derivatives (10, 20, 30, 40 and 50 µg/mL) was diluted with 100 µL of 0.1 M potassium phosphate buffer (pH 6.8) containing α-glucosidase solution (1.0 IU/mL) and was incubated in a 96-well plate at 37 ºC for 10 min. After pre incubation, 5 mM *p*-nitrophenyl-α-glucopyranoside solution (70 µL) in 0.1 M potassium phosphate buffer (pH 6.8) was added to each well at timed intervals. The reaction mixtures were incubated at 37 ºC for 60 min. The reaction was stopped by adding 0.1 M $NaCO_3$ (125 µL). The absorbance values were then measured at 405 nm using the Ivymen microplate reader (2100-C). Acarbose (10, 20, 30, 40 and 50 µg/mL) was used as the positive control, and the absolute controls contained all the reagents used in this experiment except the inhibitors. The potassium phosphate buffer was used a blank. The α-glucosidase inhibitory activity was determined as percentage of inhibition, calculated as follows:
Inhibition (%) = $((A_{control} - A_{sample})/A_{control}) \times 100\%$, where $A_{control}$ was the absorbance of the control (without the inhibitor); A_{sample} was the absorbance in the presence of TZD-derivatives.

2.6.3. Aldose Reductase Inhibition Assay

The aldose reductase inhibition assay was performed according to the method described by Kazeem *et al.* with minor modifications [193, 194]. AR activity is assayed spectrophotometrically by measuring the reduction in absorption of NADPH at 340 nm over a period of time with DL-glyceraldehyde as a substrate.

In this assay, the reaction mixture contained 0.3 mM NADPH, 10 mM DL-glyceraldehyde, 5 µL of aldose reductase (6.5 IU/mg), and 100 µL of TZD-derivatives (10, 20, 30, 40 and 50 µg/mL) or distilled water in a total volume of 300 µL in 0.05 M sodium phosphate buffer (pH 6.2). The reaction mixtures were incubated at 37 ºC for 5 min, the reaction was initiated by addition of the enzyme, and then the change in absorbance was measured at 340 nm for 10 min using the SpectraMax M3 multi-mode microplate reader (California, USA). The inhibition assay of the standard (quercetin) was performed using the same procedure but replacing the TZD-derivatives with quercetin (10, 20, 30, 40 and 50 µg/mL).

Quercetin was used as a positive control because it is a flavonoid that is an effective aldose reductase inhibitor. The absolute standard contained all the reagents used except for the inhibitor compounds. Sodium phosphate buffer was used as the blank. The assay was done in triplicates. The aldose reductase inhibition activity was calculated as percentage inhibition from:

% Inhibition = $[(\Delta Abs_{control} - \Delta Abs_{sample})/ \Delta Abs_{control}] \times 100\%$, where ΔAbs is the change is absorbance.

2.6.4. Protein Tyrosine Phosphatase Inhibition Assay

The protein tyrosine phosphatase-1B (PTP1B) inhibition assay was performed according to the method described by Song *et al.* with some modifications [195, 196]. Protein tyrosine phosphatase down-regulates insulin and leptin signalling by catalysing tyrosine dephosphorylation of insulin receptors (IR), insulin receptor substrate (IRS), and leptin receptors. The inhibitory effects are assayed using p-nitrophenyl phosphate (*p*-NPP) as the substrate; the amount of p-nitrophenol, the catalytic product of PTP1B enzyme, is determined spectrophotometrically at 405 nm absorbance.

In the assay procedure, the buffer solution consisted of 25 mM Tris-HCl (pH 7.5), 2 mM β-mercaptoethanol, 1 mM EDTA, and 1 mM dithiothreitol (DTT). The assay was performed by adding 20 µL of test compound solution to 40 µL of enzyme (0.1 µg/mL), and then mixing with 80 µL of 4 mM *p*NPP in 130 µL of the buffer (pH 7.5) in the 96 well plate and incubated at 37 ºC for 10 min. During the enzymatic reaction, the *p*NPP produced was monitored by SpectraMax M3 multi-mode microplate reader (California, USA) at 405 nm for 30 min. Sodium orthovanadate (10, 20, 30, 40 and 50 µg/mL) was used as the positive control for inhibition. Sodium orthovanadate was used as a positive control because it has been indicated as a potential PTP-1B inhibitor, and it was largely available in our laboratory. Tris-HCl was

used as the blank, and the absolute control contained al the regents used except the inhibitor compounds. The inhibition activity was calculated using:

% Inhibition = $[(\Delta Abs_{control} - \Delta Abs_{sample})/ \Delta Abs_{control}] \times 100\%$, where ΔAbs is the change is absorbance.

2.6.5. Dipeptidyl Peptidase-4 Inhibition Assay

This assay was performed according to the Dipeptidyl-peptidase-4 (DPP-4) inhibitor screening Kit (catalog number: MAK203) product information (Sigma-Aldrich.com) with minor modifications to the volumes to suit the 96 well plate assay [197]. DPP-4 is a membrane glycoprotein with serine exopeptidase activity that cleaves X-proline dipeptides from the N-terminus of polypeptides. DPP-4 activity is measured by cleaving the substrate to yield a fluorescent product (λ_{ex} = 360/ λ_{em} = 460 nm), proportional to the enzymatic activity present. The effectiveness of the test inhibitors may be compared with the DPP4 inhibitor (sitagliptin) provided as a control.

To perform this assay, the inhibitor sample solutions (10, 20, 30, 40 and 50 µg/mL) were prepared by adding 25 µL of compounds to 10 µL of DPP4 buffer (MAK203A) and aspirated into the wells of a 96 well plate. The inhibition reaction mix was prepared by adding 49 µL of the DPP4 buffer to 1 µL of the DPP4 enzyme (MAK203C), and added into the wells. The enzymatic reaction mix was prepared by mixing 23 µL of the buffer with 2 µL of the DPP4 substrate (MAK203B) then added into the wells. The positive control was prepared by adding 5 µL of (Sitagliptin) an inhibitor control to 45 µL of the DPP4 buffer. The fluorescence values were then read at excitation wavelengths of 360 nm and emission of 460 nm in kinetic mode for 30 min at 37 ºC after every minute.

The % relative inhibition was determined using the equation

$[(\Delta FLU_{control} - \Delta FLU_{sample})/ \Delta FLU_{control}] \times 100\%$, where ΔFLU is the change in fluorescence

2.7. Peroxisome Proliferator–activated Receptor-γ (PPAR-γ) Docking

The 3D crystal structure of peroxisome proliferator-activated receptor gamma (PPAR-γ) was downloaded from Protein Data Bank (PDB) (https://www.rcsb.org/) [198]. The protein (PDB entry: 4Ema) for docking was prepared using the protein preparation wizard tools of Auto dock 4.2. The ligands (**TZDD1**, **TZDD2**, **TZDD3** and **TZDD4**) were prepared using ChemDraw-AcdLabs software to generate the .dxt format and Openbabel-2.4.1 software to generate the

.pbdqt formats. The ligands imported was rosiglitazone. Rosiglitazone is a TZD, which is registered for treatment of DM, and its mode of action is PPAR-γ activation. AutoDock-4.2 was used as molecular-docking tool in order to carry out the docking simulations. The grid points in X, Y and Z axis were set at 60 × 60 × 60. The grid centre was placed in the active site pocket centre with coordinates of Central Grid Point of Maps = -4.339, -14.270, 22.436). Minimum coordinates in grid = -19.339, -29.270, 7.436 and maximum coordinates in grid = 10.661, 0.730, 37.436.

The grid boxes included the entire binding site of this protein and provided enough space for the ligand translational and rotational walk. For each ligand, a docking experiment consisting of 50 stimulations was performed and the analysis was based on binding free energies and root mean square deviation (RMSD) values, and the ligand molecules were then ranked in the order of increasing docking energies. The binding energy of each cluster is the mean binding energy of all the conformations. The clusters were ranked by the lowest-energy representative of each binding mode. The 4 TZD-derivatives and rosiglitazone as standard drug were docked against PPAR-γ using Auto Dock, results were analysed using binding energy, as well as protein plus analysis tools software (https://proteins.plus/) and Protein-Ligand Interaction Profiler (https://plip-tool.biotec.tu-dresden.de/plip-web/plip/index) to determine the binding conformations (**Figures C1 – C13 (iii), in the appendix)** [199, 200].

2.8. Anti-Alzheimer's Assays

2.8.1. Acetylcholinesterase Inhibition Assay

The inhibition of acetylcholinesterase enzyme was determined using the method developed by Ellman *et al.* and improved by Jung *et al.* with minor modifications [201, 202]. The acetylcholinesterase (AChE) assay protocol uses 5,5′-dithiobis [2-nitrobenzoic acid] (DTNB) to quantify the thiocholine produced from the hydrolysis of acetylthiocholine by AChE. The absorption intensity of DTNB adduct at 410 nm is used to measure the amount of thiocholine formed, which is proportional to the AChE activity.

In this assay, 1.71 mL of 50 mM Tris-HCl (pH 8.0) was added to test tubes, and 250 µL of the test compounds (10, 20, 30, 40 and 50 µg/mL) added. Donepezil (10, 20, 30, 40 and 50 µg/mL) was used as a positive control dissolved in 50 mM Tris-HCl buffer (pH 8.0). Donepezil is a registered AChE inhibitor. The absolute control contained all the assay reagents except the

inhibitor compounds. Tris-HCl was used as the blank. The reaction mixture was initiated by adding 6.67 IU/mL acetylcholinesterase (10 µL) and 10 mM of 5,5′-dithiobis [2-nitrobenzoic acid]. The reaction mixture was then incubated at 37 ºC for 15 min. Subsequently, 200 mM Acetylthiocholine iodide (10 µL) was added and absorbance was measured at 412 nm for 3 min every after 10 seconds using a SpectraMax M3 multi-mode microplate reader (California, USA). Inhibition activity was determined using:

% Inhibition = $[(\Delta Abs_{control} - \Delta Abs_{sample})/ \Delta Abs_{control}] \times 100\%$, where ΔAbs is the change in absorbance.

2.8.2. Matrix Metalloproteinase-1 Inhibition Assay

The matrix metalloproteinase-1 (MMP-1) inhibitory assay was performed according to the MMP-1 inhibitor screening Kit (catalog number: MAK212) product information (Sigma-Aldrich.com) with minor modifications to the volumes to suit the 96 well plate assay [203]. MMP-1 is a secreted enzyme that breaks down interstitial collagen types I, II, and III in the extracellular matrix. The MMP-1 activity is measured by hydrolysing a Förster Resonance Energy Transfer (FRET)-tagged substrate to yield a fluorescent product (λ_{ex} = 490/λ_{em} = 520 nm) proportional to the enzymatic activity present.

To perform this assay, a 20 µL of MMP-1 buffer (MAK212A) were added in a 96 well plate, after which 5 µL inhibitor sample solutions (10, 20, 30, 40 and 50 µg/mL) were added. The control was prepared by adding 1 µL of a 1 µM (GM6001) inhibitor control to 24 µL of the MMP-1 buffer. The inhibition reaction mixture which contained MMP-1 buffer (48 µL) and MMP-1 enzyme (2 µL) was then added into the reaction solution. Subsequently, the substrate (2 µL) dissolved MMP-1 buffer (23 µL) was introduced into the reaction solution. The reaction mixture was then incubated at 37 ºC for 25 min. The fluorescence was then read at excitation wavelengths of 490 nm and emission of 520 nm in kinetic mode for 30 min at 37 ºC after every 1 minute.

The % relative inhibition was then determined from $[(\Delta FLU_{control} - \Delta FLU_{sample})/ \Delta FLU_{control}] \times 100\%$, where ΔFLU is the change is fluorescence.

2.8.3. β-Amyloid Aggregation Inhibition Assay

Inhibition of $A\beta_{1-40}$ aggregation was performed using the (thioflavin T) ThT method [204]. This assay uses a fluorescent amyloid-binding dye such as ThT. ThT undergoes an absorbance

spectrum shift. Free, unbound ThT has an excitation and emission maximum of 385 and 445 nm, respectively, and these are elevated to 450 and 482 nm, respectively, upon amyloid binding. By measuring fluorescence intensity, the amyloid plaques such as fibrils and protofibrils can be quantified.

In this experiment, commercially available $A\beta_{1-40}$ protein fragment (5 μM) (A1075, Sigma-Aldrich) was dissolved in 200 μL phosphate-buffered saline (PBS) (pH 7.4), at a concentration of 10 mM and left to stand for 3 min. The TZD derivatives (10, 20, 30, 40 and 50 μg/mL) were added to the $A\beta_{1-40}$ and the mixture incubated in the assay medium containing 0.01 M NaCl in potassium phosphate buffer (pH 7.4) at 37 ºC for 96 hrs. The 100 μL $A\beta_{1-40}$ with or without the inhibitor mixture was added to thioflavin T (ThT; 200 μM) in 50 mM glycine-NaOH buffer (pH 8.0). Thereafter, the reduction in the fluorescence intensity at excitation: 448 nm and emission: 490 nm was measured at intervals of time = 0, 24, 48, 72 and 96 hrs of the aliquots using a SpectraMax M3 multi-mode microplate reader; fluorophotometer (California, USA). Rifampicin (10, 20, 30, 40 and 50 μg/mL) was tested as a positive control. The absolute control contained all the assay reagents except the inhibitor compounds and PBS was used as the blank.

2.9. Kinetics of inhibition

The mode of inhibition of the biological enzyme α-glucosidase and acetylcholinesterase by the most potent derivatives (**TZDD3**) in this study was determined using the Michaelis-Menten and Lineweaver-Burk plots to determine the kinetic constants as well as plots [205 – 207]. The inhibition of these enzyme activities was determined in the presence and absence of the **TZDD3** at a concentration of its IC_{50} and a concentration twice its IC_{50} (60 and 120 μg/mL respectively) for α-glucosidase and 150 μg/mL for AchE.

Briefly, 30 μL of α-glucosidase enzyme (0.5 IU/mL), dissolved in 0.02 M phosphate buffer (pH 6.9), was pre-incubated at 37 □C with the above-mentioned derivative (50 μL) in a 96-well plate, for 5 min. In sequence, pNPG (0.125, 0.250, 0.500, 0.750, 1.000, 1.500, 2.000, 2.500 and 5.000 mM) was added and incubated in the reaction mixture at 37 □C for 30 min. **Figure D2** shows the standard curve used to generate the amount of PNP that would give the corresponding absorbances.

To perform the acetylcholinesterase kinetic study, 10 µL of AchE enzyme (0.5 IU/mL), dissolved in 50 mM Tris-HCl (pH 8.0), was pre-incubated at 37 □C with **TZDD3** derivative (150 µL) in a 96-well plate, for 5 min. In sequence, acetylcholine (0.5, 1.0, 2.0, 2.5, 5.0, 7.5, and 10.0 mM) was added and incubated in the reaction mixture at 37 □C for 25 min.

The study of the inhibition types (competitive, uncompetitive, non-competitive or mixed) of the tested derivative was performed using the nonlinear regression Michaelis–Menten enzyme kinetics and the corresponding Lineweaver–Burk double reciprocal plots for each concentration of the inhibitor and substrate. The Ki values were calculated with GraphPad Prism 9.2.0. (332) by plotting the reciprocal of maximum velocity (1/Vmax) (y-axis) against the derivative concentrations (x-axis). The type of inhibition parameters was all calculated with GraphPad Prism 9.2.0. (332). The experiment was done in triplicates.

2.10. Statistical Analysis

Each experiment was carried out in triplicates. Statistical Analysis of results from each experiment was done using GraphPad Prism 9.2.0. (332). Further statistical analysis was done using one-way ANOVA trailed by Tukey-Kramer post-hoc test used to test the significance between a test compound and the absolute control. The statistical analysis was done on using absorbance readings obtained from spectrophotometric analysis before any normalization. Non-linear regressions were used to estimate concentrations needed to inhibit 50 % of enzyme activity (IC_{50}) under the assay conditions using GraphPap Prism inbuilt methods which use linear regression to determine concentrations needed to inhibit 50 % of enzyme activity. Raw data was used to generate these IC_{50}s. The statistical significance was accepted at a level of $p < 0.05$.

CHAPTER THREE: RESULTS

3.1. Bioavailability profiling

The BOILED-Egg model is a developed descriptive representation used to discriminate between well-absorbed and poorly absorbed molecules based on their lipophilicity and polarity, described by the n-octanol/water partition coefficient (log P) and the polar surface area (PSA). Moderately polar (PSA<79 æ2) and relatively lipophilic (log P from +0.4 to +6.0) molecules have a high probability to access the CNS. From this study, The TZD derivatives are predicted to be highly absorbed by the gastrointestinal tract but predicted not to permeate the blood-brain barrier (BBB) (**Figure 3.1 and 3.2**). Additionally, they are predicted not to be effluxed from the nervous system by the P-glycoprotein. The TZD derivatives are predicted to possess moderate water solubility, high gastrointestinal (GI) absorption, lack BBB permeability, and do not violate the Lipinski rule of 5 (RO5) (**Table 3.1**) and a consensus log $P_{o/w}$ value of 2.55 (**TZDD1**), 3.03 (**TZDD2**), 2.41 (**TZDD3**), and 2.41 (**TZDD4**). The rule-of-five by Lipinski and co-workers provides physicochemical margins outside of which the probability for a molecule to become an oral drug is low. The RO5 shed light on the relationship between bioavailability and physicochemical properties, hence the concept of drug-likeness.

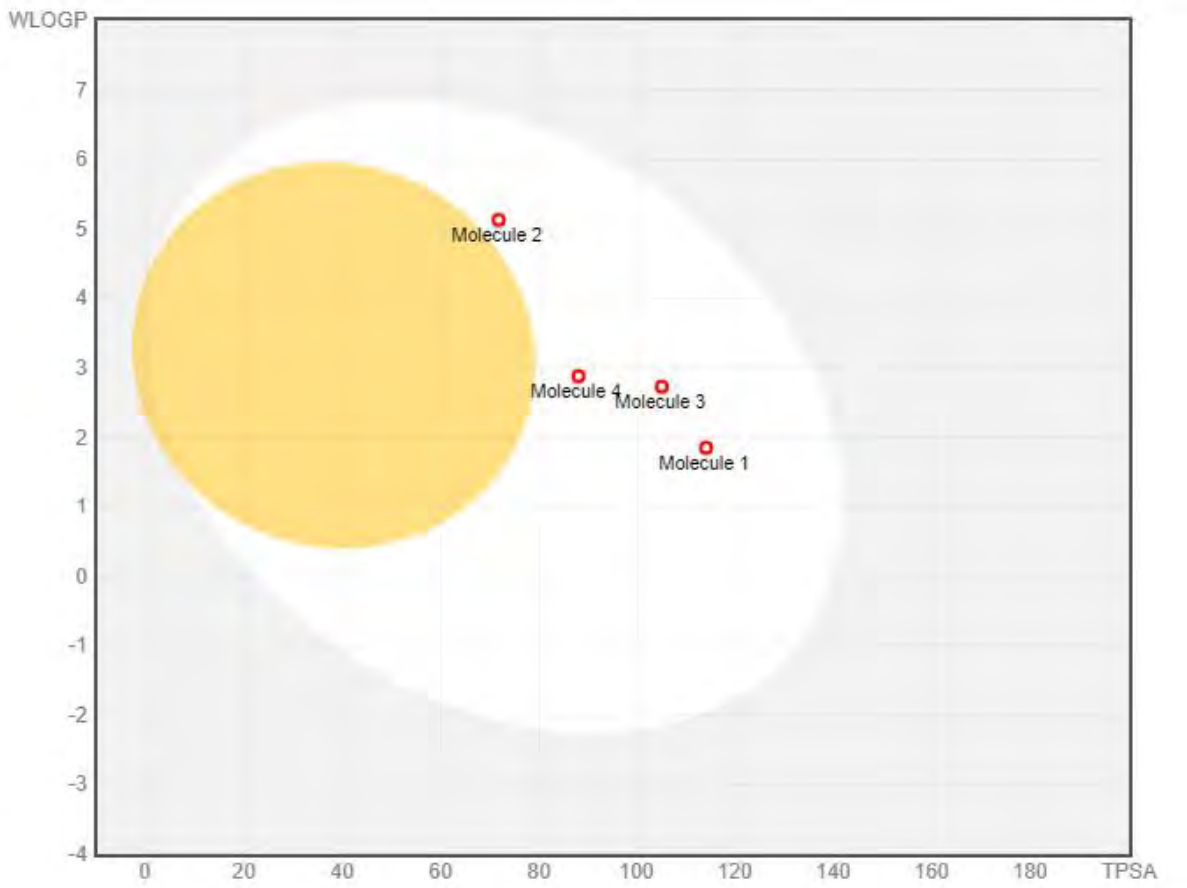

Figure 3.1: BOILED-Egg model showing molecules 1(**TZDD1**), molecule 2(**TZDD4**), molecule 3(**TZDD3**), and molecule 4(**TZDD2**). The BOILED-Egg's yolk represents a region occupied by molecules predicted to passively permeate through the blood-brain barrier and the BOILED-Egg's white, a region occupied by molecules predicted to be passively absorbed by the gastrointestinal tract. The red dots indicate that the molecules are predicted not to be effluxed from the nervous system by the P-glycoprotein.

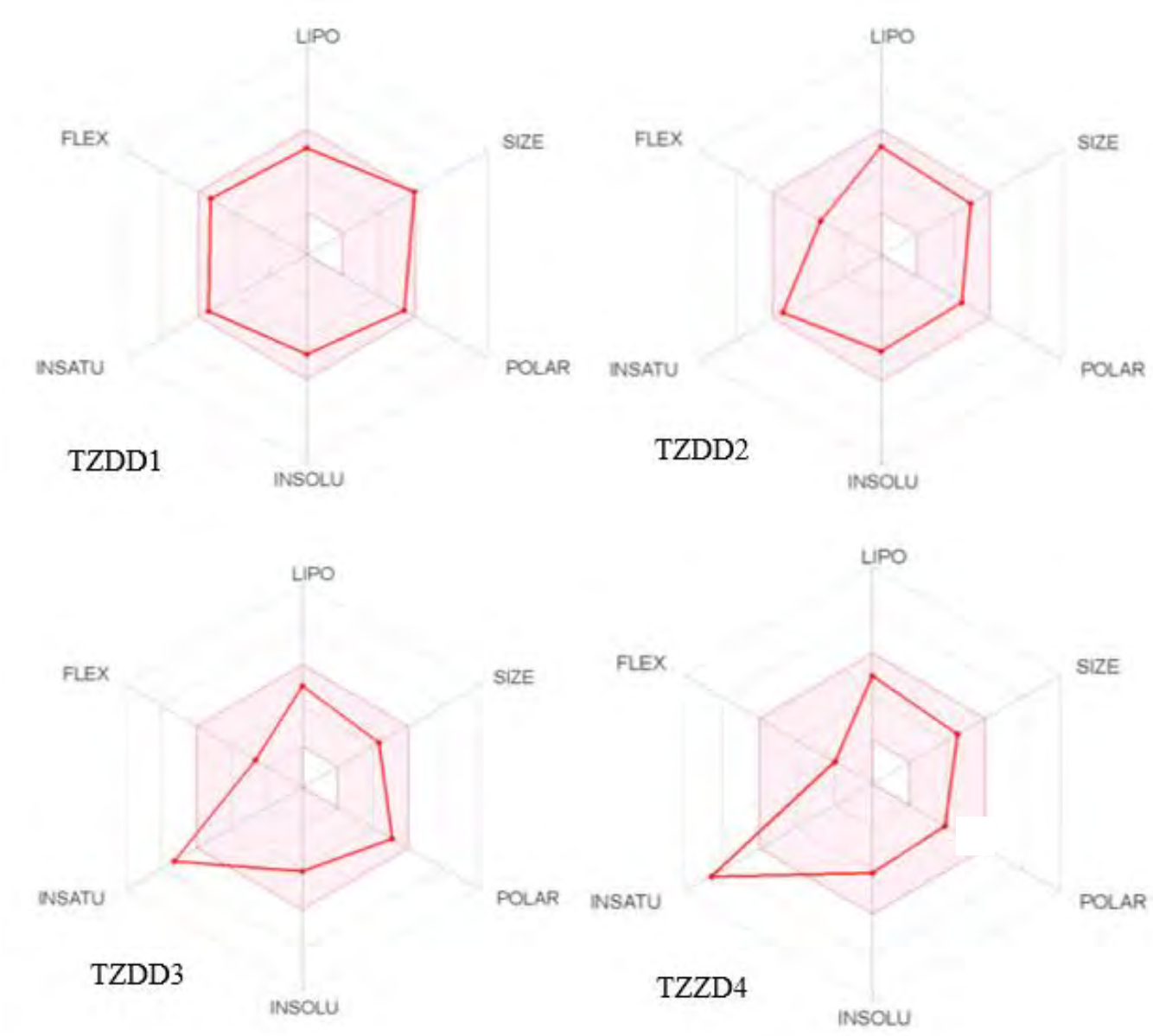

Figure 3.2: Detailed pharmacokinetic profiles of the TZD derivatives shown on the bioavailability radar. The coloured zone on the bioavailability radar is the suitable physicochemical space for oral bioavailability. LIPO(Liphophility): - 0.7 < XLOGP3 < +5.0; SIZE: 150 g/mol < MV < 500 g/mol; POLAR(Polarity): 20 Å² < TPSA < 130 Å²; INSOLU(Insolubility): 0 < Log S (ESOL) < 6; INSATU(Insaturation): 0.25 < Fraction Csp3 < 1; FLEX(Flexibility): 0 < Number of rotatable bonds < 9.

Table 3.1: ADME properties of the TZD derivatives; summarizing the Lipinski rule of 5 to establish the drug likeness, generated from SwissADME: *Sci. Rep.* (2017) 7:42717. (HBA – Hydrogen

Bond acceptors, HBD – Hydrogen Bond donors, NRB – number of rotatable bonds, TPSA – Topological Polar Surface Area, Bioavailability score of F > 10 % in rat)

Compound	MW(g/mol)	XlogP	HBA	HBD	NRB	TPSA	Bioavailability score
TZDD1	497.56	3.41	6	0	8	113.92 Å²	0.55
TZDD2	409.50	3.59	3	0	5	87.92 Å²	0.55
TZDD3	356.40	3.17	4	1	4	104.91 Å²	0.56
TZDD4	373.47	3.11	2	1	3	71.69 Å²	0.55

3.2. Antioxidant activity

3.2.1. Ferric Reducing Antioxidant Power Activity

Ferric Reducing Antioxidant Power assay (FRAP) is based on reduction of a colourless Fe^{3+}-TPTZ complex into intense blue Fe^{2+}-TPTZ once it interacts with a potential antioxidant. A darker/more intense color of Fe^{2+}-TPTZ will therefore indicate a great potential for antioxidant property of the tested compound. This can then be translated into absorbances (**Figure D1**), which were used to obtain the FRAP value. The FRAP value corelates to the antioxidant activity of the compounds, therefore, the higher the FRAP value, the higher is the antioxidant activity of the derivatives. Figure 3.3 shows the effect of TZD derivatives (10, 20, 30, 40 and 50 µg/mL) on FRAP activity. **TZDD2** and **TZDD4** showed a ferric reducing antioxidant power activity, with all concentrations showing significance by comparison to the control ($p < 0.05$). As anticipated, a significant ($p < 0.05$) free radical scavenging activity was observed with ascorbic acid. Of the four TZD derivatives investigated, **TZDD2** was most potent in ferric reducing antioxidant power activity assay as evidenced by a higher mass of Fe (II) formed across all the concentrations (**Figure 3.3**).

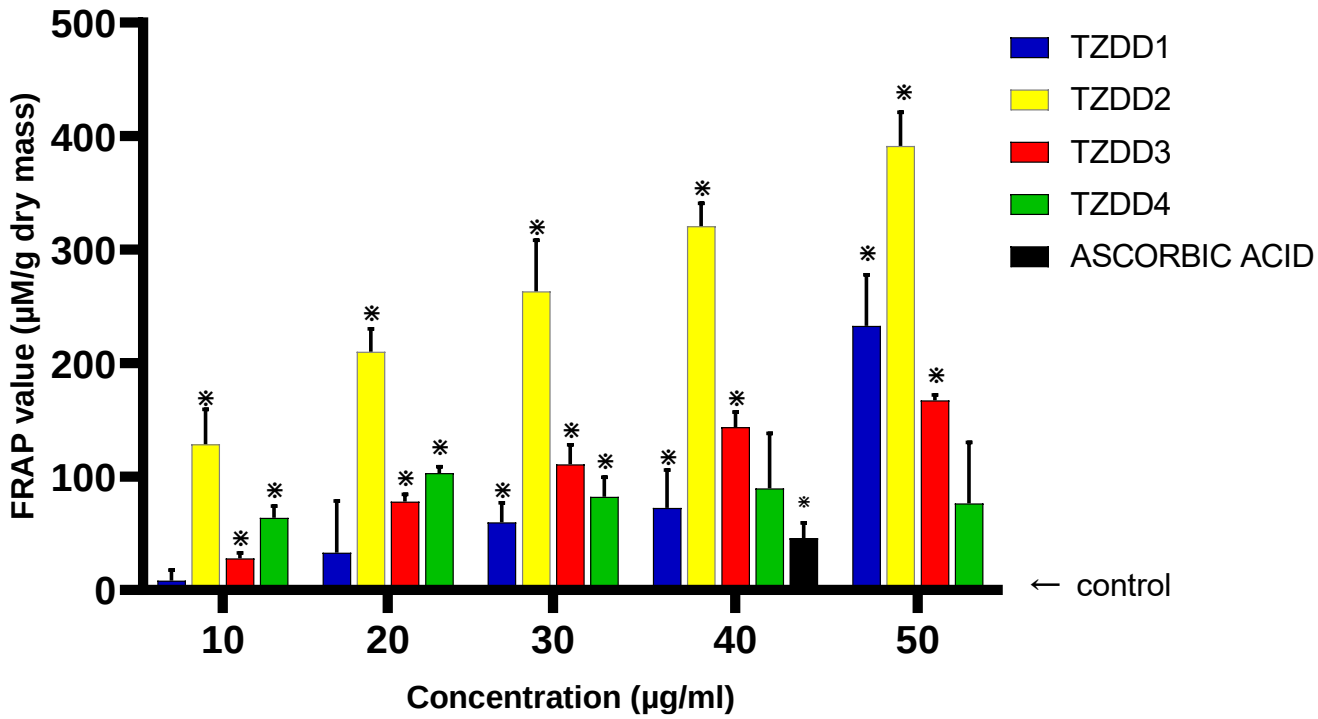

Figure 3.3: Ferric Reducing Antioxidant Power activity of the TZD-derivatives (10, 20, 30, 40 and 50 µg/mL). The results are represented in a clustered column. Data are presented as mean ± standard deviation values. The error bars correspond to the standard errors of the means and asterisks (*) indicate significant statistical difference relative to the control experiment according to ANOVA followed by Tukeys post hoc test (p value ≤ 0.05). The arrow from right pointing at the baseline at 0.0 represents the negative control which is defined to have zero percent inhibition for the purpose of data normalization.

3.2.2. Inhibition of DPPH Radical Scavenging Activity

This assay is based on the scavenging of the DPPH by the antioxidant. In its radical form, DPPH shows an active absorption band at λmax 515-517 nm, and after reaction of the antioxidant with DPPH, the DPPH accept the hydrogen donor. Therefore, the higher the antioxidant activity of the compound, the more DPPH will be scavenged. This translates to the antioxidant potential of the compounds and after analysis of the assay results, **Figure 3.4** shows the effect of TZD derivatives (10, 20, 30, 40, and 50 µg/mL) on DPPH radical scavenging activity. The **TZDD1** showed a free radical scavenging activity, with 30 µg/mL and above showing significance by comparison to the control. Similarly, **TZDD2**, **3** and **4** showed a free radical scavenging activity with 10 – 40 µg/mL showing significance ($p < 0.05$) by comparison

to the control. A significant ($p < 0.05$) free radical scavenging activity was observed with ascorbic acid in all concentrations. Of the four TZD derivatives investigated, **TZDD3** was most potent in free radical scavenging activity in DPPH assay as evidenced by smaller a smaller IC_{50} (**Table 3.2**).

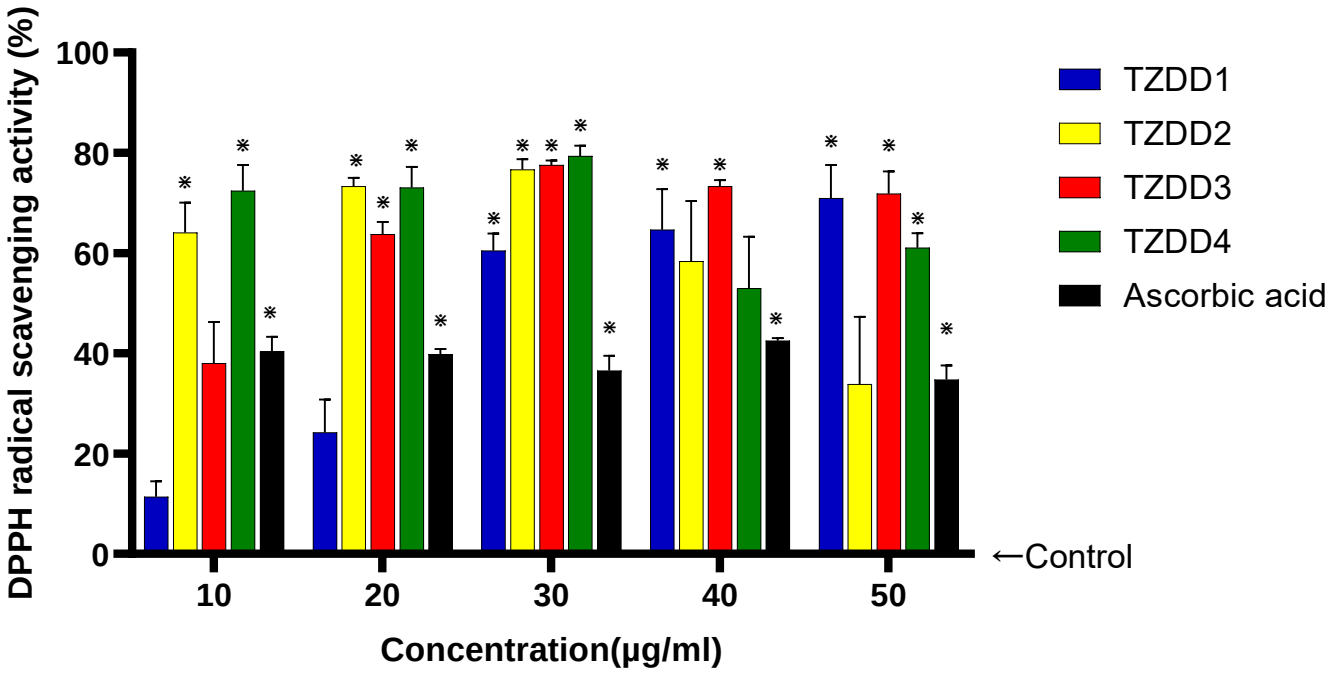

Figure 3.4: The DPPH radical scavenging activity of the TZD (10, 20, 30, 40 and 50 µg/mL). The results are represented in a clustered column. Data are presented as mean ± standard deviation values. The error bars correspond to the standard errors of the means and asterisks (*) indicate significant statistical difference relative to the control experiment according to ANOVA followed by Tukeys post hoc test (p value ≤ 0.05). The arrow from right pointing at the baseline at 0.0 represents the negative control which is defined to have zero percent inhibition for the purpose of data normalization

Table 3.2: Calculated IC50 values for the investigated TZD derivatives, from the DPPH radical scavenging activity.

Compounds	IC_{50} (µg/mL)
TZDD1	32.86 ±
TZDD2	44.92 ±
TZDD3	10.71 ±
TZDD4	71.55 ±
Ascorbic acid	28.57 ±

3.3. Antidiabetic Activity

These TZD derivatives were screened for their antidiabetic activity against enzymes, proteins and receptor proteins that are directly or indirectly involved in glucose homeostasis and/ development of diabetic complications.

3.3.1. Inhibition of α-Amylase Activity

α-amylase is the first enzyme in starch hydrolysis, and it hydrolyses dietary starch into maltose/oligosaccharides in the brush-border membrane. Inhibiting α-amylase therefore will delay starch hydrolysis and control blood glucose concentrations. In this assay to determine the inhibitory potential of the TZD derivatives, the following results were obtained. A high percentage inhibition indicates a high inhibitory potential. **Figure 3.5** shows the inhibitory properties of TZD derivatives (10, 20, 30, 40 and 50 µg/mL) on α – amylase activity. **TZDD3** showed a concentration dependent inhibitory activity, with 30 µg/mL and above showing a statistical significance ($p < 0.05$) by comparison to the control. Similarly, **TZDD1**, **2**, and **4** showed an inhibitory activity with all the concentrations showing significance ($p < 0.05$) by comparison to the control. A significant ($p < 0.05$) inhibitory activity was observed with acarbose in all concentrations. Of the four TZD derivatives investigated, **TZDD2** showed the best inhibitory activity in α – amylase inhibition assay with an IC_{50} value of 18.24 µg/mL (**Table 3.3**).

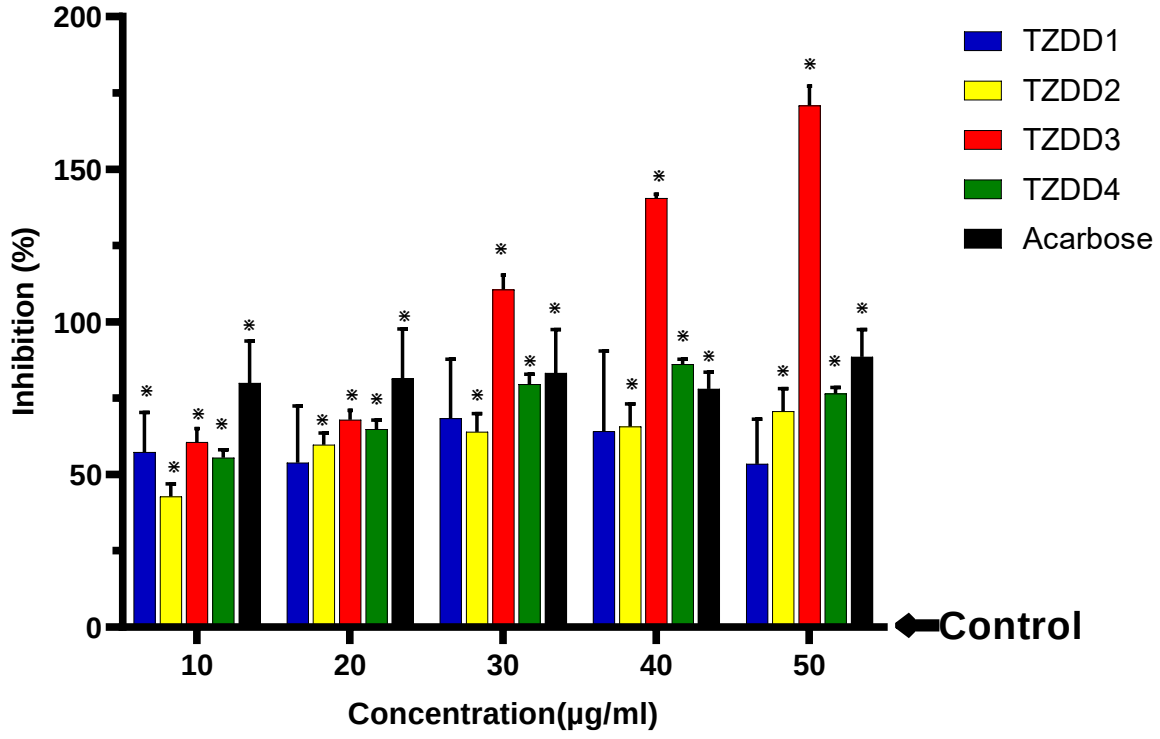

Figure 3.5: The inhibition of α-amylase activity by TZD-derivatives (10, 20, 30, 40 and 50 µg/mL). The results are represented in a clustered column. Data are presented as mean ± standard deviation values. The error bars correspond to the standard errors of the means and asterisks (*) indicate significant statistical difference relative to the control experiment according to ANOVA followed by Tukeys post hoc test (p value ≤ 0.05). The arrow from right pointing at the baseline at 0.0 represents the negative control which is defined to have zero percent inhibition for the purpose of data normalization

Table 3.3: Calculated IC_{50} values for the TZD derivatives investigated, from the α–amylase inhibitory activity assay.

Compounds	IC_{50} (µg/mL)
TZDD1	24.85 ±
TZDD2	18.24 ±
TZDD3	27.97 ±
TZDD4	24.06 ±
Acarbose	45.00 ±

3.3.2. α–Glucosidase Activity

α-glucosidase is the second enzyme involved in starch hydrolysis. α-glucosidase hydrolyses oligosaccharides to monosaccharides which can easily be absorbed and assimilated into the body. Inhibiting this enzyme provides potential control of postprandial blood glucose concentrations, hence controlling glycaemia. The higher the percentage inhibition, the higher is the potential for enzyme inhibitory activity by the derivatives. **Figure 3.6** shows the inhibitory properties of TZD derivatives (10, 20, 30, 40, and 50 µg/mL) on α–glucosidase activity. **TZDD3** showed a concentration dependent inhibitory activity. **TZDD1 - 4** showed an inhibitory activity with all concentrations showing a statistical significance ($p < 0.05$) by comparison to the control. A significant ($p < 0.05$) inhibitory activity was observed with acarbose in all concentrations. Of the four TZD derivatives investigated, **TZDD3** was more potent in inhibitory activity in this α–glucosidase inhibition assay as evidenced by smaller a smaller IC_{50} (**Table 3.4**). The kinetic analysis of α-glucosidase inhibition using Michaelis-Menten and the Lineweaver-burk plot kinetic analysis by **TZDD3** demonstrated a decrease in *Vmax* and *Km* in comparison with the uninhibited reaction (**Table 3.5**).

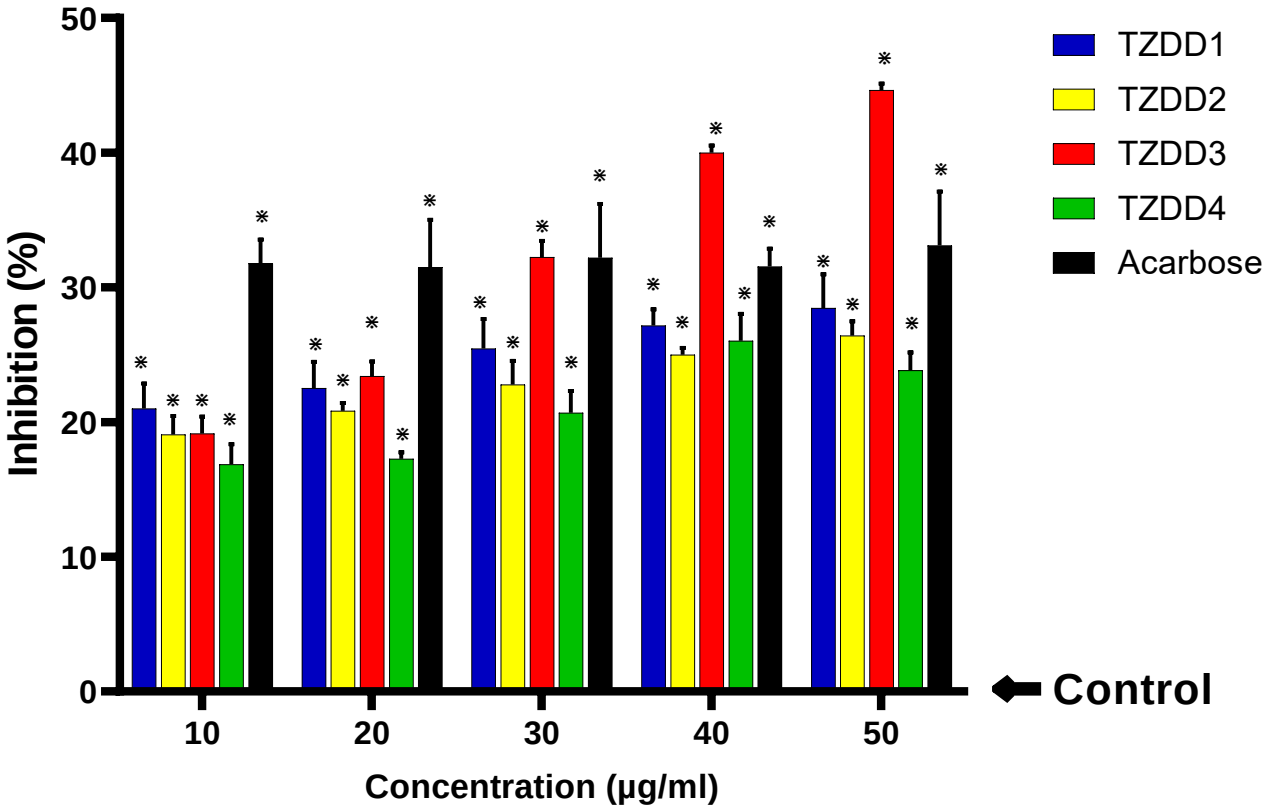

Figure 3.6: The inhibition of α-glucosidase activity by TZD-derivatives (10, 20, 30, 40 and 50 µg/mL). The results are represented in a clustered column. Data are presented as mean ± standard deviation values. The error bars correspond to the standard errors of the means and asterisks (*) indicate significant statistical difference relative to the control experiment according to ANOVA followed by Tukeys post hoc test (p value ≤ 0.05). The arrow from right pointing at the baseline at 0.0 represents the negative control which is defined to have zero percent inhibition for the purpose of data normalization

Table 34: Calculated IC_{50} values for the TZD derivatives investigated, from the α – glucosidase inhibitory activity assay.

Compounds	IC_{50} (µg/mL)
TZDD1	158.15 ±
TZDD2	174.39 ±
TZDD3	56.82 ±
TZDD4	698.92 ±
Acarbose	44.84 ±

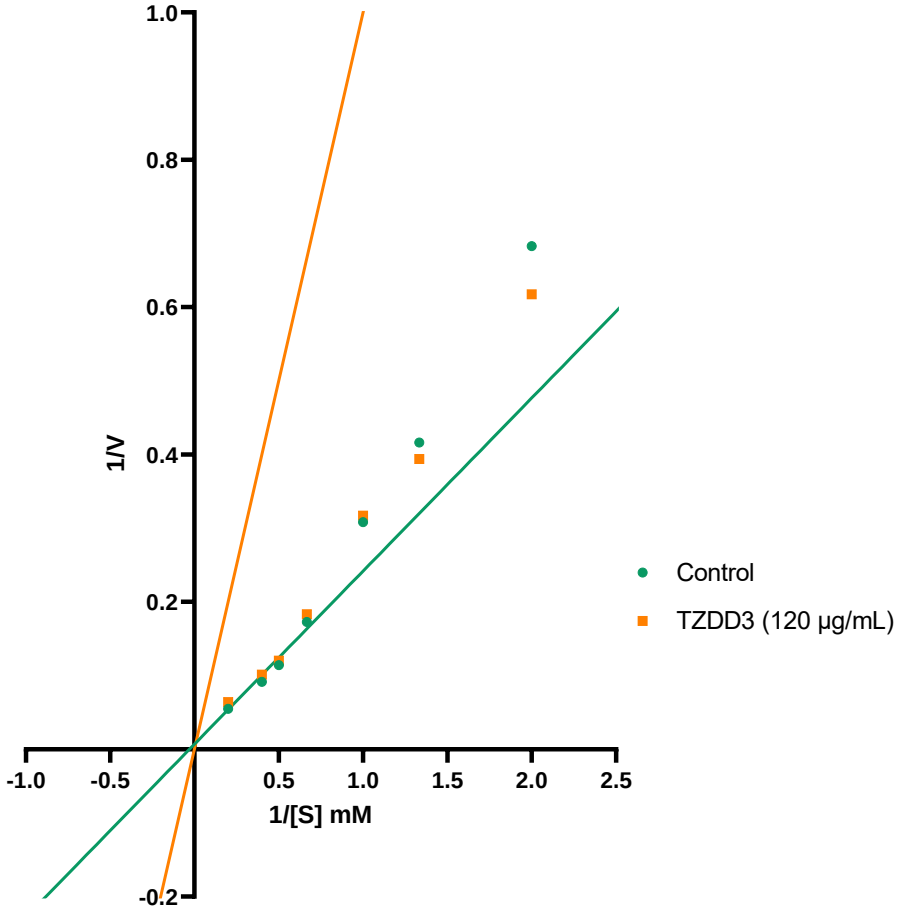

Figure 3.7: Lineweaver-burk plot of kinetic analysis of α-glucosidase inhibition by **TZDD3**.

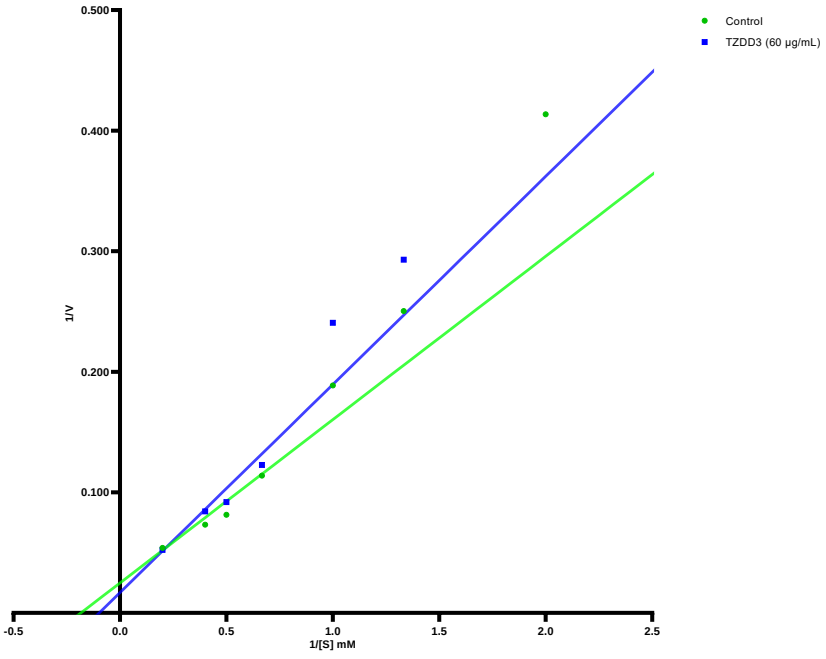

Figure 3.8: Lineweaver-burk plot of kinetic analysis of α-glucosidase inhibition by **TZDD3**.

Table 3.5: Michaelis-Menten results, control is the substrate only, and **TZDD**3 is added with substrate to determine effect on α–glucosidase inhibitory activity

	Control	TZDD3 (60 µg/mL)	TZDD3 (120 µg/mL)
Vmax	40.28	59.43	32.76
Km	5.457	10.26	4.556

3.3.3 Aldose Reductase Activity

Aldose reductase enzyme catalyses the conversion of glucose to galactitol in the polyol pathway, which is the alternate metabolism pathway for small quantities of non-phosphorylated glucose. The polyol pathway plays an important role in the aetiology of diabetic complications and therefore inhibiting aldose reductase, which is the first and rate-limiting and may provide potential treatment for long-term diabetic complications such as retinopathy. A high percentage inhibition indicates a high activity of the derivatives. **Figure 3.9** shows the effect of TZD derivatives (10, 20, 30, 40, and 50 µg/mL) on inhibition of aldose reductase activity. All the TZD derivatives showed an inhibitory activity with **TZDD1** showing a concentration dependent inhibitory activity. **TZDD1 - 4** showed an inhibitory activity with all concentrations showing significance ($p < 0.05$) by comparison to the control. As anticipated, a significant ($p < 0.05$) inhibitory activity was observed with quercetin in all concentrations. Of the four TZD derivatives investigated, **TZDD1** showed better inhibitory activity in this aldose reductase inhibition assay with an IC_{50} value of 27.54 µg/mL(**Table 3.6**).

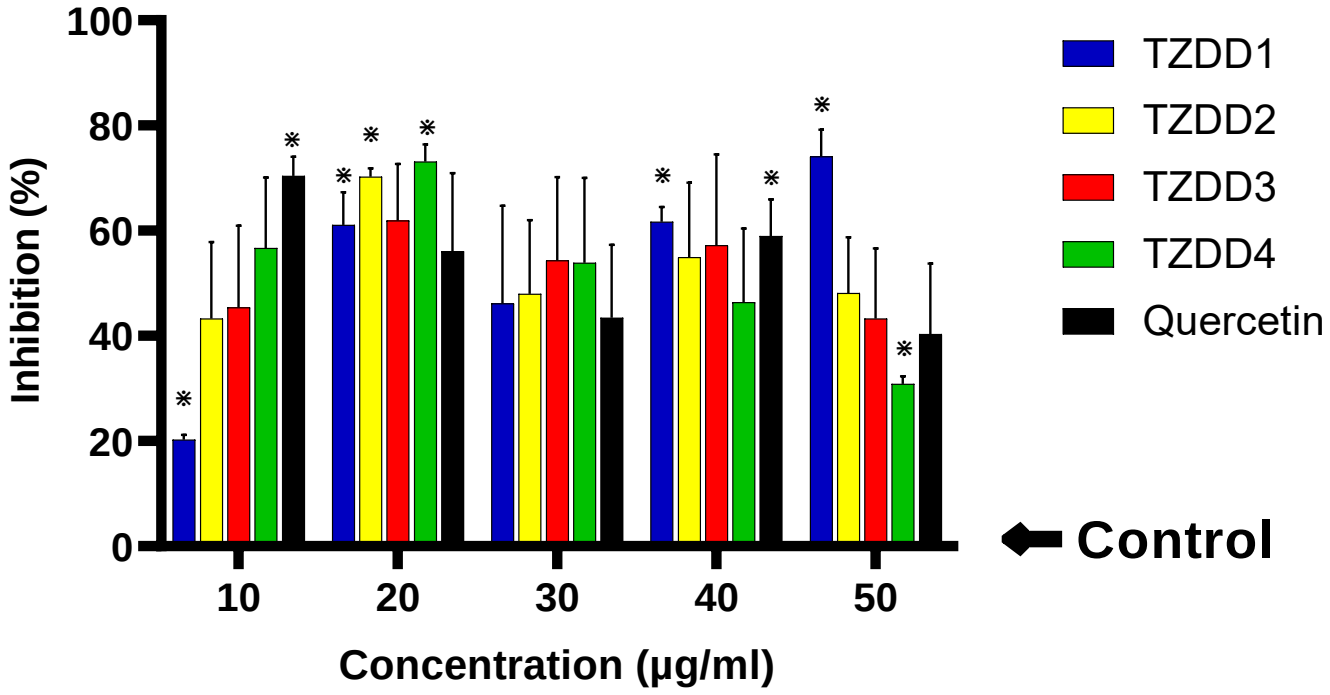

Figure 3.9: The inhibition of aldose reductase activity by TZD-derivatives (10, 20, 30, 40 and 50 µg/mL). The results are represented in a clustered column. Data are presented as mean ± standard deviation values. The error bars correspond to the standard errors of the means and asterisks (*) indicate significant statistical difference relative to the control experiment according to ANOVA followed by Tukeys post hoc test (p value ≤0.05). The arrow from right pointing at the baseline at 0.0 represents the negative control which is defined to have zero percent inhibition for the purpose of data normalization

Table 3.6: Calculated IC_{50} values for the TZD derivatives investigated, from the aldose reductase inhibitory activity assay.

Compounds	IC_{50} values (µg/mL)
TZDD1	27.54 ±
TZDD2	82.27 ±
TZDD3	57.43 ±
TZDD4	36.77 ±
Quercetin	36.71 ±

3.3.4 Protein Tyrosine Phosphatase 1B activity

Protein tyrosine phosphatase-1B catalyses the de-phosphorylation of activated insulin receptor, hence downregulating insulin signalling. Inhibiting this enzyme has potential to improve insulin signalling, and thus can be used as a potential treatment for glucose homeostasis in

T2DM. The high the percentage inhibition, the high the derivatives' activity. **Figure 3.10** shows the effect of TZD derivatives (10, 20, 30, 40, and 50 µg/mL) on inhibition of protein tyrosine phosphatase 1B activity. **TZDD1**, **2** & **4** showed weak inhibitory activity with **TZDD1** showing an inhibitory activity with all concentrations showing significance ($p < 0.05$) by comparison to the control. Of the four TZD derivatives investigated, **TZDD2** showed potent inhibitory activity in this protein tyrosine phosphatase inhibition assay with an IC_{50} value of 136.80 µg/mL (**Table 3.7**).

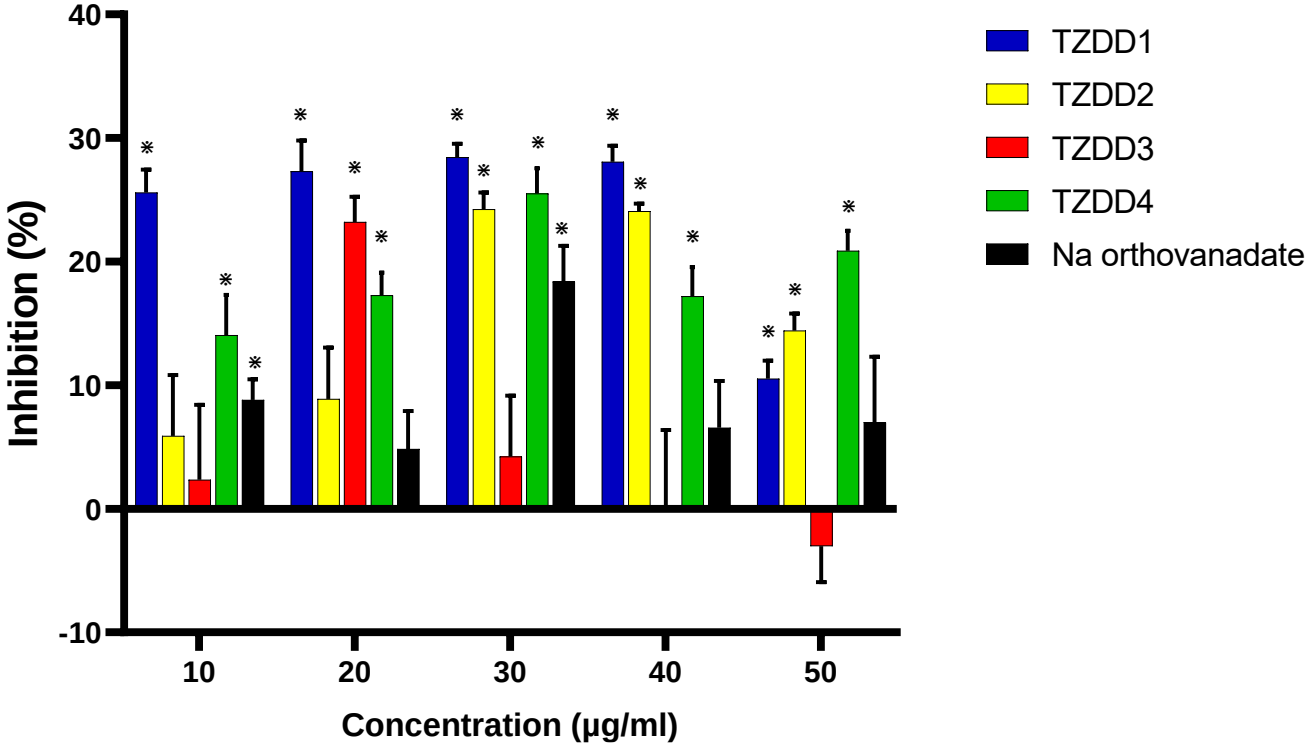

Figure 3.10: The inhibition of protein tyrosine phosphatase 1B activity by TZD-derivatives (10, 20, 30, 40 and 50 µg/mL). The results are represented in a clustered column. Data are presented as mean ± standard deviation values. The error bars correspond to the standard errors of the means and asterisks (*) indicate significant statistical difference relative to the control experiment according to ANOVA followed by Tukeys post hoc test (p value ≤0.05). The arrow from right pointing at the baseline at 0.0 represents the negative control which is defined to have zero percent inhibition for the purpose of data normalization

Table 3.7: Calculated IC_{50} values for the TZD derivatives investigated, from the protein tyrosine phosphatase 1B inhibitory activity assay.

Compounds	IC_{50} values (µg/mL)

TZDD1	unstable
TZDD2	136.80 ±
TZDD3	unstable
TZDD4	258.78 ±
Na Orthovanadate	Unstable

3.3.5 DPP4 Activity

DPP4 enzyme cleaves glucagon like peptide-1, an incretin hormone that plays an important role in glucose homeostasis and reduces its biological activity by shortening its half-life. Inhibiting DPP-4 therefore provides potential for glycaemic control. A high percentage inhibition indicates a high activity of the derivatives. **Figure 3.11** shows the effect of TZD derivatives (10, 20, 30, 40, and 50 µg/mL) on DPP4 inhibition activity. **TZDD2** showed a relatively higher activity, showing significance by comparison to the control in all the concentrations. **TZDD1**, and **3** showed a very weak inhibitory activity with no significance ($p < 0.05$) by comparison to the control. A significant ($p < 0.05$) DPP4 inhibitory activity was observed with Sitagliptin in all concentrations. Of the four TZD derivatives investigated, **TZDD2** was more potent in DPP4 activity in this DPP4 assay as evidenced by smaller a smaller IC_{50} (**Table 3.8**).

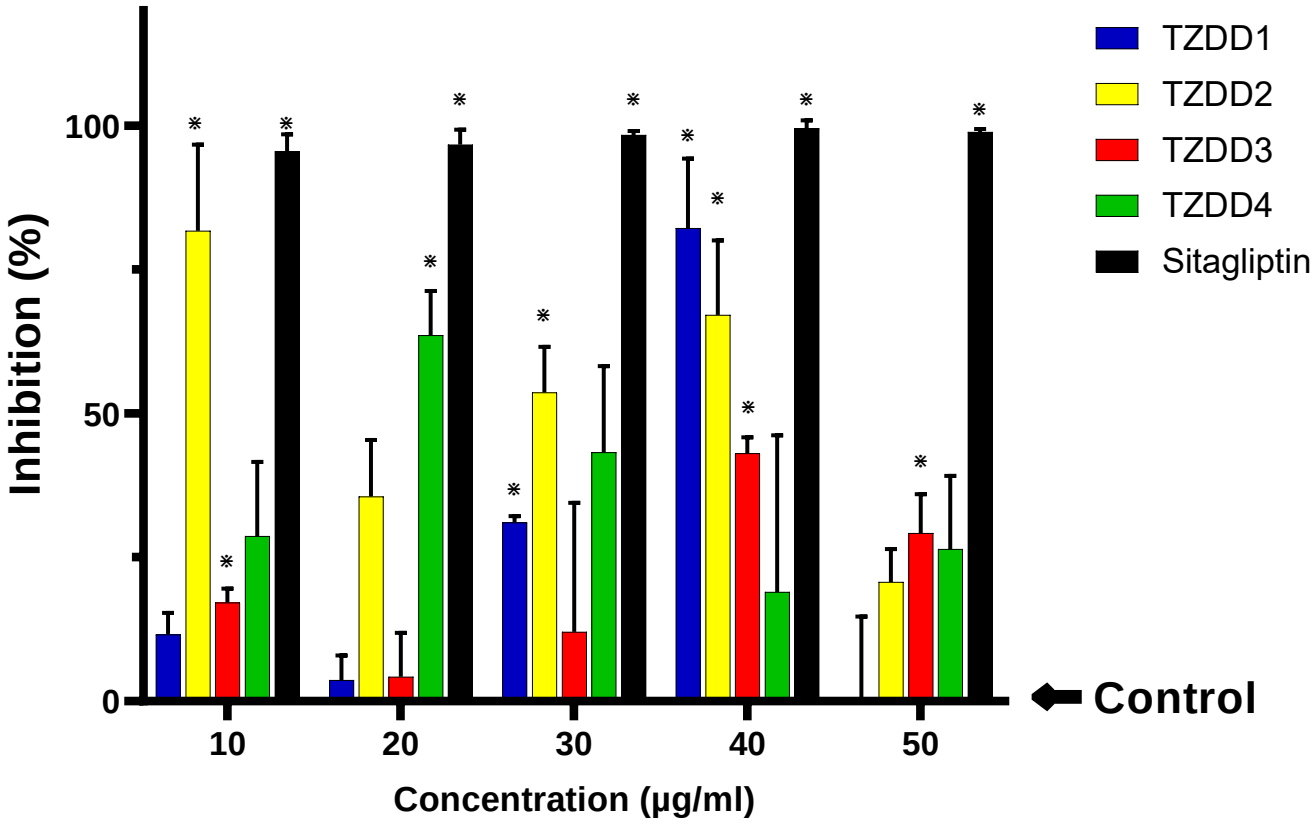

Figure 3.11: The inhibition of DPP4 activity by TZD-derivatives (10, 20, 30, 40 and 50 µg/mL). The results are represented in a clustered column. Data are presented as mean ± standard deviation values. The error bars correspond to the standard errors of the means and asterisks (*) indicate significant statistical difference relative to the control experiment according to ANOVA followed by Tukeys post hoc test (p value ≤0.05). The arrow from right pointing at the baseline at 0.0 represents the negative control which is defined to have zero percent inhibition for the purpose of data normalization

Table 3.8: Calculated IC_{50} values for the TZD derivatives investigated, from the DPP4 inhibitory activity assay.

Compounds	IC_{50} values (µg/mL)
TZDD1	73.04 ±
TZDD2	31.93 ±
TZDD3	75.82 ±
TZDD4	71.83 ±
Sitagliptin	3.31 ±

3.3.6. *In Silico* Determination of the PPAR-γ Activation

PPAR-γ is a master regulator of adipogenesis, which binds compounds such as synthetic antidiabetic thiazolidinediones that activates the trans activating function of PPAR-γ causing a powerful adipogenic response. Binding and activation of PPAR-γ by these TZD derivatives would indicate that the mode of action of TZDs have been retained. To determine this, the effect of TZDs derivatives of PPAR-γ was studied virtually through investigating the binding energies, root-mean square deviations (RMSD) values and interactions. **Figure C1-C4,** attached in the appendix show the raw data generated from docking of the TZD derivatives in autodock tools. **Figure 3.12** shows the conformations between the TZD derivatives and PPAR-γ protein. These conformations have been detailed and elaborated as shown in **figures C5(ii)**; **C5(iii)**; **C7(ii)**; **C7(iii)**; **C9(ii)**; **C9(iii)**; **C11(ii)**; **C11(iii)**; **C13(ii)**; **and C13(iii)** included in the appendix. These derivatives formed similar interactions with the PPAR-γ as the standard PPAR-γ activator used, rosiglitazone, with **TZDD2** and **TZDD4** having the most similar interactions (**Table 3.10**). The molecular interactions show hydrogen bonding, hydrophobic interactions, д- stacking interactions (**Figure 3.12**). The derivatives also showed a lower RMSD values than rosiglitazone (**Table 3.9**). **TZDD4** shows the most similar interaction to the standard (rosiglitazone) used as seen with its lowest binding energy, estimated inhibition constant, and conformation (**Figure 3.12**, **Table 3.9** and **3.10**).

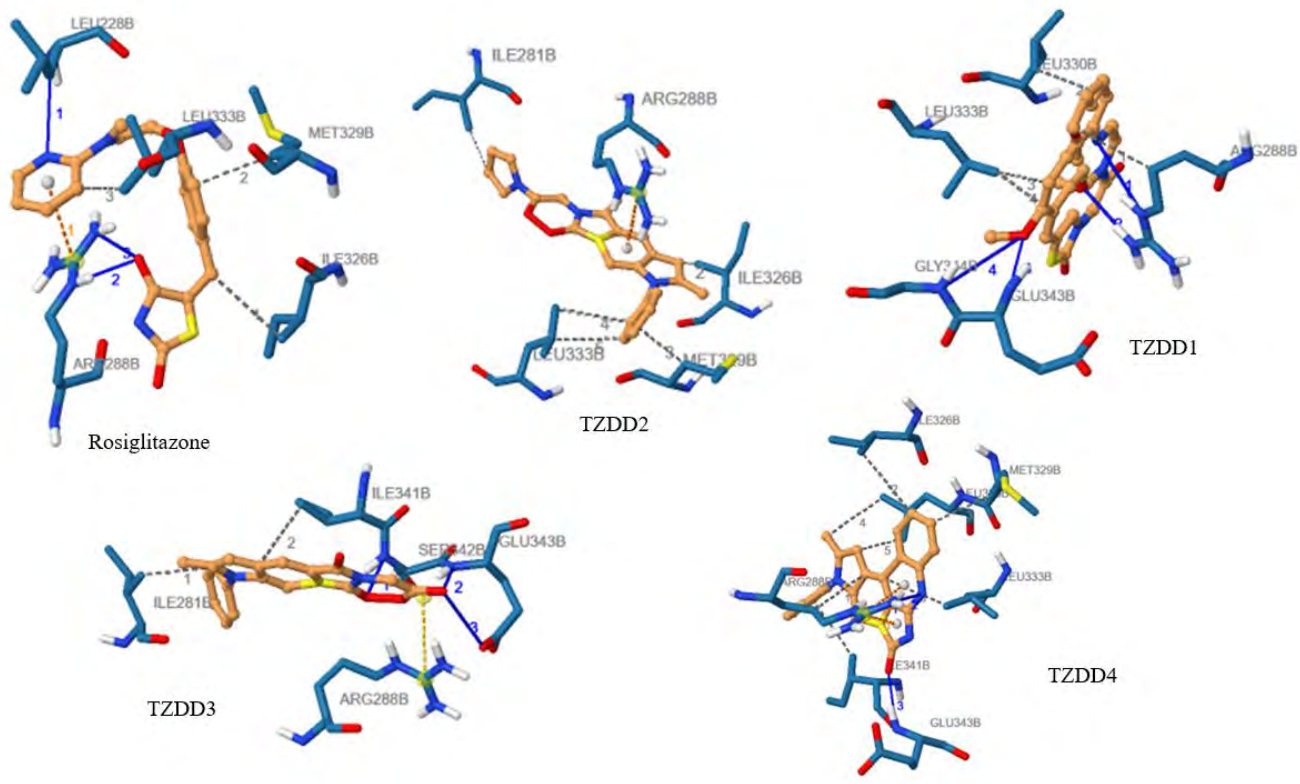

Figure 3.12: Conformations of the TZD derivatives with the PPAR-γ protein showing the different types of interactions.

Table 3.9: Low binding energies (LBE), estimated inhibition constants (EIC) and root-mean square deviations (RMSD) values of the TZD derivatives from the docking studies, temperature at 298.15K.

Compound	LBE (kcal/mol)	EIC, ki (nM)	RMSD values
TZDD1	-12.02	1.55	21.67A
TZDD2	-10.40	23.77	25.519A
TZDD3	-8.84	332.32	23.664A
TZDD4	-9.91	54.39	24.199A
Rosiglitazone	-8.63	472.78	26.194A

Table 3.10 Interaction between the TZD derivatives with the PPAR-γ protein through hydrogen bonds formed between the amino acids of the B terminus of the PPAR-γ and these

derivatives. Y is for yes, and N for no. The interactions are from the conformations of the highest ranked clusters.

Compound	LEU128	LEU333	MET329	ILE326	ARG288	ILE281	GLU343
TZDD1	N	Y	N	N	N	N	Y
TZDD2	N	Y	Y	Y	Y	Y	N
TZDD3	N	N	N	N	Y	Y	Y
TZDD4	N	Y	Y	Y	Y	N	Y
Rosiglitazone	Y	Y	Y	Y	Y	Y	N

3.4. Anti-Alzheimer's Disease Activity

3.4.1. Acetylcholinesterase Activity

Acetylcholinesterase enzyme is responsible for hydrolysing acetylcholine, a naturally occurring neurotransmitter and neuromodulator, whose deficiency is linked to the pathogenesis of AD. Inhibiting this enzyme may prolong the lifespan of acetylcholine hence controlling AD. A high percentage inhibition indicates a high activity of the derivatives. Figure 3.13 shows the inhibitory effect of TZD derivatives (10, 20, 30, 40, and 50 µg/mL) on acetylcholinesterase activity. All the four derivatives show an inhibitory effect ≥ 25 % with **TZDD1** showing more potency as evidenced by the smaller IC_{50} (**Table 3.11**). The standard (Donepezil) in this assay showed a significant ($p < 0.05$) acetylcholinesterase inhibitory activity in all concentrations. The kinetic studies of **TZDD3** showed a higher *Km* and *Vmax* than the control (**Figure 3.14**)

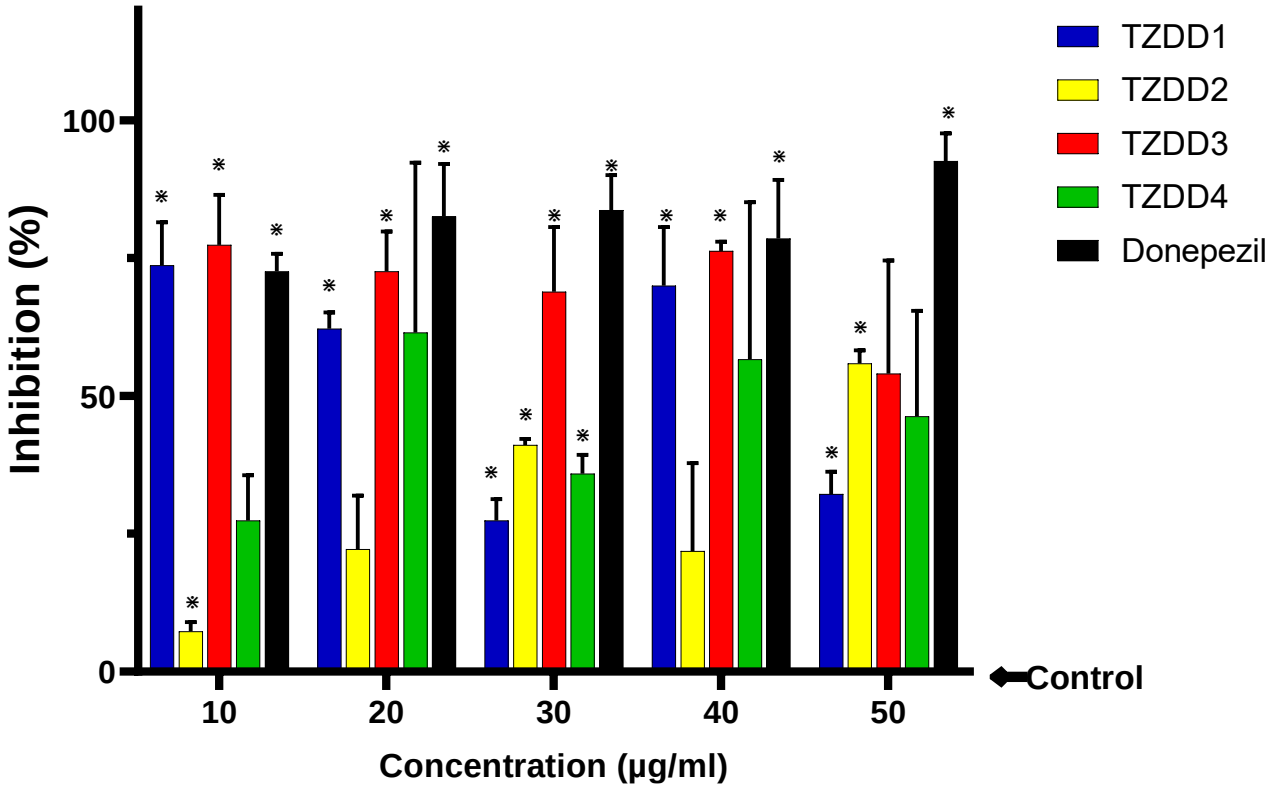

Figure 3.13: The inhibition of acetylcholinesterase activity by TZD-derivatives (10, 20, 30, 40 and 50 µg/mL). The results are represented in a clustered column. Data are presented as mean ± standard deviation values. The error bars correspond to the standard errors of the means and asterisks (*) indicate significant statistical difference relative to the control experiment according to ANOVA followed by Tukeys post hoc test (p value ≤ 0.05). The arrow from right pointing at the baseline at 0.0 represents the negative control which is defined to have zero percent inhibition for the purpose of data normalization

Table 3.11 Calculated IC50 values for the TZD derivatives investigated, in the acetylcholinesterase inhibitory activity assay.

Compounds	IC_{50} (µg/mL)
TZDD1	34.14 ±
TZDD2	50.98 ±
TZDD3	76.21 ±
TZDD4	43.48 ±
Donepezil	11.68 ±

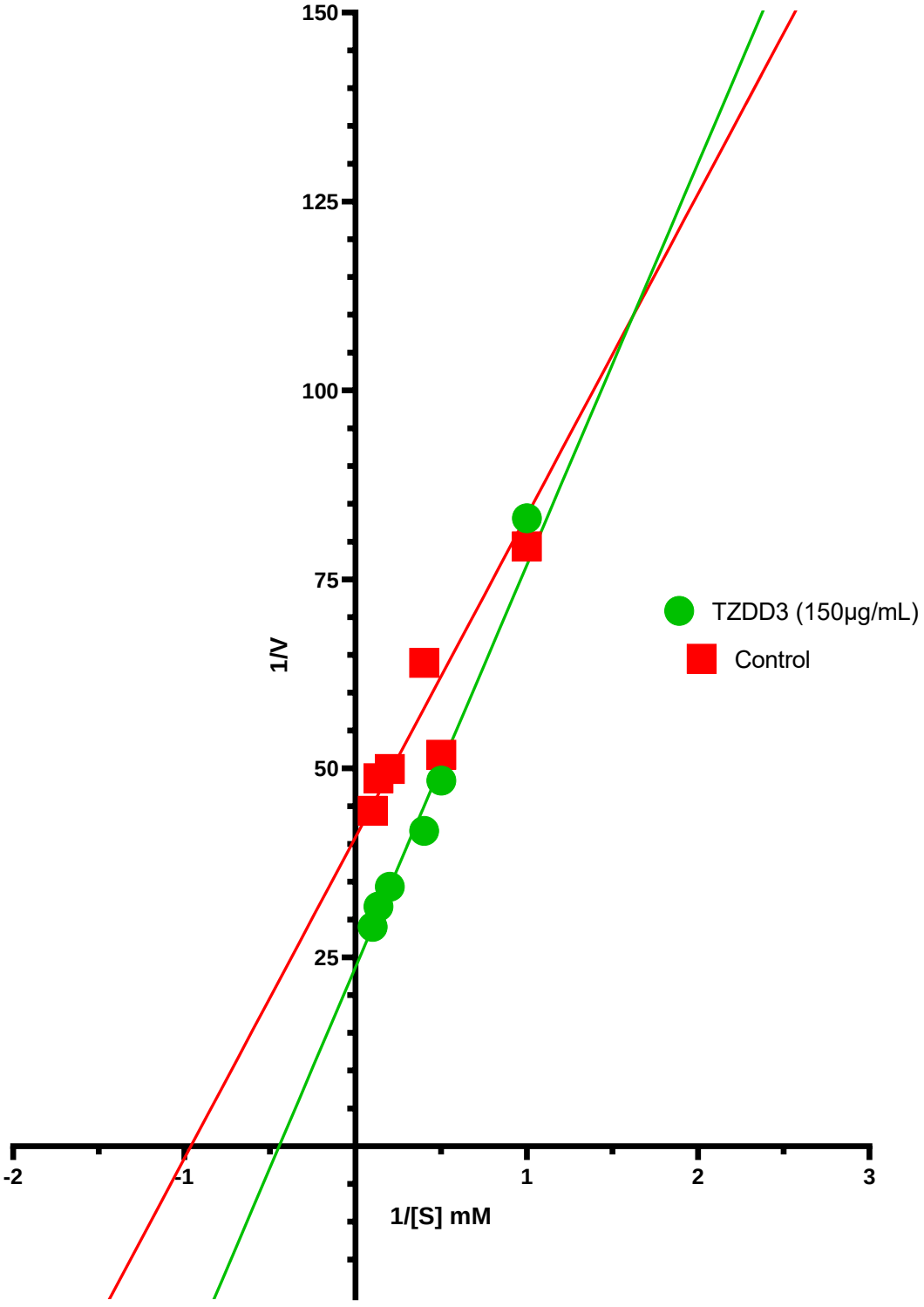

Figure 3.14: Lineweaver-burk plot of kinetic analysis of acetylcholinesterase inhibition by **TZDD3** at 150 µg/mL.

3.4.2. Matrix Metalloproteinase-1 (MMP-1) Inhibition Assay

MMP-1 enzyme is responsible for altered extracellular matrix remodelling which is associated with vascular complications in type 1 diabetes. Inhibiting this enzyme may control these diabetic complications. A high percentage inhibition indicates a high activity of the TZD derivatives. Figure 3.15 shows the effect of TZD derivatives (10, 20, 30, 40, and 50 µg/mL) on MMP-1 activity. **TZDD1** showed an inverse inhibitory activity, for 10 and 20 µg/mL and a slight inhibition for concentrations 30 – 50 µg/mL showing no significance ($p < 0.05$) by comparison to the control. **TZDD1** emerged more potent with the lowest IC_{50} value (Table 3.12). Similarly, **TZDD4** showed an inverse in MMP-1 inhibitory activity with all the concentrations showing no significance ($p < 0.05$) by comparison to the control. A significant ($p < 0.05$) MMP-1 inhibitory activity was observed with ilomastat in all concentrations.

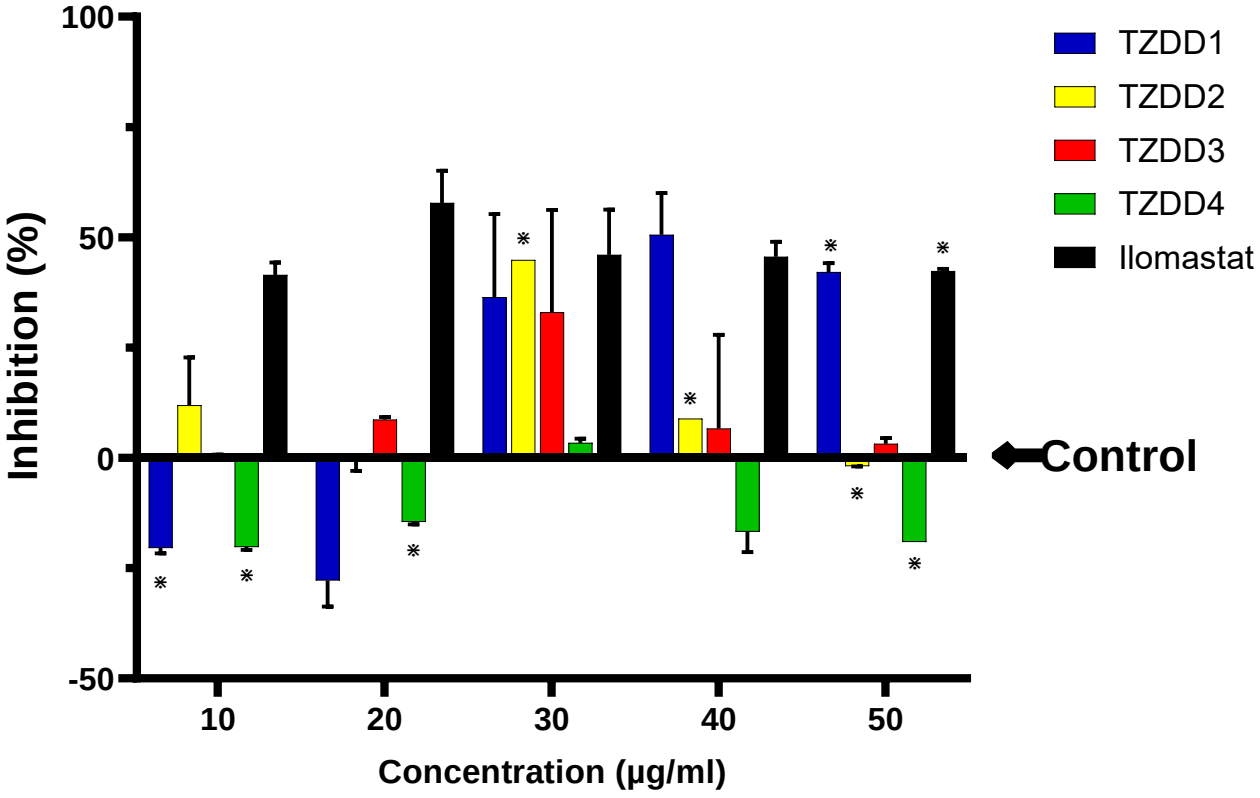

Figure 3.15: The inhibition of MMP-1 activity by TZD-derivatives (10, 20, 30, 40 and 50 µg/mL). The results are represented in a clustered column. Data are presented as mean ± standard deviation values. The error bars correspond to the standard errors of the means and asterisks (*) indicate significant statistical difference relative to the control experiment according to ANOVA followed by Tukeys post hoc test (p value ≤ 0.05). The arrow from right pointing at the baseline at 0.0 represents

the negative control which is defined to have zero percent inhibition for the purpose of data normalization

Table 3.12: Calculated IC_{50} values for the TZD derivatives investigated, in the MMP-1 inhibitory activity assay.

Compounds	IC_{50} (µg/mL)
TZDD1	51.19 ±
TZDD2	531.61 ±
TZDD3	271.32 ±
TZDD4	unstable
Ilomastat	43.33 ±

3.4.3. β-Amyloid Aggregation Inhibition Assay

β-amyloid accumulation is a hallmark in AD physiopathology. Therefore, inhibiting the accumulation of these plaques provides a potential treatment for AD. A high percentage inhibition indicates a high activity by the derivatives. **Figure 3.16** shows the effect of TZD derivatives (10, 20, 30, 40, and 50 µg/mL) on the β-amyloid aggregation. **TZDD1** and **3** showed an inhibitory activity with all concentrations showing significance ($p < 0.05$) by comparison to the control. Of the four TZD derivatives investigated, **TZDD2** and **4** showed no significance in β-amyloid aggregation activity assay as evidenced by a smaller inhibition activity. A significant ($p < 0.05$) β-amyloid aggregation inhibitory activity was observed with rifampicin at concentration 50 µg/mL.

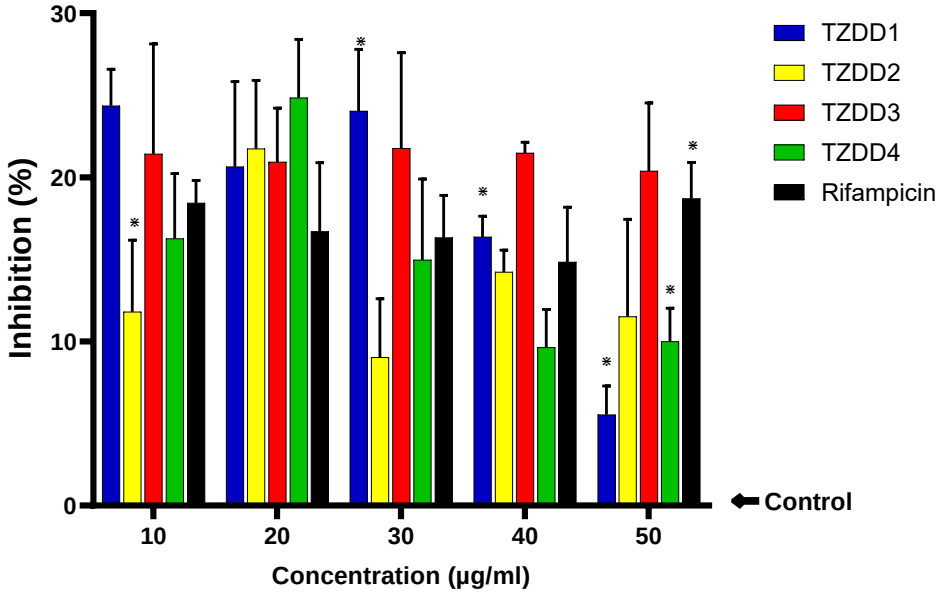

Figure 3.16: The inhibition of β-amyloid aggregation activity by TZD-derivatives (10, 20, 30, 40 and 50 µg/mL). The results are represented in a clustered column. Data are presented as mean ± standard deviation values. The error bars correspond to the standard errors of the means and asterisks (*) indicate significant statistical difference relative to the control experiment according to ANOVA followed by Tukeys post hoc test (p value ≤0.05). The arrow from right pointing at the baseline at 0.0 represents the negative control which is defined to have zero percent inhibition for the purpose of data normalization

Table 3.13: Calculated IC_{50} values for the TZD derivatives investigated, in the β-amyloid aggregation inhibitory activity assay.

Compounds	IC_{50} (µg/mL)
TZDD1	1740.52 ±
TZDD2	283.95 ±
TZDD3	134.92 ±
TZDD4	671.61 ±
Rifampicin	177.15 ±

CHAPTER FOUR: DISCUSSION

Drug discovery and development is a time and resource-consuming processes through which many molecular structures are investigated according to multiple parameters to guide the selection of robust chemical compounds to synthesise, test and promote along the discovery pipeline. The final goal is to identify those compounds with the best chance to become an effective medicine for the patients. The molecules must exhibit high biological activity together with low toxicity. Access to and concentration at the therapeutic target in the body are equally crucial [177]. Drug bioavailability is referred to as the fraction of the administered dose that enters the systemic circulation [208] . Only the intravenous administered dose achieves a 100% bioavailability due to no requirement for absorption into the blood stream. While orally administered doses encounter absorption challenges either due to water solubility, lipophilicity, or drug likeness because of their physicochemical properties. The design of successful formulations for effective therapy, requires considering these challenges including therapeutic requirements and patient compliance [209]. In this regard therefore, we conducted the bioavailability profiling to establish the pharmacokinetics of TZD derivatives investigated in this study. Initially, these compounds were designed and synthesised for their potential antimalarial activity against the *Plasmodium falciparum* parasite, a causative agent for malaria.

The TZD derivatives investigated in this study are predicted to be highly absorbed by the gastrointestinal tract according to the white region of the BOILED-Egg but are predicted not to permeate the blood-brain barrier according to the yolk of the BOILED-Egg (**Figure 3.1**). This would make their oral formulations (oral bioavailability predicted, **Figure 3.2**) a lot easier. However, further studies such as *in vitro* experiments would be necessary to establish their absorption when mixed with various excipients for oral dose formulations for effective therapeutic effects. It would, however, pose a challenge to deliver these compounds into the brain and hence would need drug delivery systems technologies to successfully access the brain bypassing the BBB for treating diseases such as Alzheimer's disease.

The brain remains highly inaccessible with more than 98% of small molecule drugs unable to cross the BBB [210 - 212]. Therefore, it is imperative that these molecules be studied further and incorporating the new available drug delivery systems to enable them effectively cross the BBB but protecting their therapeutic activity once in the brain [212]. The pathogenesis of AD involves

chronic neuro-inflammation, the progressive deposition of insoluble amyloid-beta or tau aggregates, and neural degeneration. New drugs that both attack these multiple sites in AD, and which have been coupled with BBB drug delivery technology can lead to new and effective treatments of this serious disorder [211].

Early prediction and analysis of pharmacokinetic parameters of drug molecules ensures that bioavailability challenges are addressed through structural optimization and formulations for optimal drug design. This reduces rates of failures of the drugs during clinical trials [213]. These predictions of bioavailability (**Figure 3.1 and 3.2**, **Table 3.1**) can enhance optimisation of drug design and development. For successful BBB permeability, drug molecules need to have a MW ≤ 400 Da, the polar functional groups on the drug need to form ≤ 7 hydrogen bonds and the polar surface area (PSA) of the drug should not exceeds 80 $Å^2$, which corresponds to a MW of 400 Da. BBB transfer decreases exponentially when the PSA increases from 52 $Å^2$, which corresponds to a MW of 300 Da, to a PSA of 105 $Å^2$, which corresponds to a MW of 450 Da [211]. Therefore, some of the derivatives investigated can be modified into small molecules with the aim of reducing the TPSA to less than 80 $Å^2$ in order to obtain BBB permeability. Currently, **TZDD1** has a TPSA of 113.92 $Å^2$, **TZDD2** of 87.92 $Å^2$, **TZDD3** of 104.91 $Å^2$, and **TZDD4** of 71.69 $Å^2$. The first and the only small molecules approved for AD are the acetylcholinesterase inhibitors, and these drugs have MW ranging from 179 to 380 Da, and form ≤ 5 hydrogen bonds with solvent water [211]. These include donepezil, rivastigmine, and galantamine whose symptomatic efficacy is attained through their augmentation of acetylcholine-mediated neuron-to-neuron transmission as we will discuss at a later stage. The predicted high solubility of the investigated derivatives indicates that the challenge of drug absorption in the intestines will be minimal and hence able to exert therapeutic effect at this therapeutic target site.

In humans, α–amylase is present in both salivary and pancreatic secretions. This enzyme is responsible for cleaving large malto-oligosaccharides to maltose, which then is a substrate for α–glucosidase in the intestines [214]. *α*-Glucosidase is a membrane-bound enzyme in the epithelium of the small intestine that hydrolyses the cleavage of glucose from disaccharides and oligosaccharides and thereby facilitates their absorption [204]. Inhibitors of α-amylase and α-glucosidase delay the breaking down of carbohydrate in the small intestine and diminish the postprandial blood glucose excursion in a diabetic person [215]. One of the strategies and methods adopted to cure diabetes mellitus involves the inhibition of carbohydrate digesting

enzymes such as α-amylase and α-glucosidase in the gastrointestinal glucose absorption which lowers postprandial glucose concentration [216].

In this study, the effect of TZD derivatives on the activities of α-amylase and α-glucosidase was evaluated. The derivatives showed high potent inhibition of α-amylase activity, showing ≥ 50 % in all concentrations (10, 20, 30, 40 and 50 μg/mL) with **TZDD3** exhibiting a dose dependent activity. These observations may suggest that clinically, low doses would be required which agrees with previous reports indicating that excessive inhibition of pancreatic α-amylase could result in the excessive bacterial fermentation of undigested carbohydrates in the colon and therefore mild α-amylase inhibition activity is desirable [217]. Interestingly, α-glucosidase inhibition activity was much lower, with all the four derivatives exhibiting an inhibition between 15 -50 %. However, **TZDD3** again emerged as the most potent compound with an IC_{50} value close to that of acarbose in this study. Acarbose is structurally similar to natural oligosaccharides but has 10^4 to 10^5 times higher affinity for alpha glucosidase which makes it a competitive inhibitor. Similarly, TZDD3 exhibited a high enzyme affinity (Km = 4.556), which suggest that its mode of inhibition of the alpha glucosidase enzyme is competitive.

Lineweaver-Burk plot also showed that **TZDD3** inhibited α-glucosidase competitively. This suggests that the active functional group in the derivative compete with the substrate for binding to the active site of the enzyme which prevents the breaking down of oligosaccharides to disaccharides [218, 219]. Competitive inhibition may result in an increase in the apparent affinity ($Km^{app} < Km$), which means that *Km* value appears to decrease when the inhibitor binds favourably to the enzyme–substrate complex.

From available literature, several studies have identified hydrogen bonds and hydrophobic interactions with the amino acid residues of α-amylase as the mode of inhibition of compounds which have shown activity against α-amylase [220, 221]. Presence of lipophilic amino acid residues Leu162, Leu165 and Ile235 in the active site of α-amylase could be essential in the formation of the hydrophobic interactions with inhibitor compounds [222]. Furthermore, the existence of functional groups such as the methoxy group, carboxylic acid group and the aliphatic CH groups may be crucial for binding [222]. Another important note is the starch binding site, which is located on a loop between A and C domains and binds the polysaccharide chain extending from the active site. The plasticity of the active-site groove in the proximity to the catalytic centre might be substantial for both formations of the productive substrate-enzyme

complex as well as for the release of the product from the +1 to +n subsites [223, 224]. It can be postulated that the lipophilic tail and the methyl groups present in the derivative forms hydrophobic interactions with the amino acid residues of the binding site in α-amylase through д-stacking. The ketone group persevered on 4C may be involved in forming hydrogen bonds with the amino acid residues further making the enzyme-inhibitor complex stronger, hence the higher inhibition activity.

The inhibitory activity exhibited in the α-glucosidase assay could be that the derivatives, especially **TZDD3** are interacting with the orthosteric binding site (OBS) of the enzyme. Acarbose, a recognized competitive inhibitor of α-glucosidase, showed that acarbose was surrounded by residues of His111, Asp214, Glu276, Asp343, and His348 in the OBS of α-glucosidase, supporting the results of many previous studies [225, 226]. In a study by Chen *et al*., Glu426 and Lys155 were found to be particularly crucial for formation of key hydrogen bonds between the ligand and receptor, and there were π-π stack interaction between the aromatic ring A of cyanidin and residue Phe311 of α-glucosidase, which might play a critical role in the binding [227]. Additionally, a Pi-anion electrostatic interaction and a Pi-alkyl hydrophobic interaction were found between the skeleton of cyanidin and Asp232, Ile416 of α-glucosidase, respectively [227, 228]. Similarly, we can postulate that the investigated TZD derivatives are forming interactions with the α-glucosidase residues in the binding site through hydrogen bonds, π-π stack interaction between the aromatic tail rings, aliphatic chains on the side of the ring with the Phe311 residue of the enzyme.

One disadvantage of competitive inhibition is that it is affected by substrate concentrations. Therefore, with higher carbohydrate intake, higher concentrations of the drug will be required to achieve the same effect [229]. Researchers have described the following characteristics of α-glucosidase inhibitors: (1) sugar (substrate)- mimic structures, (2) potency to establish ionic bonds with nucleophilic catalysing residues, (3) transition state-like structures, (4) potency to construct hydrogen bonds with catalytic acid residues, (5) potency to construct ionic and hydrophobic interactions at sites other than the active site, and (6) potency to construct covalent bond with enzymes through an epoxy or aziridine group [229]. Further studies (*in silico*) should be directed towards confirming the observed mode of inhibition using other parameters.

The digestion and absorption of glucose trigger secretion of hormones such as GLP-1 and GIP which stimulate glucose dependent insulin secretion. However, GLP-1 and GIP are enzymatically inactivated by DPP-4. DPP-4 is a membrane glycoprotein with serine

exopeptidase activity that cleaves X-proline dipeptides from the N-terminus of these polypeptides. Inhibitors of DPP4 block the degradation of glucose-dependent insulinotropic polypeptide and glucagon-like peptide-1 by DPP-4 and have emerged as oral anti-diabetic agents [230]. Sitagliptin which is a selective DPP-4 inhibitor prolongs the activity of naturally occurring incretin hormones; GLP-1 and GIP which are metabolized by the activity of DPP-4, resulting in enhanced glucose-dependent insulin secretion from the pancreas and decreased hepatic glucose production [231]. The DPP-4 inhibitors bind to the DPP-4-GLP-1 interacting site and hence these inhibitors may be considered as protein-protein interaction (PPI) inhibitors. It has been reported that the evolved PPI inhibitors tend to be larger, highly hydrophobic, very rigid, and contain multiple aromatic rings [232].

In a study done by Arulmozhiraja *et al*., it was found that DPP-4 inhibitors reside inside the hydrophobic cavity made up of Arg125, Glu205, Glu206, Tyr547, Tyr662, Tyr666, Ser630, and Phe357 [233]. It is further known that DPP-4 inhibitors interact strongly with the Glu206 and Glu205 amino acids in the S_2 subsite by forming salt bridges with them. Sitagliptin is known to form the strongest bonding with Glu206 and Glu205 residues through its amine group. Its trifluorophenyl ring binds to the S_1 subsite and has only moderate interactions with Tyr662 and Tyr666, respectively. The other strong interaction comes through Phe357 – the triazolopyrazine moiety π-π stacks with this phenylalanine. CF_3 group interacts moderately with Arg358 [233]. From our study results (**Figure 3.11**), Sitagliptin exhibited maximum inhibitory activity as to be expected of about 100% in all the concentrations. We can therefore predict that the TZD derivatives did not form strong interaction bonds either due to their chain length or size and hence the weak inhibitory effect.

Soluble DPP-4 has been shown to induce inflammation and proliferation of human smooth muscle cells (hSMC) through activation of extra cellular signal regulated kinase (ERK) and nuclear factor kappa B (NF-κB) signalling pathway in a PAR2 dependent manner leading to pro-atherogenic changes in hSMC like increased proliferation and inflammation. In accordance with DPP-4 induced stress and inflammatory signalling, DPP-4 also increases the expression and secretion of pro-inflammatory cytokines like interleukin–6 (IL-6), interleukin–8 (IL-8) and monocyte chemoattractant protein–1 (MCP-1). The activation of NF-κB and SMAD signalling further stimulates the activation of fibroblasts resulting in fibrosis. Both the expression and secretion of cytokines, as well as the activation of ERK and NF-κB can be completely blocked by DPP-4 inhibitors which block proteinase-activated receptor-2 (PAR2) [230]. Therefore,

inhibiting the DPP-4 enzyme is beneficial in supressing inflammation and fibrosis. We can postulate that the derivatives investigated in this study slightly inactivated DPP4, therefore, blunting the ERk & NF-κB signalling pathway. This is paramount considering inflammation observed in diabetes.

DPP-4 has been recognized as a corona virus co-receptor protein for intracellular entry of SARS-CoV-2 [234]. Within the immune system, DPP-4 proteins may be involved in amplifying the signals derived from interactions with an antigen, thereby leading to T-cell activation [235]. Therefore, it is of clinical importance that we search for more DPP-4 inhibitors since they are proving to broadly achieve numerous therapeutic treatments. Hence, there is a great need to pursue more studies such as *in silico* and *in vitro* to ascertain the level activity of the TZD derivatives against DPP4.

It is important to note that the investigated TZD derivatives contain a TZD moiety, which has proven anti-hyperglycaemic activity through peroxisome proliferator-activated receptor gamma (PPARγ) activation. TZDs bind avidly to PPARγ and the activation of PPARγ by TZDs influences several genes expression which are involved in lipid and glucose metabolism and preadipocyte differentiation. They enhance the sensitivity to insulin and promote the utilization of glucose by peripheral tissues [236]. Binding of the agonists/ligands with the ligand binding region of peroxisome proliferator-activated receptors (PPARs) causes the translocation of PPARs to the nucleus and produces heterodimers with another nuclear receptor, the retinoid X receptor (RXR). The PPARs then bind with specific regions on DNA of the target genes which are named as peroxisome proliferator hormone response elements (PPREs) [237-240].

It has been shown that rosiglitazone binds to PPARγ forming hydrogen bonds between the residues Ser289, His323 and Tyr473 and the TZD group of rosiglitazone in the polar part of the binding site. This hydrogen bonding pattern is expected to be essential for the formation of a tight binding ligand complex, which stabilizes a charge clamp between the C-terminal activation function 2 (AF-2) helix and a conserved lysine residue on the surface of the receptor [241]. Further studies have shown that PPARs have a Y-shaped binding cavity of ligand binding domain (LBD) in both PPAR isoforms which is made up of 34 amino acid residues. The amino acid residues in arm I of PPARγ has His323 and Phe363, which have a marked influence on the ligand specificity since the polar head groups of the ligands interact with the binding pockets located in this arm. Arm II containing Gly284 is hydrophobic and provides

characteristic specificity for PPARγ. Arm III, which is the ligand entrance site, contains Arg288 [238, 240]. Generally, TZDs interact by forming hydrogen bonds with His323 (H4), His449 (H11), and Tyr473 residue of helix 12 of PPARγ LBD, associated with AF2 domain. It may also form hydrogen bond with Ser289 (H3) and the oxygen, nitrogen atoms of the ring function as both hydrogen bond acceptors and donors. The hydrophobic tail moiety of rosiglitazone may also interact with helix 3, 5, 6, 7, and the β strand, occupying arm II and arm III of the LBD, through van der Waals and hydrophobic interactions which accounts for the efficiency of binding and potency of the molecule. The central phenyl ring is accommodated beneath helix 3 by hydrophobic interactions [242].

In this investigation however, rosiglitazone formed interactions with residues Leu128, Leu333, Met329, Ile326 and Arg288 while **TZDD2** and **TZDD4**, formed interactions with similar residues in addition to Ile281 and Glu345 respectively, and both did not interact with Leu128. **TZDD3** formed with Arg288, Ile281 and Glu345 while **TZDD1** only interacted with Leu333 and Glu345 (**Figures 3.12**; **C5(ii)**; **C5(iii)**; **C7(ii)**; **C7(iii)**; **C9(ii)**; **C9(iii)**; **C11(ii)**; **C11(iii)**; **C13(ii)**; **and C13(iii)**). The interactions included hydrogen bonding, д -cation interactions, salt bridges, and hydrophobic interactions. We can therefore suggest that these derivatives were binding to another minor binding site as literature suggests there are about 32 amino acid residues which can easily form interactions with ligands [243]. Reports on structure-activity relationships of TZD derivatives suggest that the structure of the lipophilic tail region and the conformation of the molecule are important for high potency. The amine group of TZD acid head plays an important role in the inhibitory potency of hydrogen bonding which is essential to orient the molecule more favourably toward the binding site of the enzyme [244].

With the understanding of the mode of action of TZD derivatives and analysis of binding activity of the investigated TZD derivatives, we then hypothesise that binding to the PPARγ would result in its activation. Rosiglitazone which is a known activator was used as the standard. Analysis of the conformations of the docking results, shows that these TZD derivatives formed interactions to the PPARγ at the same positions and amino acids as the standard (rosiglitazone) with **TZZD2** and **TZDD4** forming the most similar interactions. **TZZD1** formed the least similar interactions (**Figure 3.12**, **Table 3.9**). **TZDD3** however, obtained a similar low binding energy, a close estimated inhibition constant and root mean square deviation value to that of rosiglitazone in this study. With these observations, we can postulate that these TZD derivatives exhibit a PPARγ activation mode of action and need to be

studied further *in vivo* to establish the mode of action. Most TZDs have been withdrawn due to their toxicity, and this has magnified the interest in investigating TZD derivatives with the aim of achieving similar therapeutic effect but with less or no toxicity challenges [244]. For example, our derivatives were synthesized by pharmacophore hybridization in which TZD and *N*-arylpyrrole frameworks were integrated into a single structure entity to overcome the toxicity challenge while improving potency.

Earlier studies have shown that TZD-derived hybrids with *N*-functionalized side chain on the *N*-3 nitrogen TZD ring displayed improved efficacy and that such modifications exhibited low toxicity towards primary cultured non-malignant human hepatocytes. In addition, a large number of clinically approved drugs are having *N*-heterocyclic ring as a subunit of their chemical structures and mefloquine and levofloxacin are two representative examples of drugs with *N*-heterocyclic ring. On the basis of the above observations, the synthesis explored the use of *N*-heterocyclic amines as an appendant on the *N*-3 of the TZD scaffold and this should render these derivatives with less or no toxicity challenges [178].

The presence and increase in blood glucose concentration normally triggers secretion of insulin from β-cells of Islets of Langerhans in pancreatic cells. Insulin exerts its pleiotropic biological effects by binding to its receptor on insulin target tissues (adipose, liver, skeletal muscle). The insulin receptor is an α2β2 heterotetrametric receptor in which the α and β subunits are linked by disulphide bonds. The β subunits contain the tyrosine kinase catalytic domain. Insulin binding induces a conformational change that results in tyrosine kinase activation. The β subunits undergo autophosphorylation, followed by phosphorylation of downstream effector molecules on tyrosine residues. These proximal tyrosine phosphorylation events are essential for the initiation of insulin action, and for the full complement of insulin-regulated biological responses to occur. Many of these responses are also dependent on insulin-mediated changes (both increases and decreases) in serine and threonine phosphorylation brought about by the regulation of serine/threonine kinase and phosphatase activities [245].

The insulin receptor substrates (IRS)-1 and 2 play a central role in insulin signalling [246]. Several signalling proteins interact with IRS-1 or IRS-2 in an insulin dependent manner [247]. It should be noted that all of the phosphorylation events triggered by insulin are transient. This is the case for insulin receptor autophosphorylation as well as for tyrosine phosphorylation of downstream targets, such as IRS-1 and IRS-2. The action of PTPases has been implicated in this process. PTP-1B is an intracellular PTP that has been implicated as a key negative regulator

of the insulin and leptin signalling pathways [248, 249]. It acts by dephosphorylating specific phosphotyrosine (pTyr) residues on both the insulin receptor and insulin receptor substrate proteins, therefore rendering the insulin signalling pathway inactive [250]. The important roles of PTPases in the regulation of various signal transduction pathways qualify these enzymes as interesting therapeutic targets for drug discovery and provide new opportunities for therapeutic intervention.

Recent studies have shown that the inhibitory mechanism of action of PTP-1B with TZDs illustrated that a pair of hydrogen bonding interactions are made from Gln266 and the backbone amino group of Ser216 to the carbonyl oxygen substituents on the TZD frame [251]. The acidic proton occupying the amidic position seemed to be close to Cys215 and Arg221. Further interaction within the catalytic site could be observed through hydrophobic interactions between the inhibitor's aromatic rings and surrounding hydrophobic residues, including Tyr46, Val49, Phe182, Ala217 and Ile218 [251]. Our attempt to establish the activity of these TZD derivatives against the activity of PTP-1B yielded a very low inhibitory activity below 30% in all the derivatives investigated. **TZDD1** showed a dose independent activity while **TZDD2** and **TZDD4**, a dose dependent activity. However, **TZDD3** exhibited a decrease in activity as the concentrations increased from 10 through to 50 µg/mL. The poor exhibited inhibition activity could be due to weak van der Waals forces of attraction formed and the inability of the molecules to align properly in the binding site. Interestingly, the results suggest that **TZDD3** increases the activity of PTPases at 50 µg/mL. This observation may indicate activation of this enzyme which would exacerbate the hyperglycaemia. Further studies need to be conducted to establish the mode of interaction of these compounds with these therapeutic targets

Despite the inhibition of α-amylase, α-glucosidase, DPP-4, PTP-1B, target hyperglycaemia to halt the progression of diabetes, often the development of diabetes complications is inevitable. As such, several processes have been targeted in the pathogenesis and progression of diabetes as possible therapeutic targets. These include the hexosamine pathway, protein glycosylation, oxidative stress, and polyol pathway [252]. As earlier indicated in literature, several studies have also established the inevitable link between polyol pathway and development of diabetic complications like kidney disease, cataract, and cardiovascular disorder [253]. Furthermore, oxidative stress and AGEs formation which are myriad of pathological processes resulting from accumulation of sorbitol and fructose in the polyol pathway, are implicated in retinopathy, neuropathy, and nephropathy [194].

In this study, we evaluated the inhibitory effect of the rate limiting enzyme for polyol pathway enzyme, aldose reductase by our four TZD derivatives as a possible mechanism underlying hypoglycaemic potential of the derivatives. These derivatives exhibited a significant inhibitory activity against aldose reductase. Of these derivatives, **TZDD1** displayed the lowest IC_{50} (27.54 µg/mL) for the inhibition of aldose reductase (**Table 3.6**). This is an indication that these derivatives effectively inhibited the activity of this enzyme which is the rate limiting in the polyol pathway. The mechanism involved is that the enzyme inhibition prevents the intracellular accumulation of sorbitol and fructose [254]. This mitigates osmotic stress and glycation, respectively. It also prevents the depletion of NADPH [255], which is normally required by the cell for regeneration of reduced glutathione, which plays the role of antioxidant.

Inhibition of this enzyme by the derivatives, therefore, may prevent cellular oxidative stress and redox imbalance, thereby ameliorating diabetic complications. The fact that IC_{50} values (for the inhibition of aldose reductase) exhibited by **TZDD4** (IC_{50} = 36.77 ± 5.10 µg/mL) is similar to the standard (quercetin; IC_{50} value = 36.71 ± 11.15 µg/mL), and **TZDD1** (IC_{50} = 27.54 ± 5.34 µg/mL) is lower than that of the standard, depicts the high potency of **TZDD4** and **TZDD1**. This is because quercetin has been demonstrated to possess strong inhibition against enzymes in the polyol pathway and is therefore used widely as positive control [256]. More importantly, quercetin possesses structural features such as hydroxyl group at 3′ position in the B ring, 2′,3 double bond and the 4-oxo group in the C ring which are required for binding to the active site of the enzymes. Quercetin also inhibits aldose reductase in a variety of mechanism including competitive, non-competitive, and uncompetitive inhibition [257].

Similarly, the investigated TZD derivatives possess a double bond on the substituent on C5 of the TZD acid head, one oxo group in **TZDD1** and **2**, two oxo groups in **TZDD3**. This observation can be used to predict that the derivatives form the required interactions in the binding site hence the potent inhibitory effect of the TZD derivatives on aldose reductase depicted. Therefore, it can be postulated that the derivatives investigated in this study displayed significant inhibitory properties against aldose reductase due to the mentioned structural features. The inhibition of polyol pathway enzymes by the derivatives may contribute to the amelioration of diabetic complications, which will need confirmation in an *in vivo* model of diabetic complication.

During the polyol pathway, free radicals are formed in biological systems and are associated with extreme damage in free radical pathology, capable of injuries to almost every molecule found in living cells [258]. These "free radicals" are usually removed by the antioxidant defence system of the body which scavenges for ROS and prevent generation of oxidative stress thus minimizing oxidative stress – induced tissue damage. However, an absolute or relative deficiency of antioxidant defences results in oxidative stress as observed in the pathophysiology of DM and AD [65–80].

This therefore, creates a potential therapeutic opportunity for use of antioxidant molecules such as ascorbic acid to scavenge ROS. Using the FRAP assay, we determined the antioxidant properties of these TZD derivatives, and they exhibited a significant FRAP activity with **TZDD1**, **TZDD2** and **TZDD3** showing a concentration dependent activity. **TZDD4** (FRAP value ≥ 50 μM/g dry mass across concentrations) however, exhibited an almost constant activity with an increase in concentrations (**Figure 3.3**). **TZDD2** (FRAP value > 120 μM/g dry mass in all concentrations) was most potent. The good antioxidant activity exhibited can be attributed to the presence of electron donating groups like the aromatic ring at the tail position, carbonyl group on 4C of the acid TZD ring, and OCH_3 groups in **TZDD1**. The relatively low antioxidant activity exhibited by **TZDD4** and **1**, however can be attributed to the electron withdrawing species such as the phenylpiperazine ring in **TZDD1** and the secondary tertiary amine in **TZDD4**.

Furthermore, in the evaluation of these TZD derivatives for their possible potential to antioxidant activity, we carried out the DPPH radical scavenging method. This test is widely accepted as a model for evaluating the free radical scavenging activity of any new drug [259]. The DPPH scavenging method has been used to evaluate the antioxidant activity of compounds due to its simplicity, rapidity, sensitivity and reproducibility [260, 261]. Similarly, the mode of action of these derivatives can be predicted as explained in this method through their hydrogen donating ability. All the four compounds exhibited significant DPPH radical scavenging activity compared to the control, with **TZDD1** exhibiting a concentration dependent activity, **TZDD3** had an activity greater than 50 % in all the concentrations (10 – 50 μg/mL) (**Figure 3.4**). The higher the DPPH radical scavenging activity is associated with a lower IC_{50} value and therefore, **TZDD3** had a potentially higher radical scavenging activity. In addition to FRAP activity of these derivatives, the observed DPPH radical scavenging activity suggests that these

derivatives have a potential antioxidant activity and therefore can be used to defend against ROS, to supplement and increase the effectiveness of the bodily antioxidant defence system.

Uncontrolled ROS is detrimental to the brain and is a precursor for accumulation of amyloid β proteins in the amyloid plaques of extracellular system, intracellular neurofibrillary tangles by the phosphorylated tau protein and cholinergic neurons degeneration in basal forebrain [262]. Preventing or limiting the aggregation of these plaques is a possible therapeutic target in the treatment of AD. In the evaluation of our derivatives against, β – amyloid aggregation, a slight insignificant activity was observed. However, **TZDD1** and **TZDD3** showed some promising inhibition activity. These may be possible therapeutic mode of action of these derivatives against AD, however, more studies would need to be done to completely ascertain that possibility.

Although AD is primarily associated with extracellular Aβ plaques and neurofibrillary tangles in the brain, recent studies have indicated that intra-neuronal accumulation of Aβ also accelerates AD progression by promoting degeneration and loss of neurons [263]. Currently, a monoclonal antibody (Aducanumab) is licenced for therapeutic treatment of AD. Aducanumab is a human monoclonal antibody that selectively targets aggregated Aβ. In a transgenic mouse model of AD, aducanumab is shown to enter the brain, bind parenchymal Aβ, and reduce soluble and insoluble Aβ in a dose-dependent manner [263]. In patients with prodromal or mild AD, one year of monthly intravenous infusions of aducanumab reduces brain Aβ in a dose- and time-dependent manner.

In addition to alleviating ROS, it is imperative that we consider mechanisms of controlling and alleviating inflammation that may result from the activities of MMP-1 activation. MMP-1 is a secreted enzyme capable of breaking down interstitial collagen types I, II and III in the extracellular matrix. Matrix metalloproteinases have important functions in morphogenesis, angiogenesis, apoptosis, tissue remodelling and repair, and tumour metastasis [264].
The TZD derivatives exhibited a non-significant inhibitory activity against MMP-1, and **TZDD1** and **TZDD4** exhibited an activation activity at lower concentrations of 10 and 20 µg/mL. The potential activation of MMP-1 would be of clinical importance because it can be a cause for deteriorating instead of management of DM and AD due to aggravated chronic inflammatory disease. It is an established view that the balance between the production of active enzymes and their inhibition is critical to avoid the conditions of uncontrolled

extracellular matrix (ECM) turnover, inflammation, and dysregulated cell growth and migration, which would result in disease or worsening thereof. For example, the deregulation of MMPs result in tissue damage which is a precursor in brain degenerative diseases such as AD. The two major inhibitors of MMPs in body fluids and tissues are α_2-macroglobulin and tissue inhibitors of proteinases (TIMPs), respectively.

The naturally occurring inhibitors of human MMP activity are four members of the TIMPs. Each TIMP molecule consists of around 190 amino acids composed of two distinct domains, a larger N-terminal and a smaller C-terminal domain, each one stabilised by three conserved di-sulfide bonds. The N-terminal domaincan fold independently and is fully functional to inhibit MMPs by chelating their catalytic zinc atom with a 1:1 molar ratio. The function of the C-terminal domain is not fully understood, but it has been shown that it can bind tightly to the haemopexin domain of latent MMPs [265]. The investigated derivatives all possess a sulphide group in the acidic TZD head, and therefore we can postulate that the exhibited activity could be due to this group. Currently, meloxicam, tenoxicam, piroxicam, and sodium alendronate are known inhibitors of MMPs. In addition, batimastat (a hydroxamic acid derivative that mimics the peptide structure of natural substrates) and marimastat (hydroxamic acid analog that is structurally similar to batimastat) are in clinical trials as MMPs inhibitors. A study on the inhibitory activities of meloxicam, tenoxicam, piroxicam, and sodium alendronate suggested that inhibition of the MMPs is of clinical significance since there is a series of metalloproteinases in the connective matrix, all of which have similar structure but with diverse participation in different pathologies.

If there is continued deregulation of MMPs, then degeneration of neurons sets in which will result in drop of cholinergic function. The cholinergic hypothesis of AD proposes that the degeneration of cholinergic neurons occurs in the basal forebrain and is associated with loss of cholinergic neurotransmission in the cerebral cortex. This is therapeutically important since the basal forebrain cholinergic system is known to be involved in the cognitive processing of memory and attention [265]. Currently, it is believed that prolonging the availability of acetylcholine released into the neuronal synaptic cleft improves the cholinergic function in patients with AD by inhibiting acetylcholine hydrolysis [266].

The screening of these TZD derivatives showed a relatively significant inhibition activity against AchE with **TZDD3** having a dose independent activity while **TZDD2** showed a dose dependent activity. **TZDD1** exhibited the most potent activity with the lowest IC_{50} (**Figure**

3.13 and **Table 3.11**). This can be one of the modes of action of these derivatives against Alzheimer's disease in which they can enable and enhance direct neuron-to-neuron signalling. AChE catalytic site consists of the Ser200–Glu327–His440 (SEH) triad which is responsible for its resultant hydrolysis, and a so-called anionic subsite, located at the bottom of a deep and narrow gorge [267, 268]. This anionic subsite recognizes the quaternary ammonium group of the substrate. A second, 'peripheral', anionic site exists 14 Å apart from the active site. The catalytic triad is named 'the aromatic gorge', and several studies invoke aromatic groups as a general feature of quaternary-ligand binding sites [267-272]. The investigated TZD derivatives all have prominent aromatic groups, all have the aromatic ring in the tail region, **TZDD1** has an extra ring on the 5C substituent, **TZDD2** and **3** have a second ring on the linker group, and **TZDD4** has two extra aromatic rings onto the 5C substituent.

We can therefore attribute the activity of these compounds to the presence of these groups. Drugs such as tacrine, donepezil, galantamine, and physostigmine are some classical AChE inhibitors. AChE catalyses the hydrolysis of the neurotransmitter ACh at the synaptic cleft into its two components choline and acetic acid. Therefore, inhibiting its activity will promote availability of acetylcholine. Some of AChE inhibitors are competitive with ACh in order to prevent its hydrolysis. Notwithstanding, acylation of OH group of S200 is also inhibited in order to yield a carbamyl ester. This is more stable than the acetate and less capable of leaving the active site [241]. To achieve therapeutic effect from the investigated derivatives however, the TZD derivatives would need to be delivered across the BBB as they exhibited no BBB permeability. In clinical setting, this could be why most clinical studies have failed to deliver treatment of AD due to challenges of the BBB. Further studies would be required to establish the delivery systems for therapeutic effect.

CONCLUSIONS

Diabetes mellitus and Alzheimer's disease are pathologies of global concern and pose a serious public health challenge worldwide. Recent studies show a direct link between the two diseases. Several researchers worldwide are striving to search for novel forms of treatment and prevention of diabetes as well as Alzheimer's disease. However, to date, there is no therapy able to induce management and treatment of both diseases. The current therapies aim at management of each disease (diabetes and Alzheimer's) and in some instances are only palliative such as for Alzheimer's disease. This continues to promote polypharmacy as a result of co-morbidities in patients. In this line, the discovery of new therapies is undoubtedly an important goal, in order to provide better and more efficient treatment for patients with both diabetes and Alzheimer's disease. Oxidative stress is an important pathological factor in both diabetes mellitus and Alzheimer's disease, and it serves as an important therapeutic target for the development of remediation noble therapies. In this context, antioxidants are remarkable contributors for these therapeutic purposes, along with therapeutic target on amyloid β and tau aggregation. In this investigation, our TZD derivatives (**TZDD1**, **2**, **3** and **4**) exhibited substantial antioxidant activities with potential to interfere with amyloid β aggregation.

Furthermore, from the enzymatic (α–amylase, α–glucosidase, aldose reductase, PTP1B, DPP4) inhibition assays targeting critical stages of glucose homeostasis, showed relative inhibition activity, further promising anti-hyperglycaemic activity. However, this also raises a risk for hypoglycaemia and therefore more *in vivo* and *in silico* studies are necessary to quantify and eliminate this risk. These derivatives also exhibited a relatively promising acetylcholinesterase inhibition activity. Since pathological processes of diabetes mellitus and Alzheimer's disease are interlinked, effective treatment of diabetes mellitus can alleviate Alzheimer's disease and in an interesting finding, these derivatives can be targeted at both these two pathologies. Furthermore, *in silico* ADME profiling predicted that these derivatives have moderate to good solubility in the GI and hence good bioavailability as well as desired drug-likeness. However, they are predicted to have poor BBB penetration, and this will also require further studies to establish their mode of drug delivery across the BBB if developed as therapeutic treatments against Alzheimer's disease.

STUDY LIMITATIONS AND FUTURE STUDIES

In this investigation, each assay experiment was conducted once and replicated to generate results. There is a need for more studies to be conducted to establish with absolute confidence the activity of these derivatives by repeating some of these assays. This could not be achieved with our study due to the limiting resources such as screening kits and enzymes for inhibition assays, which are expensive and therefore, only one assay could be performed.

Furthermore, there is a need to carry out studies using cells to measure glucose uptake in presence of these investigated TZD derivatives. It is believed that these preliminary results would be a helpful subject on the reported compounds to further studies such as their toxicology profiles to aid their optimization. Toxicology profiles have not been done in this study due to limited resources and laboratory equipment to facilitate toxicology studies. Lastly, it will be necessary to utilize new docking tools to quantify further specific interaction as well as the required conformations essential for activity of these compounds.

REFERENCES

1. Atun, R., Davies, J. I., Gale, E. A., Bärnighausen, T., Beran, D., Kengne, A. P., Sobngwi, E. (2017). Diabetes in sub-Saharan Africa: from clinical care to health policy. *The Lancet Diabetes & Endocrinology Commission*, 5(8); 622-667.
2. Bradshaw, D., Norman, R., Pieterse, D., Levitt, N. S., &the South African Comparative Risk Assessment Group (2007). Estimating the burden of disease attributable to diabetes South Africa in 2000. *South African Medical Journal*, 96(7); 700-705.
3. Hu, F. (2011). Globalization of diabetes: The role of diet, lifestyle, and genes. *Diabetes Care*, 34; 1249-1257.
4. Aynalem, S. B. & Zeleke, A. J. (2018). "Prevalence of Diabetes Mellitus and Its Risk Factors among Individuals Aged 15 Years and Above in Mizan-Aman Town, Southwest Ethiopia, 2016: A Cross Sectional Study". *International Journal of Endocrinology*, 2018.
5. Pheiffer, C., Pillay-van Wyk,V., Joubert, J.D., *et al*. (2018). The prevalence of type 2 diabetes in South Africa: a systematic review protocol. *British Medical Journal Open*, 8(7).
6. Erasmus, R., Soita, D., Hassan, M., Blanco-Blanco, E., Vergotine, Z., Kengne, A., & Matsha, T. (2012). High prevalence of diabetes mellitus and metabolic syndrome in a South African coloured population: Baseline data of a study in Bellville, Cape Town. *South African Medical Journal, 102*(11); 841-844.
7. Melanie, Y., Bertra, M., Aneil, V.S., Jaswal, Pillay Van Wyk, V., Levitt, N. S. & Hofman, K. J. (2013). The non-fatal disease burden caused by type 2 diabetes in South Africa 2009. *Global Health Action*, 6(1).
8. Stokes, A., Berry, K. M., Mchiza, Z., Parker, W., Labadarios, D., Chola, L., *et al*. Prevalence and unmet need for diabetes care across the care continuum in a national sample of south African adults: evidence from the SANHANES-1, 2011-2012. *PloS One*;12(10).
9. Lalkhen, H. & Mash, R. (2015). Multimorbidity in non-communicable diseases in South African primary healthcare, *South African Medical Journal*, 105(2); 134-138.
10. NCD Risk Factor Collaboration (2016). Worldwide trends in diabetes since 1980: A pooled analysis of 751 population-based studies with 4.4 million participants. Lancet. *NCD Risk Factor Collaboration*, 387; 1513–1530.

11. Bertram, M. Y., Jaswal, A. V. S., Van Wyk, V. P., Levitt, N. S. & Hofman, K. J. (2013). The non-fatal disease burden caused by type 2 diabetes in South Africa, 2009. *Global Health Action*, 6(1).
12. International Diabetes Federation (IDF). IDF Diabetes Atlas 2019: Diabetes increase the risk of health complications. *9th. Edition 2019*.
13. Coetzee, A., Beukes, A., Dreyer, R., Solomon, S., van Wyk, L., Mistry, R., Conradie, M. & van de Vyver, M. (2019). The prevalence and risk factors for diabetes mellitus in healthcare workers at Tygerberg hospital, Cape Town, South Africa: a retrospective study. *Journal of Endocrinology, Metabolism and Diabetes of South Africa*, 24(3); 77-82.
14. International Diabetes Federation (2017). IDF Diabetes atlas 8th Edition [Internet]. *Brussels, Belgium*.
15. Govender, R. D., Gathiram, P. & Panajatovic, M. (2017). Poor control and management of type 2 diabetes mellitus at an under-resourced South African Hospital: is it a case of clinical inertia? *South African Family Practice*, 59(5); 154-159.
16. Erzse, A., Stacey, N., Chola, L., Tugendhaft, A., Freeman, M. & Hofman, K. (2019). The direct medical cost of type 2 diabetes mellitus in South Africa: a cost of illness study. *Global Health Action*, 12(1).
17. Hunter-Adams, J. & Battersby, J. (2020). Health care providers' perspectives of diet-related non-communicable disease in South Africa. *BioMed Central Public health*, 20; 262.
18. Aruoma, O. I., Narrain, D., Indelicato, J., Bourdon, E., Murad, F., Bahorun, T. (2014). Cognitive impairment in patients with type 2 diabetes mellitus: Perspectives and challenges. *Archives of Medical and Biomedical Research*, 1(2); 79-89.
19. Biessels, G.J., Staekenborg, S., Brunner, E., Brayne, C., Scheltens, P. (2006). Risk of dementia in diabetes mellitus: a systematic review. *Lancet Neurology*, 5(1); 64-74.
20. van Rensburg, S. J., Daniels, W. M. U., Potocnik, F. C. V., van Zyl, J. M., Taljaard, J. J. F., & Emsley, R. A. (1997). A new model for the pathophysiology of Alzheimer's disease: Aluminium toxicity is exacerbated by hydrogen peroxide and attenuated by an amyloid protein fragment and melatonin. *South African Medical Journal*, 87; 1111-1115.
21. de Jager, C. A., Joska, J. A., Hoffman, M., Borochowitz, K. E., & Combrinck, M. I. (2015). Dementia in rural South Africa: A pressing need for epidemiological studies. *South African Medical Journal*, 105(3); 189-190.

22. Alzheimer's Association (2012). Alzheimer's disease facts and figures. *Alzheimers Dement*, 8(2); 131-168.
23. Alam, Q., ZubairAlam, M., Karim, S., Gan, S. H., Kamal, M. A., Jiman-Fatani, A., Damanhouri, G. A., Abuzenadah, A. M., Chaudhary, A. G., & Haque, A. (2014). A nanotechnological approach to the management of Alzheimer disease and type 2 diabetes. *CNS & neurological disorders drug targets*, 13(3), 478–486.
24. Whalen, K. (2015). Lippincott Illustrated Reviews: Pharmacology (6th ed.). (F. Richard, & P. Thomas A., Eds.) Blatimore, New York, London: Wolters Kluwer. 349 – 362.
25. Deutschländer, M.S., Lall, V. & van de Venter, M. (2009). Plant species used in the treatment of diabetes by South African traditional healers: An inventory. *Pharmaceutical Biology*, 47(4); 348-365.
26. Yee Tan, S., Ling Mei Wong, J., Jinn Sim, Y., Sie Wong, S., Elhassan, S. A. M., Hong Tan, S., Pei Ling Lim, G., Wuen Rong Tay, N., Annan, N. C., Bhattamisra, S. K. & Candasamy, M. (2019). Type 1 and 2 diabetes mellitus: A review on current treatment approach and gene therapy as potential intervention, Diabetes & Metabolic Syndrome. *Clinical Research & Reviews*, 13(1); 364-372.
27. Szablewski, L. Glucose Homeostasis – Mechanism and Defects, November 2011: 227 – 247.
28. Foulis A.K., Mc Gill M. & Farquharson M.A. (1991). Insulitis in type 1 (insulin-dependent) diabetes mellitus in man – macrophages, lymphocytes, and interferon-gamma containing cells. *The Journal of Pathology*, 165(2); 97-103.
29. Todd, J.A. (1999). From genome to aetiology in a multifactorial disease type-1 diabetes. *BioEssay,* 21(2); 164-173.
30. Gilespie K.M. (2006). Type 1 diabetes: pathogenesis and prevention (Review). *Canadian Medical Association Journal*, 175(2); 165-170.
31. Atkinson M.A. & Eisenbarth G.S. (2001). Type 1 diabetes: new perspectives on disease pathogenesis and treatment. *Lancet*, 358(9277); 221-229.
32. Rabinovitch A. (2000). Autoimmune diabetes mellitus. *Science and Medicine*, 7(3); 18-27.
33. Haller M.J., Atkinson M.A. & Schatz D. (2005). Type 1 Diabetes Mellitus: Aetiology, presentation and management. *Pediatric Clinics of North America*, 52(6); 1553-1578.
34. Warram J.H., Krolewski A.S. & Kahn C.R. (1988). Determinants of IDDM and perinatal mortality in children of diabetic mothers. *Diabetes,* 37(10); 1328-1334.

35. Risch N. (1987). Assessing the role of HLA-linked and unlinked determinants of disease. *American Journal of Human Genetics,* 40(1); 1-14.
36. Todd J.A. & Wicker L.S. (2001). Genetic protection from the inflammatory disease type 1 diabetes in humans and animal models. *Immunity*, 15(3); 387-395
37. Peakman M. (2001). Advance in understanding the immunopathology of type 1 diabetes mellitus. *CPD Bulletin of Immunology and Allergy*, 2(1); 23-26.
38. Bell G.I., Horita S. & Karam J.H. (1984). A polymorphic locus near the insulin gene is associated with insulin-dependent diabetes mellitus. *Diabetes*, 33(2); 176- 183.
39. Concannon P., Gogolin-Ewans K.J., Hinds D.A. *et al* (1998). A second-generation screen of the human genome for susceptibility to insulin-dependent diabetes mellitus. *Nature Genetics*, 19(3); 292-296.
40. Cox N.J., Wapelhorst B., Morrison V.A. *et al*. (2001). Seven regions of the genome show evidence of linkage to type 1 diabetes in a consensus analysis of 767 multiplex families. *American Journal of Human Genetics*, 69(4); 820-830.
41. Dorman J.S. & Bunker C.H. (2000). HLA-DQ locus of the human leucocyte antigen complex and type 1 diabetes mellitus: a HUGE review. *Epidemiological Reviews,* 22(2); 218-227.
42. Lin Y. & Sun Z. (2010). Current views on type 2 diabetes. *Journal of Endocrinology,* 204; 1-11.
43. Poulsen P., Kyvik K.O., Vaag A. & Beck-Nielsen H. (1999). Heritability of type II (non- insulin-dependent) diabetes mellitus and abnormal glucose tolerance – a population-based twin study. *Diabetologia,* 42(2);139-145.
44. Majithia A.R. & Florez C.J. (2009). Clinical translation of genetic predictors for type 2 diabetes. *Current Opinion in Endocrinology, Diabetes and Obesity,* 16(2); 100-106.
45. Doria A., Patti M-E. & Kahn C.R. (2008). The emerging genetic architecture of type 2 diabetes. *Cell Metabolism,* 8(3); 186-200.
46. Staiger H., Machicao F., Fritsche A. & Häing H-U. (2009). Patho-mechanisms of type 2 diabetes genes. *Endocrine Reviews,* 30(6); 557-585.
47. Ridderstrale M. & Groop L. (2009). Genetic dissection of type 2 diabetes. *Molecular and Cellular Endocrinology,* 297(1-2); 10-17.
48. Bjornholm M. & Zierath J. (2005). Insulin signal transduction in human skeletal muscle: identifying the defects in type 2 diabetes. *Biochemical Society Transactions*, 33(2); 354-357.

49. Drucker, D. J. (2007). The role of gut hormones in glucose homeostasis. *The Journal of Clinical Investigation*, 117(1); 24-32.
50. Usdin, T.B., Mezey, E., Button, D.C., Brownstein, M.J., Bonner, T.I. (1993). Gastric inhibitory polypeptide receptor, a member of the secretin-vasoactive intestinal peptide receptor family, is widely distributed in peripheral organs and the brain. *Endocrinology*, 133:2861-2870.
51. Mayo, K.E., *et al*. (2003). International Union of Pharmacology. XXXV. The glucagon receptor family. *Pharmacology. Review.*, 55:167-194.
52. Yip, R.G., Boylan, M.O., Kieffer, T.J., Wolfe, M.M. (1998). Functional GIP receptors are present on adipocytes. *Endocrinology*, 139:4004-4007.
53. Gromada, J., *et al*. (1998). Glucagon-like peptide 1 (7-36) amide stimulates exocytosis in human pancreatic beta-cells by both proximal and distal regulatory steps in stimulus-secretion coupling. *Diabetes*, 47:57-65.
54. Trumper, A., *et al*. (2001). Glucose-dependent insulinotropic polypeptide is a growth factor for beta (INS-1) cells by pleiotropic signalling. *Molecular Endocrinology*, 15:1559-1570.
55. Trumper, A., Trumper, K., Horsch, D. (2002). Mechanisms of mitogenic and anti-apoptotic signalling by glucose-dependent insulinotropic polypeptide in beta (INS-1)-cells. *Journal of Endocrinology*, 174:233-246.
56. Mentlein, R., Gallwitz, B., & Schmidt, W.E. (1993). Dipeptidyl-peptidase IV hydrolyses gastric inhibitory polypeptide, glucagon-like peptide-1(7-36) amide, peptide histidine methionine and is responsible for their degradation in human serum. *European Journal of Biochemistry*, 214:829-835.
57. Ahrén, B. & Schmitz, O. (2004). GLP-1 receptor agonists and DPP-4 inhibitors in the treatment of type 2 diabetes. *Hormone and Metabolic Research*, 36(11-12); 867-876.
58. Kim, D.J., Kang, Y.H., Kim, K.K., *et al*. (2017 Jun). Increased glucose metabolism and alpha-glucosidase inhibition in Cordyceps militaris water extract-treated HepG2 cells. Nutrition Research and Practice. 11(3):180-189.
59. Peyrot des Gachons, C., & Breslin, P. A. (2016). Salivary Amylase: Digestion and Metabolic Syndrome. *Current diabetes reports*, *16*(10), 102.
60. Butterworth, P., Warren, F., & Ellis, P. (2011). Human α-amylase and starch digestion: An interesting marriage. *Starch - Stärke.* 63, 395-405.

61. Phielix E., & Mensink M. (2008). Type 2 diabetes mellitus and skeletal muscle metabolic function. *Physiology & Behavior*, 94(2); 252-258.
62. Evans, J. & Jallal, B. (1999). Protein tyrosine phosphatases: Their role in insulin action and potential as drug targets. Expert opinion on investigational drugs 8(2). 139-160.
63. Blanco, C.L., McGill-Vargas, L.L., Gastaldelli, A., Seidner, S.R., McCurnin, D.C., Leland, M.M., Anzueto, D.G., Johnson, M.C., Liang, H., DeFronzo, R.A., Musi, N. (2015). Peripheral insulin resistance and impaired insulin signaling contribute to abnormal glucose metabolism in preterm baboons. *Endocrinology*, 156(3); 813-823.
64. Aronoff, S. L., Berkowitz, K., Shreiner, B., Want, L. (2004). Glucose Metabolism and Regulation: Beyond Insulin and Glucagon. *Diabetes spectrum*, 17 (3); 183-190.
65. Horowitz, M., Edelbroek, M. A., Wishart, J. M., Straathof, J. W. (1993). Relationship between oral glucose tolerance and gastric emptying in normal healthy subjects. *Diabetologia*, 36; 857–862.
66. Hunt, J.V., Dean, R. T. & Wolff, S. P. (1988). Hydroxyl radical production and autoxidative glycosylation. Glucose autoxidation as the cause of protein damage in the experimental glycation model of diabetes mellitus and ageing. *Biochemical Journal*, 256(1), 205–212.
67. Bonnefont-Rousselot, D. (2002). Glucose and reactive oxygen species. *Current Opinion in Clinical Nutrition and Metabolic Care*, 5(5); 561-568.
68. Tarr, J. M., Kaul, K., Chopra, M., Kohner, E. M., & Chibber, R. (2013). Pathophysiology of diabetic retinopathy. *ISRN ophthalmology*, *2013*, 343560.
69. Bonnefont-Rousselot, D., Beaudeux, J. L., Thérond, P., Peynet, J., Legrand, A., Delattre, J. (2004). Diabetes mellitus, oxidative stress and advanced glycation end-products. *Annales Pharmaceutiques Francaises*, 62(3); 147-157.
70. Sheikh-Ali, M., Chehade, J. M., Mooradian, A. D. (2011). The antioxidant paradox in diabetes mellitus. *American Journal of Therapeutics*, 18(3); 266-278.
71. Shi, Y., & Vanhoutte, P. M. (2009). Reactive oxygen-derived free radicals are key to the endothelial dysfunction of diabetes. *Journal of Diabetes*, 1(3):151-162.
72. Jaganjac, M., Tirosh, O., Cohen, G., Sasson, S. & Zarkovic, N. (2013). Reactive aldehydes: second messengers of free radicals in diabetes mellitus. *Free Radical Research*, 47(1); 39–48.
73. Giacco, F., & Brownlee, M. (2010). Oxidative stress and diabetic complications. *Circulation research*, *107*(9), 1058–1070.

74. Giacco, F., & Brownlee, M. (2010). Oxidative stress and diabetic complications. *Circulation Research*, 107(9); 1058-1070.
75. Tiwari, B. K., Pandey, K. B., Abidi, A. B. & Rizvi, S. I. (2013). Markers of Oxidative Stress during Diabetes Mellitus. *Journal of Biomarkers*, 2013; 1-8.
76. Brownlee, M. (2005). The pathobiology of diabetic complications: a unifying mechanism. *Diabetes*, 54(6); 1615–1625.
77. Yamagishi, S.-i. (2013). Advanced Glycation End-Products. Editor(s): Maloy, S., & Hughes, K. *Brenner's Encyclopedia of Genetics* (Second Edition), *Academic Press*, 36-38.
78. Yamagishi, s., Nakamura, K., Matsui, T., Ueda, S., Noda, Y., & Imaizumi, T. (2008). Inhibitors of Advanced Glycation End Products (AGEs): Potential Utility for the Treatment of Cardiovascular Disease. *Cardiovascular Therapeutics*, 26(1); 50-58.
79. Sivitz, W. I. & Yorek, M. A. (2010). Mitochondrial dysfunction in diabetes: from molecular mechanisms to functional significance and therapeutic opportunities. *Antioxidants and Redox Signalling*, 12(4); 537–577.
80. Teixeira, J. P., de Castro, A. A., Soares, F. V., da Cunha, E., & Ramalho, T. C. (2019). Future Therapeutic Perspectives into the Alzheimer's Disease Targeting the Oxidative Stress Hypothesis. *Molecules*, *24*(23); 4410.
81. English, P. & Williams, G. (2000). Hyperglycaemic crises and lactic acidosis in diabetes mellitus. *Postgraduate Medical Journal*, 80(943); 253–261.
82. Umpierrez, G. U., Murphy, M. B. & Kitabchi, A. E. (2002). Diabetic ketoacidosis and hyperglycemic hyperosmolar syndrome. *Diabetes Spectrum*, 15(1); 28–36.
83. American Diabetes Association (1998). Economic consequences of diabetes mellitus in the U.S. in 1997. *Diabetes Care*, 21(2); 296–309.
84. DeFronzo, R. A. & Ferrannini, E. (1991). Insulin resistance: a multifaceted syndrome responsible for NIDDM, obesity, hypertension, dyslipidemia, and atherosclerotic cardiovascular disease. *Diabetes Care*, 14(3); 173–194.
85. Al-Khalifa, A., Mathew, T. C., Al-Zaid, N. S., Mathew, E. & Dashti, H. (2011). Low carbohydrate ketogenic diet prevents the induction of diabetes using streptozotocin in rats. *Experimental and Toxicologic Pathology*, 63(7-8); 663–669.
86. Mezzetti, A., Cipollone, F. & Cuccurullo, F. (2000). Oxidative stress and cardiovascular complications in diabetes: isoprostanes as new markers on an old paradigm. *Cardiovascular Research*, 47(3); 475–488.

87. Leung, G. M. & Lam, K. S. (2000). Diabetic complications and their implications on health care in Asia. *Hong Kong Medical Journal*, 6(1); 61–68.
88. Philippe, J. & Raccah, D. (2009). Treating type 2 diabetes: how safe are current therapeutic agents? *International Journal of Clinical Practice*, 63(2); 321–332.
89. Kahn, C. R. (1985). The molecular mechanism of insulin action. *Annual Review of Medicines*, 36; 429-451.
90. Henquin, J. C. (2009). Regulation of insulin secretion: a matter of phase control and amplitude modulation. *Diabetologia*, 52; 739 –751.
91. Hayes, M. R. *et al*. (2014). Incretins and amylin: neuroendocrine communication between the gut, pancreas, and brain in control of food intake and blood glucose. *Annual review of nutrition*, 34; 237-260.
92. Thornberry, N. A. & Gallwitz, B. (2009). Mechanism of action of inhibitors of dipeptidyl-peptidase-4 (DPP-4). *Best Practice & Research Clinical Endocrinology & Metabolism*, 23(4); 479-486.
93. Rolee, P. & Bridgeman, M. B. (2010). Dipeptidyl Peptidase-4 (DPP-4) Inhibitors in the Management of Diabetes. *P & T: a peer-reviewed journal for formulary management*, 35(9); 509-513.
94. Panten, U., Schwanstecher, M. & Schwanstecher, C. (1996). Sulfonylurea receptors and mechanism of sulfonylurea action. *Experimental and clinal Endocrinology & Diabetes*, 104(1); 1-9.
95. Sehra, D., Sehra, S. & Tej Sehra, S. (2011). Sulfonylureas: Do we need to introspect safety again? Expert Opinion on Drug Safety, 10(6); 851-861.
96. Füchtenbusch, M., Standl, E. & Schatz, H. (2000). Clinical efficacy of new thiazolidinediones and glinides in the treatment of type 2 diabetes mellitus. *Experimental and Clinical Endocrinology & Diabetes*, 108(3), 151-163.
97. Murad, M. H., Coto-Yglesias, F., Wang, A. T., Sheidaee, N., Mullan, R. J., Elamin, M. B., Erwin, P. J. & Montori, V. M. (2009). Drug-Induced Hypoglycemia: A Systematic Review. *The Journal of Clinical Endocrinology & Metabolism*, 94(3); 741–745.
98. Bodmer, M., Meier, C., Krähenbühl, S., Jick, S. S. & Meier, C. R. (2008). Metformin, Sulfonylureas, or other Antidiabetes Drugs and the Risk of Lactic Acidosis or Hypoglycemia: A nested case-control analysis. *American Diabetes Association*: *Diabetes Care*, 31 (11); 2086-2091.

99. Rachmani R, Slavachevski I, Levi Z, Zadok B, Kedar Y, Ravid M (2002). Metformin in patients with type 2 diabetes mellitus: reconsideration of traditional contraindications. *European Journal of Internal Medicine,* 13:428.

100. Kalra, S. (2014). Alpha glucosidase inhibitors. *The Journal of the Pakistan Medical Association*, *64*(4); 474–476.

101. Eberhard, S. & Schnell, O. (2015). Alpha-Glucosidase Inhibitors 2012 – Cardiovascular Considerations and Trial Evaluation. *Diabetes and Vascular Disease Research* x, 163–169.

102. Peters, A. L., Buschur, E. O., Buse, J. B., Cohan, P., Diner, J. C. & Hirsch, I. B. (2015). Euglycemic Diabetic Ketoacidosis: A Potential Complication of Treatment with Sodium–Glucose Cotransporter 2 Inhibition. *American Diabetes Association*: *Diabetes Care*, 38(9); 1687-1693.

103. Vergès, B. & Halimi, S. (2014). Adverse effects and safety of SGLT-2 inhibitors. *Diabetes & Metabolism*, 40(6).

104. Davis, S. N., & Umpierrez, G. E. (2007). Diabetic ketoacidosis in type 2 diabetes mellitus--pathophysiology and clinical presentation. *Nature clinical practice. Endocrinology & metabolism*, *3*(11), 730–731.

105. Plamboeck, A., Holst, J. J., Carr, R. D., & Deacon, C. F. (2005). Neutral endopeptidase 24.11 and dipeptidyl peptidase IV are both mediators of the degradation of glucagon-like peptide 1 in the anaesthetised pig. *Diabetologia*, *48*(9), 1882-1890.

106. Willard, J. R., Barrow, B. M., & Zraika, S. (2017). Improved glycaemia in high-fat-fed neprilysin-deficient mice is associated with reduced DPP-4 activity and increased active GLP-1 levels. *Diabetologia*, *60*(4), 701-708.

107. Nougué, H., Pezel, T., Picard, F., Sadoune, M., Arrigo, M., Beauvais, F., ... & Logeart, D. (2019). Effects of sacubitril/valsartan on neprilysin targets and the metabolism of natriuretic peptides in chronic heart failure: a mechanistic clinical study. *European journal of heart failure*, *21*(5), 598-605.

108. Vodovar, N., Nougue, H., Launay, J. M., Solal, A. C., & Logeart, D. (2017). Sacubitril/valsartan in PARADIGM-HF. *The lancet Diabetes & endocrinology*, *5*(7), 495-496.

109. Wang, C. H., Leung, N., Lapointe, N., Szeto, L., Uffelman, K. D., Giacca, A., ... & Lewis, G. F. (2003). Vasopeptidase inhibitor omapatrilat induces profound insulin sensitization and increases myocardial glucose uptake in Zucker fatty rats: Studies comparing a vasopeptidase inhibitor, angiotensin-converting enzyme inhibitor, and angiotensin II type I receptor blocker. *Circulation*, *107*(14), 1923-1929.

110. Campbell, D. J., Anastasopoulos, F., Duncan, A. M., James, G. M., Kladis, A., & Briscoe, T. A. (1998). Effects of neutral endopeptidase inhibition and combined angiotensin converting enzyme and neutral endopeptidase inhibition on angiotensin and bradykinin peptides in rats. *Journal of Pharmacology and Experimental Therapeutics*, *287*(2), 567-577.

111. Henriksen, E. J., Jacob, S., Fogt, D. L., & Dietze, G. J. (1998). Effect of chronic bradykinin administration on insulin action in an animal model of insulin resistance. *American Journal of Physiology-Regulatory, Integrative and Comparative Physiology*, *275*(1), R40-R45.

112. Northridge, D., Alabaster, C., Connell, J. C., Dilly, S., Lever, A., Jardine, A., ... & Samuels, G. R. (1989). Effects of UK 69 578: a novel atriopeptidase inhibitor. *The Lancet*, *334*(8663), 591-593.

113. Scranton, R. & Cincotta, A. (2010). Bromocriptine unique formulation of a dopamine agonist for the treatment of type 2 diabetes. *Expert opinion on pharmacotherapy*, 11; 269-279.

114. Thulé, P. M. (2012). Mechanisms of current therapies for diabetes mellitus type 2. *Advances in Physiology Education*, 36; 275–283.

115. Wahlqvist, M. L., Lee, M. S., Hsu, C. C., Chuang, S. Y., Lee, J. T., Tsai, H. N. (2012). Metformin-inclusive sulfonylurea therapy reduces the risk of Parkinson's disease occurring with Type 2 diabetes in a Taiwanese population cohort. *Parkinsonism Relat Disord*, 18(6); 753-758.

116. Izzo, A. & Andrew, R. (2017). Principles of pharmacological research of nutraceuticals. *British Journal of Pharmacology*, 174(11); 1177-1194.

117. Esch, T., Fricchione, G. & Stefano, G. (2003). The therapeutic use of the relaxation response in stress-related diseases. *Medical science monitor: international medical journal of experimental and clinical research*, 9. RA23-34.

118. Odeyemi, S. W. (2015). A comparative study of the in vitro antidiabetic properties, cytotoxicity and mechanism of action of Albuca 91 racteate and Albuca setosa bulb extracts. *Doctoral dissertation [Doctoral, thesis]*, University of Fort Hare.

119. ADA (American Diabetes Association) (Jan 2006). Diagnosis and classification of diabetes mellitus. *Diabetes Care*, 29(Suppl 1); S43–S48.

120. Sagbo, I. J., van de Venter, M., Koekemoer, T. & Bradley, G. (2018). *In Vitro* Antidiabetic Activity and Mechanism of Action of *Brachylaena elliptica* (Thunb.) DC. *Evidence-Based Complementary and Alternative Medicine*.

121. Wan, Z., Lee, J., Hotchandani, R., Moretto, A., Binnun, E., Wilson, D., Kirincich, S., Follows, B., Ipek, M., Xu, W., Joseph-McCarthy, D., Zhang, Y., Tam, M., Erbe, D., Tobin, J., Li, W., Tam, S., Mansour, T., & Wu, J. (2008). Structure-Based Optimization of Protein Tyrosine Phosphatase-1 B Inhibitors: Capturing Interactions with Arginine 24, *ChemMed Chem* 3(10), 1525-1529

122. DeFronzo, R. A., (2000). Pharmacologic therapy for type 2 diabetes mellitus. *Ann. Intern. Med.*, 133 (1); 73–74.

123. Yoshioka, T., Fujita, T., Kanai, T., Aizawa, Y., Kurumada, T., Hasegawa, K., Horikoshi, H., (1989). Studies on hindered phenols and analogues. Hypolipidemic and hypoglycemic agents with ability to inhibit lipid peroxidation. *Journal of Medicinal Chemistry*, 32(2), 421– 428.

124. Momose, Y., Meguro, K., Ikeda, H., Hatanaka, C., Oi, S., & Sohda, T. (1991). Studies on antidiabetic agents: Synthesis and biological activities of pioglitazone and related compounds. *Chemical and Pharmaceutical Bulletin (Tokyo)*, 39(6); 1440–1445.

125. Cantello, B. C. C., Cawthorne, M. A., Haigh, D., Hindley, R. M., Smith, S. A., & Thurlby, P. L. (1994). The synthesis of BRL 49653 – a novel and potent anti-hyperglycaemic agent. *Bio-organic Medicinal Chemistry Letters*, 4(10); 1181–1184.

126. Krook, A., Bjo¨ rnholm, M., Galuska, D., Jiang, X. J., Fahlman, R., Myers Jr., M. G., Wallberg Henriksson, H., & Zierath, J. R. (2000). Characterization of signal transduction and glucose transport in skeletal muscle from type 2 diabetic patients. *Diabetes*, 49(2); 284– 292.

127. Scheen, A. J. (2001). Hepatotoxicity with thiazolidinediones: is it a class effect? *Drug Safety*, 24(12); 873–888.

128. Kahn, S. E., Haffner, S. M., Heise, M. A., Herman, W. H., Holman, R. R., Jones, N. P., Kravitz, B. G., Lachin, J. M., O'Neill, M. C., Zinman, B., Viberti, G. ADOPT

Study Group. (2006). glycaemic durability of rosiglitazone, metformin, or glyburide monotherapy. *New England Journal of Medicine*, 355(23); 2427–2443.

129. Lo, C., Shropshire, E. Y., & Croxall, W. J. (1953). 5- Aralkylidene-3-isobutyl-2,4-thiazolidinediones. *Journal of American Chemical Society*, 75; 4845-4846.

130. Monforte, P., Fenech, G., Basile, M., Ficarra, P. & Silvestro, A. (1979). 4-Thiazolidinones and 2,4-thiazolidinediones from α- mercaptopropionic acid and carbodiimides. *Journal of Heterocyclic Chemistry*, 16; 341-345.

131. Sohda, T., Mizuno, K., Momose, Y., Ikeda, H., Fujita, T., & Meguro, K. (1992). Studies on antidiabetic agents: Novel thiazolidinedione derivatives as potent hypoglycaemic and hypolipidemic agents. *Journal of Medicinal Chemistry*, 35; 2617-2626.

132. Koro, C., Barrett, S. & Qizilbash, N. (1999). Cancer risks in thiazolidinedione users compared to other anti-diabetic agents. *Diabetic Medicine*, 16; 485-492.

133. Banerjee, M., Sahoo, S. & Sahu, S. K. (2016). *in silico* designing and molecular docking studies on selected reported & proposed new compounds against ppar-γ receptor for type-2-diabetes. *World Journal of Pharmacy and Pharmaceutical Sciences*, 5; 1022–1030.

134. Kharbanda, C., Alam, M. S., Hamid, H., Javed, K., Bano, S., Ali, Y., Dhulap, A., Alam, P. & Pasha, M. A. Q. (2016). Novel Piperine Derivatives with Antidiabetic Effect as PPAR-c Agonists. *Chemical Biology & Drug Design*,88.

135. Rakowitz, D., Maccari, R., Ottana, R. & Vigorita, M. G. (2006). *In vitro* aldose reductase inhibitory activity of 5-benzyl-2,4- thiazolidinediones. *Bioorganic & Medicinal Chemistry*, 14; 567–574.

136. Mohammed Iqbal, A. K., Khan, A. Y., Kalashetti, M. B., Belavagi, N. S., Gong, Y. & Khazi, I. A. M. (2012). Synthesis, hypoglycaemic and hypolipidemic activities of novel thiazolidinedione derivatives containing thiazole/triazole/oxadiazole ring. *European Journal of Medicinal Chemistry*, 53; 308- 315.

137. Bhattarai, B. R., Kafle, B., Hwang, J., Ham, S. W., Lee, K., Park, H., Han, I., & Cho, H. (2010). Novel thiazolidinedione derivatives with anti-obesity effects: Dual action as PTP1B inhibitors and PPAR-c activators. *Bioorganic & Medicinal Chemistry Letters*, 20; 6758–6763.

138. Maccari, R., Ciurleo, R., Giglio, M. *et al*., (2010). Identification of new non-carboxylic acid containing inhibitors of aldose reductase. *Bioorganic & Medicinal Chemistry*, 18, 4049–4055.

139. Hidalgo Figueroa, S., Estrada-Soto, S., Ramírez-Espinosa, J., Paoli, P., Lori, G., Rivera, I., Navarrete-Vázquez, G. (2018). Synthesis and evaluation of thiazolidine-2,4-dione/benzazole derivatives as inhibitors of protein tyrosine phosphatase 1B (PTP-1B): Antihyperglycemic activity with molecular docking study. *Biomedicine & Pharmacotherapy*, 107(c), 1302-1310.

140. Ghanemi, A. (2015). Alzheimer's disease therapies: Selected advances and future perspectives. *Alexandria Journal of Medicine*, 51; 1–3.

141. Salawu, F. K., Umar, J. T. & Olokoba, A. B. (2011). Alzheimer's disease: A review of recent developments. *Annals of African Medicine*, 10(2); 73-79.

142. Kumawat, M., Sharma, T. K., Singh, I., Singh, N., Ghalaut, V. S., Vardey, S. K., & Shankar, V. (2013). Antioxidant Enzymes and Lipid Peroxidation in Type 2 Diabetes Mellitus Patients with and without Nephropathy. *North American journal of medical sciences*, *5*(3), 213–219. https://doi.org/10.4103/1947-2714.109193

143. Sinclair, A.J., 1993. Free radical mechanisms and vascular complications of diabetes mellitus. *Diabetes Rev*, *2*(2), pp.7-10.

144. Jennings, P.E. and Barnett, A.H., 1988. New approaches to the pathogenesis and treatment of diabetic microangiopathy. *Diabetic medicine*, *5*(2), pp.111-117.

145. Ganjifrockwala, F. A., Joseph, J. T. & George, G. (2017). Decreased total antioxidant levels and increased oxidative stress in South African type 2 diabetes mellitus patients. *Journal of Endocrinology, Metabolism and Diabetes of South Africa*, 22(2); 21–25.

146. Lehericy, S., Hirsch, E. C., Cervera-Pierot, P., Hersh, L. B., Bakchine, S., Piette, F., Duyckaerts, C., Hauw, J. J., Javoy-Agid, F. & Agid, Y. (1993). Heterogeneity and selectivity of the degeneration of cholinergic neurons in the basal forebrain of patients with Alzheimer's disease. *Journal of Comparative Neurology*, 330; 15-31.

147. Picciotto, M. R., Higley, M. J., & Mineur,Y. S. (2012). Acetylcholine as a Neuromodulator: Cholinergic Signaling Shapes Nervous System Function and Behavior. *Neuron*, 76(1); 116-129.

148. Liu, P. P., Xie, Y., Meng, X. Y. *et al.* (2019). History and progress of hypotheses and clinical trials for Alzheimer's disease. *Signal Transduction and Targeted Therapy*, 4(29).

149. Mullane, K. & Williams, M. (2019). Preclinical Models of Alzheimer's Disease: Relevance and Translational Validity. *Current Protocols in Pharmacology*, 84(1).

150. Stanciu, G. D., Luca, A., Rusu, R. N., Bild, V., Beschea Chiriac, S. I., Solcan, C., Bild, W., & Ababei, D. C. (2020). Alzheimer's Disease Pharmacotherapy in Relation to Cholinergic System Involvement. *Biomolecules*, 10(1); 40.

151. Picciotto, M. R., Caldarone, B. J., King, S. L., & Zachariou, V. (2000). Nicotinic receptors in the brain: Links between molecular biology and behavior. *Neuropsychopharmacology: official publication of the American College of Neuropsychopharmacology*, *22*(5); 451–465.

152. Picciotto, M. R., Higley, M. J., & Mineur, Y. S. (2012). Acetylcholine as a Neuromodulator: Cholinergic Signalling Shapes Nervous System Function and Behaviour. *Neuron*, 76(1); 116-129.

153. Stefanescu, R., Stanciu, G. D., Luca, A., Paduraru, L., & Tamba, B. I. (2020). Secondary Metabolites from Plants Possessing Inhibitory Properties against Beta-Amyloid Aggregation as Revealed by Thioflavin-T Assay and Correlations with Investigations on Transgenic Mouse Models of Alzheimer's Disease. *Biomolecules*, 10(6); 870.

154. Games, D., Adams, D., Alessandrini, R. *et al.* (1995). Alzheimer-type neuropathology in transgenic mice overexpressing V717F β-amyloid precursor protein. *Nature*, 373; 523–527.

155. Panche, A., Chandra, S., Diwan, A., & Harke, S. (2015). Alzheimer's And Current Therapeutics: A Review. *Asian Journal of Pharmaceutical and Clinical Research*, 8(3); 14 – 19.

156. Tabet, N. (2006). Acetylcholinesterase inhibitors for Alzheimer's disease: Anti-inflammatories in acetylcholine clothing! *Age and ageing*, 35(4); 336-338.

157. Tabet, N. (2006). Acetylcholinesterase inhibitors for Alzheimer's disease: anti-inflammatories in acetylcholine clothing. *Age and Ageing*, 35(4); 336–338.

158. Adewusi, E. A., Moodley, N. & Steenkamp, V. (2010). Medicinal plants with cholinesterase inhibitory activity: A Review. *African Journal of Biotechnology*, 9(49); 8257-8276.

159. Lee, J., Kim, M. & Park, S. (2017). Effect of natural antioxidants on the aggregation and disaggregation of beta-amyloid. *Tropical Journal of Pharmaceutical Research*, 16 (11); 2629-2635.

160. Wang, J., Hu, S., Nie, S., Yu, Q., & Xie, M. (2016). Reviews on Mechanisms of In Vitro Antioxidant Activity of Polysaccharides. *Oxidative Medicine and Cellular Longevity*, 2016, 569-285.

161. Obrenovich, M. E., Nair, N. G., Beyaz, A., Aliev, G., & Reddy, V. P. (2010). The role of polyphenolic antioxidants in health, disease, and aging. *Rejuvenation Research*, 13; 631-643.

162. Yaari, R., Corey-Bloom, J. (2007). Alzheimer's disease. *Seminars in Neurology*, 27:32-41.

163. Doody, R. S., Stevens, J. C., Beck, C., Dubinsky, R. M., Kaye, J. A., Gwyther, L., *et al*. (2001). Practice parameter: Management of dementia (an evidence-based review): Report of the Quality Standards Subcommittee of the American Academy of Neurology. *Neurology*, 56; 1154-1166.

164. Sugimoto, H. (2004). Scope and limitations of acetylcholinesterase inhibitors. *Nihon Yakurigaku Zasshi*, 124(3); 163-170.

165. Coelho dos, S. T., Thaís Mota, G., Araújo Serra, P. B., Leandro, C. A., & de Andrade, P. A. M. (2018). Naturally Occurring Acetylcholinesterase Inhibitors and their Potential Use for Alzheimer's Disease Therapy. *Frontiers in Pharmacology*, 9; 1192.

166. Witt, A., Macdonald, N., & Kirkpatrick, P. (2004). Memantine hydrochloride. *Nat Rev Drug Discov*, 3; 109-110.

167. Atri, A., Shaughnessy, L. W., Locascio, J. J., Growdon, J. H. (2008). Long- term course and effectiveness of combination therapy in Alzheimer' disease. *Alzheimer Dis Assoc Disord*, 22; 209-221.

168. Guo, T., Zhang, D., Zeng, Y. *et al* (2020). Molecular and cellular mechanisms underlying the pathogenesis of Alzheimer's disease. *Mol Neurodegeneration* **15,** 40.

169. Fuster, J. J., Ouchi, N., Gokce, N., & Walsh, K. (2016). Obesity-Induced Changes in Adipose Tissue Microenvironment and Their Impact on Cardiovascular Disease. *Circulation research*, *118*(11), 1786–1807.

170. Kumawat, M., Sharma, T. K., Singh, I., Singh, N., Ghalaut, V. S., Vardey, S. K., & Shankar, V. (2013). Antioxidant Enzymes and Lipid Peroxidation in Type 2 Diabetes Mellitus Patients with and without Nephropathy. *North American journal of medical sciences*, *5*(3), 213–219.

171. West, I.C., 2000. Radicals and oxidative stress in diabetes. *Diabetic medicine*, *17*(3), pp.171-180.

172. Jakus, V., 2000. The role of free radicals, oxidative stress and antioxidant systems in diabetic vascular disease. *Bratislavske lekarske listy*, *101*(10), pp.541-551.

173. Yang, Y. & Song, W. (2013). Molecular links between Alzheimer's disease and diabetes mellitus. *Neuroscience*. 250.

174. Sharma, R. K., Younis, Y., Mugumbate, G., Njoroge, M., Gut, J., Rosenthal, P. J., & Chibale, K. (2015). Synthesis and structure-activity-relationship studies of thiazolidinediones as antiplasmodial inhibitors of the Plasmodium falciparum cysteine protease falcipain-2. *European journal of medicinal chemistry*, 27(*90)*, 507–518.

175. Salamone, S., Colin, C., Grillier-Vuissoz, I., *et al*. (2012). Synthesis of new troglitazone derivatives: anti-proliferative activity in breast cancer cell lines and preliminary toxicological study. *European Journal of Medicinal Chemistry*, 51, 206-215.

176. Stocks, P. A., Raynes, K. J., Bray, P, G., Park, B. K., O'Neill, P. M., & Ward, S. A. (2002). Novel Short Chain Chloroquine Analogues Retain Activity Against Chloroquine Resistant K1 Plasmodium falciparum. *Journal of Medicinal Chemistry*, *45* (23), 4975-4983.

177. Maia, R., Tesch, R., & Fraga, C. (2012). Phenylpiperazine derivatives: A patent review (2006 – Present). *Expert opinion on therapeutic patents*, 22(10), 1169-1178.

178. Oderinlo, O. O. (2019). Synthesis, characterisation and biological evaluation of novel anti-infective compounds bearing ferrocene, arylpyrrole, thiazolidinedione, quinoline and triazole moieties. *Doctoral dissertation [Doctoral, thesis]*, Rhodes university.

179. Cardoso, S., & Moreira, P. (2020). Antidiabetic drugs for Alzheimer's and Parkinson's diseases: Repurposing insulin, metformin, and thiazolidinediones. *International Review of Neurobiology*, *155*, 37-64.

180. Pérez, M., & Quintanilla, R. (2015). Therapeutic Actions of the Thiazolidinediones in Alzheimer's Disease. *PPAR Research*, *2015*, 1-8.

181. Zolezzi, J. M., & Inestrosa, N. C. (2013). Peroxisome proliferator-activated receptors and Alzheimer's disease: hitting the blood–brain barrier. *Molecular neurobiology*, *48*(3), 438-451.

182. Heneka, M. T., Fink, A., & Doblhammer, G. (2015). Effect of pioglitazone medication on the incidence of dementia. *Annals of neurology*, *78*(2), 284-294.

183. Cheng, H., Shang, Y., Jiang, L., Shi, T. L., & Wang, L. (2016). The peroxisome proliferators activated receptor-gamma agonists as therapeutics for the treatment of

Alzheimer's disease and mild-to-moderate Alzheimer's disease: a meta-analysis. *International Journal of Neuroscience*, *126*(4), 299-307.

184. Dello Russo, C., Gavrilyuk, V., Weinberg, G., Almeida, A., Bolanos, J., & Palmer, J. *et al*. (2003). Peroxisome Proliferator-activated Receptor γ Thiazolidinedione Agonists Increase Glucose Metabolism in Astrocytes. *Journal Of Biological Chemistry*, *278*(8), 5828-5836.

185. Feinstein, D. L., Galea, E., Gavrilyuk, V., Brosnan, C. F., Whitacre, C. C., Dumitrescu-Ozimek, L., ... & Heneka, M. T. (2002). Peroxisome proliferator-activated receptor-γ agonists prevent experimental autoimmune encephalomyelitis. *Annals of Neurology: Official Journal of the American Neurological Association and the Child Neurology Society*, *51*(6), 694-702.

186. Heneka, M. T., Landreth, G. E., & Feinstein, D. L. (2001). Role for peroxisome proliferator-activated receptor-γ in Alzheimer's disease. *Annals of Neurology: Official Journal of the American Neurological Association and the Child Neurology Society*, *49*(2), 276-276.

187. Heneka, M. T., Feinstein, D. L., Galea, E., Gleichmann, M., Wüllner, U., & Klockgether, T. (1999). Peroxisome proliferator-activated receptor gamma agonists protect cerebellar granule cells from cytokine-induced apoptotic cell death by inhibition of inducible nitric oxide synthase. *Journal of neuroimmunology*, *100*(1-2), 156-168.

188. Daina, A., Michielin, O. & Zoete, V. (2017). SwissADME: a free web tool to evaluate pharmacokinetics, drug-likeness and medicinal chemistry friendliness of small molecules. *Scientific Report* **7,** 42717.

189. Benzie, I.F., & Strain, J.J. (1996). The ferric reducing ability of plasma (FRAP) as measurement of "antioxidant power" The FRAP assay. *Analytical Biochemistry*, 239(1),70–76.

190. Kwon, Y.I., Apostolidis, E., Kim, Y.C., Shetty, K. (2007). Health benefits of traditional corn, beans and pumpkin: in vitro studies for hyperglycaemia and hypertension management. Journal of Medicinal Food. 10, 266–275.

191. Worthington Biochemical Corp., 1993a. Alpha amylase. In: V. Worthington (Eds.), *Worthington Enzyme Manual. Freehold*, 36–41.

192. Worthington Biochemical Corp., 1993b. Maltase-a-glucosidase. In: V. Worthington (Eds.), Worthington Enzyme Manual. Freehold, 261.

193. Fatmawati, S., Ersam, T., Shimizu, K. (2015). The inhibitory activity of aldose reductase in vitro by constituents of Garcinia mangostana Linn. *Phytomedicine*, 22(1), 49–51.

194. Kazeem, M. I., Adeyemi1, A. A., Adenowo, A. F., & Akinsanya, M. A. (2020). Carica papaya Linn. Fruit extract inhibited the activities of aldose reductase and sorbitol dehydrogenase: possible mechanism for amelioration of diabetic complications. *Future Journal of Pharmaceutical Sciences*, 6, 96.

195. Ang L, Cao J, Duan L, *et al*. (2014). Protein tyrosine phosphatase 1B (PTP1B) and a-glucosidase inhibitory activities of Schisandra chinensis (Turcz.) Baill. *Journal of Functional Foods*, 9, 264–270.

196. Song, Y. H., Uddin, Z., Jina, Y. M., Lia, Z., Curtis-Longb, M. J., Kimc, K. D., Choa, J. K., & Parka, K. H. (2017) Inhibition of protein tyrosine phosphatase (PTP1B) and a-glucosidase by geranylated flavonoids from Paulownia tomentosa. *Journal of Enzyme Inhibition and Medicinal Chemistry*, 32(1), 1195–1202.

197. Sigma-aldrich. DPP4 inhibitor screening Kit (MAK203).

198. Liberato, M.V., Nascimento, A.S., Polikarpov, I. Human peroxisome proliferator-activated receptor gamma in complex with rosiglitazone**.**

199. ProteinsPlus, a free web tool, ZBH – centre for Bioinformatics; available from: https://proteins.plus/

200. Dasme, M. F. *et al*. Protein-Ligand Interaction Profiler (PLIP) 2021: expanding the scope of the protein–ligand interaction profiler to DNA and RNA. Nucl. Acids Res. 2021.

201. Ellman, G.L., Courtney, K.D., Andres, V.J., & Featherstone, R.M. (1961). A new and rapid colorimetric determination of acetylcholinesterase activity. *Biochemical Pharmacology,* 7, 88–95.

202. Yousof Ali, M., Jung, H.A. & Choi, J.S. (2015). Anti-diabetic and anti-Alzheimer's disease activities of *Angelica decursiva*. *Archives of Pharmacal Research,* 38(12)**,** 2216–2227.

203. Sigma-aldrich. MMP-1 inhibitor screening Kit (MAK212).

204. Ozadali-Sari, K., Tüylü Küçükkılınç, T., Ayazgok, B., Balkan, A., & Unsal-Tan, O. (2017). Novel multi-targeted agents for Alzheimer's disease: Synthesis, biological evaluation, and molecular 98eview98ng of novel 2-[4-(4-substitutedpiperazin-1-yl)phenyl]benzimidazoles. *Bioorganic chemistry*, *72*, 208–214.

205. Bowden, A.C. (1974). A simple method for determining the inhibition constants of mixed, uncompetitive and non-competitive inhibitors. *Biochemistry Journal,* 137, 143–144.

206. Dixon, M. (1953). The determination of enzyme inhibitor constants. *Biochemistry Journal*, 55, 170–171.

207. Balan, K., Ratha, P., Prakash, G., Viswanathamurthi, P., Adisakwattana, S., Palvannan, T. (2017). Evaluation of invitro α-amylase and α-glucosidase inhibitory potential of N2O2 schiff base Zn complex, *Arabian Journal of Chemistry*, 10(5), 732-738.

208. Yin, N., Cai, X., Wang, P., Feng, R., Du, H., Fu, Y., Sun, G, & Cui, Y. (2021). Predictive capabilities of in vitro colon bio-accessibility for estimating in vivo relative bioavailability of arsenic from contaminated soils: Arsenic speciation and gut microbiota considerations, *Science of The Total Environment*.

209. Souto E.B., Müller R.H. (2010) Lipid Nanoparticles: Effect on Bioavailability and Pharmacokinetic Changes. In: Schäfer-Korting M. (eds) *Drug Delivery*. *Handbook of Experimental Pharmacology*, 197, 115-141.

210. Brinton, R.D., Yamazaki, R.S. (1998). Advances and Challenges in the Prevention and Treatment of Alzheimer's Disease. *Pharmaceutical Research*, 15**,** 386–398.

211. Pardridge W. M. (2020). Treatment of Alzheimer's Disease and Blood-Brain Barrier Drug Delivery. *Pharmaceuticals (Basel, Switzerland)*, *13*(11), 394.

212. Pardridge, W.M. (2005). The blood-brain barrier: Bottleneck in brain drug development. *NeuroRx*, 2, 3–14.

213. Bonate, P. Pharmacokinetic-Pharmacodynamic Modeling and Simulation. Pharmacokinetic-Pharmacodynamic Modeling and Simulation (2006). 1-387.

214. Ramasubbu, N., Ragunath. C., Mishra, P.J., Thomas, L.M., Gyemant, G., & Kandra, L. (2004). Human salivary alpha-amylase Trp58 situated at subsite-2 is critical for enzyme activity. *European Journal of Medicinal Chemistry*, 271, 2517-2529.

215. Kwon, Y. I., Apostolidis, E., & Shetty, K. (2007). Evaluation of pepper (Capsicum annuum) for management of diabetes and hypertension. *Journal of Food Biochemistry*, *31*(3), 370-385.

216. Mccue, P., Kwon, Y. I., & Shetty, K. (2005). Anti-amylase, anti-glucosidase and anti-angiotensin i-converting enzyme potential of selected foods. *Journal of food biochemistry*, *29*(3), 278-294.

217. Apostolidis, E., Kwon, Y. I., & Shetty, K. (2007). Inhibitory potential of herb, fruit, and fungal-enriched cheese against key enzymes linked to type 2 diabetes and hypertension. *Innovative Food Science & Emerging Technologies*, *8*(1), 46-54.

218. Matsuda, H., Morikawa, T., & Yoshikawa, M. (2002). Antidiabetogenic constituents from several natural medicines. *Pure and Applied Chemistry*, *74*(7), 1301-1308.

219. Shai, L. J., Masoko, P., Mokgotho, M. P., Magano, S. R., Mogale, A. M., Boaduo, N., & Eloff, J. N. (2010). Yeast alpha glucosidase inhibitory and antioxidant activities of six medicinal plants collected in Phalaborwa, South Africa. *South African Journal of Botany*, *76*(3), 465-470.

220. Amtul, Z., Rahman, A., Siddiqui, R., Choudhary, M. I. (2002). Chemistry and Mechanism of Urease Inhibition. *Current medicinal chemistry*, 9, 1323-1348.

221. Giuberti, G., Rocchetti, G., & Lucini, L. (2020). Interactions between phenolic compounds, amylolytic enzymes and starch: an updated overview. *Current Opinion In Food Science*, *31*, 102-113.

222. Marwa, T., Elisabetta, R., Niccoletta, B., Grazia, C. M., Ranjana, R., Guillaume, S., & Aldo, B. R. (2015). Strategies for the chemical and biological functionalization of scaffolds for cardiac tissue engineering: a review. *Journal of Royal Society Interface*, 12(108).

223. Baroroh, U., Yusuf, M., Rachman, S. D., Ishmayana, S., Syamsunarno, M. A. A., Levita, J., & Subroto,T. (2017). "The Importance of Surface-Binding Site towards Starch-Adsorptivity Level in *α*-Amylase: A Review on Structural Point of View", *Enzyme Research*.

224. Guan, Lan & Hu, Yonglin & Kaback, Ronald. (2003). Aromatic Stacking in the Sugar Binding Site of the Lactose Permease. Biochemistry. 42(6). 1377-1382.

225. Park, H., Hwang, K. Y., Kim, Y. H., Oh, K. H., Lee, J. Y., & Kim, K. (2008). Discovery and biological evaluation of novel α-glucosidase inhibitors with in vivo antidiabetic effect. *Bioorganic & medicinal chemistry letters*, *18*(13), 3711-3715.

226. Li, N., Wang, F., Niu, S., Cao, J., Wu, K., Li, Y., … & Yin, Y. (2009). Discovery of novel inhibitors of Streptococcus pneumoniae based on the virtual screening with the homology-modeled structure of histidine kinase (VicK). *BMC microbiology*, *9*(1), 1-11.

227. Chen, J., Wu, S., Zhang, Q., Yin, Z., Zhang, L. (2020). α-Glucosidase inhibitory effect of anthocyanins from Cinnamomum camphora fruit: Inhibition kinetics and

mechanistic insights through in vitro and in silico studies, *International Journal of Biological Macromolecules*, 143, 696-703.

228. Fettach, S., Thari, F. Z., Hafidi, Z., Tachallait, H., Karrouchi, K., El achouri. M., Cherrah, Y., Sefrioui, H., Bougrin, K. & Faouzi, M. E. A. (2021). Synthesis, α-glucosidase and α-amylase inhibitory activities, acute toxicity and molecular docking studies of thiazolidine-2,4-diones derivatives, *Journal of Biomolecular Structure and Dynamics*.

229. Maher, S., & Brayden, D. J. (2021). Formulation strategies to improve the efficacy of intestinal permeation enhancers, *Advanced Drug Delivery Reviews*, 177, 113925.

230. Avogaro, A., Dardano, A., de Kreutzenberg, S. V., & Del Prato, S. (2015). Dipeptidyl peptidase-4 inhibitors can minimize the hypoglycaemic burden and enhance safety in elderly people with diabetes. *Diabetes, obesity & metabolism*, *17*(2), 107–115.

231. Thornberry, N. A., & Gallwitz, B. (2009). Mechanism of action of inhibitors of dipeptidyl-peptidase-4 (DPP-4). *Best practice & research. Clinical endocrinology & metabolism*, *23*(4), 479–486.

232. Guo, W., Wisniewski, J. A., & Ji, H. (2014). Hot spot-based design of small-molecule inhibitors for protein–protein interactions. *Bioorganic & medicinal chemistry letters*, *24*(11), 2546-2554.

233. Arulmozhiraja, S., Matsuo, N., Ishitsubo, E., Okazaki, S., Shimano, H., & Tokiwa, H. (2016). Comparative Binding Analysis of Dipeptidyl Peptidase IV (DPP-4) with Antidiabetic Drugs – An Ab Initio Fragment Molecular Orbital Study. *PloS one*, *11*(11).

234. Gadanec, L. K., McSweeney, K. R., Qaradakhi, T., Ali, B., Zulli, A., & Apostolopoulos, V. (2021). Can SARS-CoV-2 Virus Use Multiple Receptors to Enter Host Cells?. *International journal of molecular sciences*, *22*(3), 992.

235. Gorkhali, R., Koirala, P., Rijal, S., Mainali, A., Baral, A., & Bhattarai, H. K. (2021). Structure and Function of Major SARS-CoV-2 and SARS-CoV Proteins. *Bioinformatics and biology insights*, *15*.

236. Lalloyer, F. & Staels, B. (2010). "Fibrates, glitazones, and peroxisome proliferator-activated receptors," *Arteriosclerosis, Thrombosis, and Vascular Biology*, 30(5), 894–899.

237. Shulman, A. I. & Mangelsdorf, D. J. (2005). "Retinoid X receptor heterodimers in the metabolic syndrome," *New England Journal of Medicine*, 353(6), 604–615.

238. Heikkinen, S., Auwerx, J. & Argmann, C. A. “PPARγ in human and mouse physiology,” *Biochimica et Biophysica Acta: Molecular and Cell Biology of Lipids*, 1771(8), 999– 1013.

239. Viswakarma, N., Jia, Y., & Bai, L. (2010). “Coactivators in PPAR regulated gene expression,” *PPAR Research*.

240. Yu, S. & Reddy, J. K. (2007). “Transcription coactivators for peroxisome proliferator-activated receptors,” *Biochimica et Biophysica Acta—Molecular and Cell Biology of Lipids*, 1771(8), 936–951.

241. Choi, J., Ko, Y., Lee, H. S., Park, Y. S., Yang, Y, & Yoon, S. (2010). Identification of (β-carboxyethyl)-rhodanine derivatives exhibiting peroxisome proliferator-activated receptor γ activity. *European Journal of Medicinal Chemistry*, 45(1), 193-202.

242. Kroker, A. J., Bruning, J. B. (2015). "Review of the Structural and Dynamic Mechanisms of PPARγ Partial Agonism", *PPAR Research*, 2015, 1-15.

243. Long, N., Le Gresley, A., & Wren, S. P. (2021). Thiazolidinediones: An In–Depth Study of Their Synthesis and Application to Medicinal Chemistry in the Treatment of Diabetes Mellitus, 16(11); 1717-1736.

244. Purohit, S. S., Alman, A., & Shewale, J. (2012). Synthesis and antimicrobial activity of a new series of 3, 5-disustitutedthiazolidine-2, 4-diones. *International Journal of Pharmacy and Pharmaceutical Science*, *4*(3), 273-276.

245. Avruch, J. (1998). Insulin signal transduction through protein kinase cascades. *Molecular and Cellular Biochemistry.*, 182(1-2): 31-48.

246. White, M. F. (1997). The insulin signalling system and the IRS proteins. *Diabetologia*, 40, S2-S17.

247. Holman, G.D., Kasuga, M. (1997). From receptor to transporter: insulin signalling to glucose transport. *Diabetologia*, 40: 991-1003.

248. Yousof Ali, M., Jung, H. A., & Choi, J. S. (2015). Anti-diabetic and anti-Alzheimer's disease activities of Angelica decursiva. *Archives of pharmacal research*, *38*(12), 2216–2227.

249. Johnson, T.O., Ermolieff, J. & Jirousek, M.R. (2002). Protein tyrosine phosphatase 1B inhibitors for diabetes. *Nature Reviews Drug Discovery*, 1: 696–709.

250. Zhang, Z. (2002). Protein tyrosine phosphatases: Structure and function, substrate specificity, and inhibitor development. *Annual Review of Pharmacology and Toxicology*, 42: 209–234.

251. Bhattarai, B. R., Kafle, B., Hwang, J. S., Khadka, D., Lee, S. M., Kang, J. S., ... & Cho, H. (2009). Thiazolidinedione derivatives as PTP1B inhibitors with antihyperglycemic and anti-obesity effects. *Bioorganic & medicinal chemistry letters*, *19*(21), 6161-6165.

252. Oyedemi, S.O., Oyedemi, B.O., Arowosegbe, S., Afolayan, A.J. (2012). Phyto-chemicals analysis and medicinal potentials of hydroalcoholic extract from Curtisia dentata (Burm. F) Ca Sm stem bark. *International Journal of Molecular Science*, 13(5): 6189–6203.

253. Chung, S.S.M., Ho, E.C.M., Lam, K.S.L., Chung, S.K. (2003). Contribution of polyol pathway to diabetes-induced oxidative stress. *Journal of American Society of Nephrology*, 14(suppl 3): S233–S236.

254. Beaufils, C., Man, H., De Poulpiquet, A., Mazurenko, I. & Lojou, E. (2021). From Enzyme Stability to Enzymatic Bioelectrode Stabilization Processes. Catalysts. 11(4).

255. Saad, M.I., Abdelkhalek, T.M., Saleh, M.M. *et al.* (2015). Insights into the molecular mechanisms of diabetes-induced endothelial dysfunction: focus on oxidative stress and endothelial progenitor cells. *Endocrine* 50**,** 537–567.

256. Akter, R., Afrose, A., Rahman, M. R., Chowdhury, R., Nirzhor, S., Khan, R. I., & Kabir, M. T. (2021). A Comprehensive Analysis into the Therapeutic Application of Natural Products as SIRT6 Modulators in Alzheimer's Disease, Aging, Cancer, Inflammation, and Diabetes. *International journal of molecular sciences*, *22*(8), 4180.

257. Veeresham, C., Rao, A. Asres, K. (2014). Aldose Reductase Inhibitors of Plant Origin. *Phytotherapy research*, 28(3).

258. Lobo, V., Patil, A., Phatak, A., & Chandra, N. (2010). Free radicals, antioxidants and functional foods: Impact on human health. *Pharmacognosy reviews*, *4*(8), 118–126.

259. Wagner, H, Bladet, S, et.al. (1996). Plant Drug Analysis-A TLC Atlas, 1st Edn, Springer verlag Berlin, Heidel berg, New York, 195-214.

260. Handa, S.S, Vasisht, K, et.al. (2006). Compendium of Medicinal and Aromatic Plants-Asia, II, ICS-UNIDO, AREA Science Park, Padriciano, Trieste, Italy, 79-83.

261. Balan, K., Ratha, P., Prakash, G., Viswanathamurthi, P., Adisakwattana, S., & Palvannan, T. (2017). Evaluation of invitro α-amylase and α-glucosidase inhibitory potential of N2O2 schiff base Zn complex, *Arabian Journal of Chemistry*, 10 (5), 732-738.

262. Sehlin, D., Fang, X.T., Cato, L., Antoni, G., Lannfelt, L., & Syvänen, S. (2016). Antibody-based PET imaging of amyloid beta in mouse models of Alzheimer's disease *Nature Communications*, 7, Article 10759.

263. Winblad, B., Andreasen, N., Minthon, L., Floesser, A., Imbert, G., Dumortier, T., Maguire, R., Blennow, K., Lundmark, J., Staufenbiel, M., Orgogozo, J., Graf, A. (2012). Safety, tolerability, and antibody response of active A?? immunotherapy with CAD106 in patients with Alzheimer's disease: Randomised, double-blind, placebo-controlled, first-in-human study. *Lancet neurology*, 11(7), 597-604.

264. Maradni, A., Khoshnevisan, A., Mousavi, S. H., Emamirazavi, S. H., & Noruzijavidan, A. (2013). Role of matrix metalloproteinases (MMPs) and MMP inhibitors on intracranial aneurysms: a review article. *Medical journal of the Islamic Republic of Iran*, *27*(4), 249–254.

265. Francis, P.T., Palmer, A.M., Snape, M. (1999). The cholinergic hypothesis of Alzheimer's disease: A review of progress. *Journal of Neurology, Neurosurgery and Psychiatry*, 54: 137–147.

266. Kwon, S.H., H.K. Lee, J.A. Kim, S.I. Hong, H.C. Kim, and T.H. Jo. (2010). Neuroprotective effects of chlorogenic acid on scopolamine- induced amnesia via anti-acetylcholinesterase and antioxidative activities in mice. *European Journal of Pharmacology*, 649: 210–217.

267. Érica C.M. Nascimento, João B.L. Martins, Maria L. dos Santos, R. Gargano. (2008). Theoretical study of classical acetylcholinesterase inhibitors, *Chemical Physics Letters*, 458(4 – 6), 285-289.

268. Axelsen, P.H., Harel, M., Silman, I., Sussman, J.L. (1994) *Protein Science.*, 3, 188.

269. Zhang, Y., Kua, J., & McCammon, J. (2002). Role of the Catalytic Triad and Oxyanion Hole in Acetylcholinesterase Catalysis: An ab initio QM/MM Study. *Journal Of The American Chemical Society*, *124*(35), 10572-10577

270. Sussman, J., & Silman, I. (1992). Acetylcholinesterase: structure and use as a model for specific cation—protein interactions. *Current Opinion In Structural Biology*, *2*(5), 721-729.

271. Harel, M., Schalk, I., Ehret-Sabatier, L., Bouet, F., Goeldner, M., & Hirth, C. *et al*. (1993). Quaternary ligand binding to aromatic residues in the active-site gorge of acetylcholinesterase. *Proceedings Of The National Academy Of Sciences*, *90*(19), 9031-9035.

272. Rosenberry, T. (2009). Strategies to Resolve the Catalytic Mechanism of Acetylcholinesterase. *Journal Of Molecular Neuroscience*, *40*(1-2), 32-39.

APPENDICES

Appendix A: Abstract submitted and presented on during the faculty of pharmacy postgraduate conference 2021

Mr Charles Arineitwe

- M.Sc. Candidate

In-Vitro Screening of Thiazolidinedione-Derivatives on Diabetes and Alzheimer's Therapeutic Targets

C.Arineitwe, N. Sibiya, S.D. Khanye

Pharmacology/Pharmaceutical Sciences

There has been an increased prevalence of diabetes and other non-communicable diseases in Sub-Saharan Africa and globally [1-3]. In South Africa, the prevalence of type 2 DM is currently estimated at 9.0% in people aged 30 and older, and is expected to increase [4]. Diabetes-related complications result in acute alterations in the mental state due to poor metabolic control as well as greater rates of decline in cognitive functioning with age, higher prevalence of depression and increased risk of Alzheimer's disease (AD) [5]. AD is the most common form of dementia in older adults and possibly contributes to 60 - 70% of cases [6]. AD remains incurable, its progression inevitable with the currently available symptomatic therapies being palliative while the treatment of diabetes relies on insulin preparations and other glucose-lowering agents. Current DM treatment options have numerous side effects such as hypoglycaemia, diarrhoea, weight gain and abnormal liver function [7]. New generations of small molecules are being investigated which exhibit improved efficacy and safety profiles [8]. Several studies have shown that thiazolidinediones and their corresponding derivatives exhibit a broad spectrum of biological activities including anti-inflammatory, and antioxidant activities. Furthermore, recent evidence from experimental, epidemiological and clinical studies have proven the utility of antioxidants which might therefore be helpful for treating diabetes and its complication, and suppressing glycaemia has been shown to be beneficial in AD treatment. This study, therefore, aimed at in-vitro screening for anti-diabetic and anti-Alzheimer's properties of synthesized thiazolidinedione-derivates owing to their antioxidant properties.

REFERENCES

1. Bradshaw, D., Norman, R., Pieterse, D., Levitt, N. S., &the South African Comparative Risk Assessment Group. Estimating the burden of disease attributable to diabetes South Africa in 2000. *South African Medical Journal* (2007), 96(7); 700-705.

2. Pheiffer, C., Pillay-van Wyk,V., Joubert, J.D., et al. The prevalence of type 2 diabetes in South Africa: a systematic review protocol. *British Medical Journal Open* (2018), 8(7), doi:10.1136/ bmjopen-2017-021029

3. Erasmus, R., Soita, D., Hassan, M., Blanco-Blanco, E., Vergotine, Z., Kengne, A., & Matsha, T. High prevalence of diabetes mellitus and metabolic syndrome in a South African coloured population: Baseline data of a study in Bellville, Cape Town. *South African Medical Journal* (2012), *102*(11); 841-844, doi:10.7196/SAMJ.5670

4. Govender, R. D., Gathiram, P. & Panajatovic, M. Poor control and management of type 2 diabetes mellitus at an under-resourced South African Hospital: is it a case of clinical inertia? *South African Family Practice* (2017), 59(5); 154-159, doi: 10.1080/20786190.2017.1307909

5. Aruoma, O. I., Narrain, D., Indelicato, J., Bourdon, E., Murad, F., Bahorun, T. Cognitive impairment in patients with type 2 diabetes mellitus: Perspectives and challenges. *Arch Med Biomed Res* (2014), 1 (2); 79-89.

6. Alzheimer's Association. Alzheimer's disease facts and figures. *Alzheimers Dement* (2012), 8(2); 131-168, doi: 10.1016/j.jalz.2012.02.001

7. Odeyemi, S. W. A comparative study of the in vitro antidiabetic properties, cytotoxicity and mechanism of action of Albuca racteate and Albuca setosa bulb extracts. *Doctoral dissertation [Doctoral, thesis]* (2015), University of Fort Hare.

8. Mohammed Iqbal, A. K., Khan, A. Y., Kalashetti, M. B., Belavagi, N. S., Gong, Y. & Khazi, I. A. M. Synthesis, hypoglycaemic and hypolipidemic activities of novel thiazolidinedione derivatives containing thiazole/triazole/oxadiazole ring. *European Journal of Medicinal Chemistry* (2012), 53; 308- 315.

Appendix B: ADME profiling of our TZD-derivatives

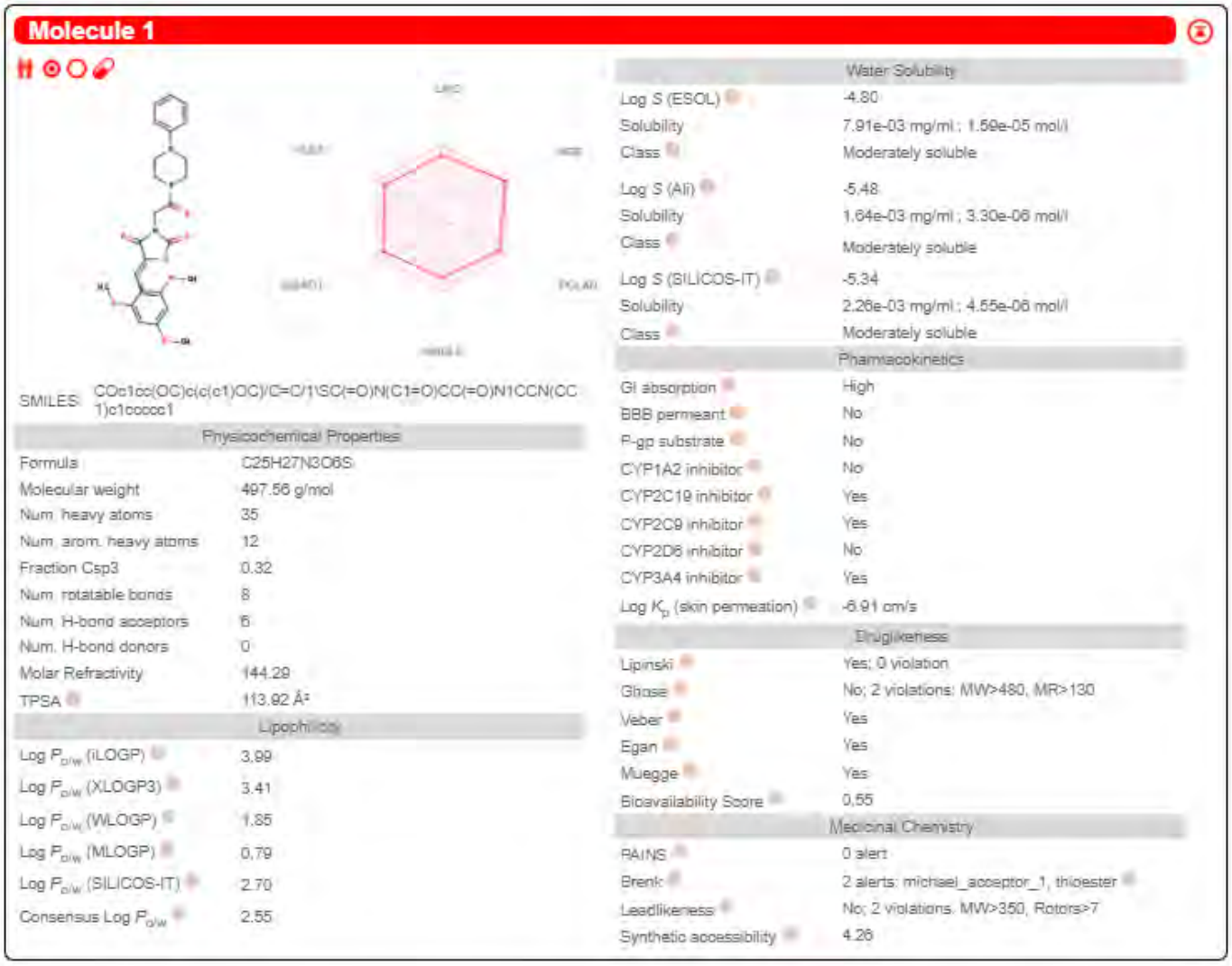

Figure B1: Detailed ADME profiling of TZDD1, generated from SwissADME: *Sci. Rep.* (2017) 7:42717.

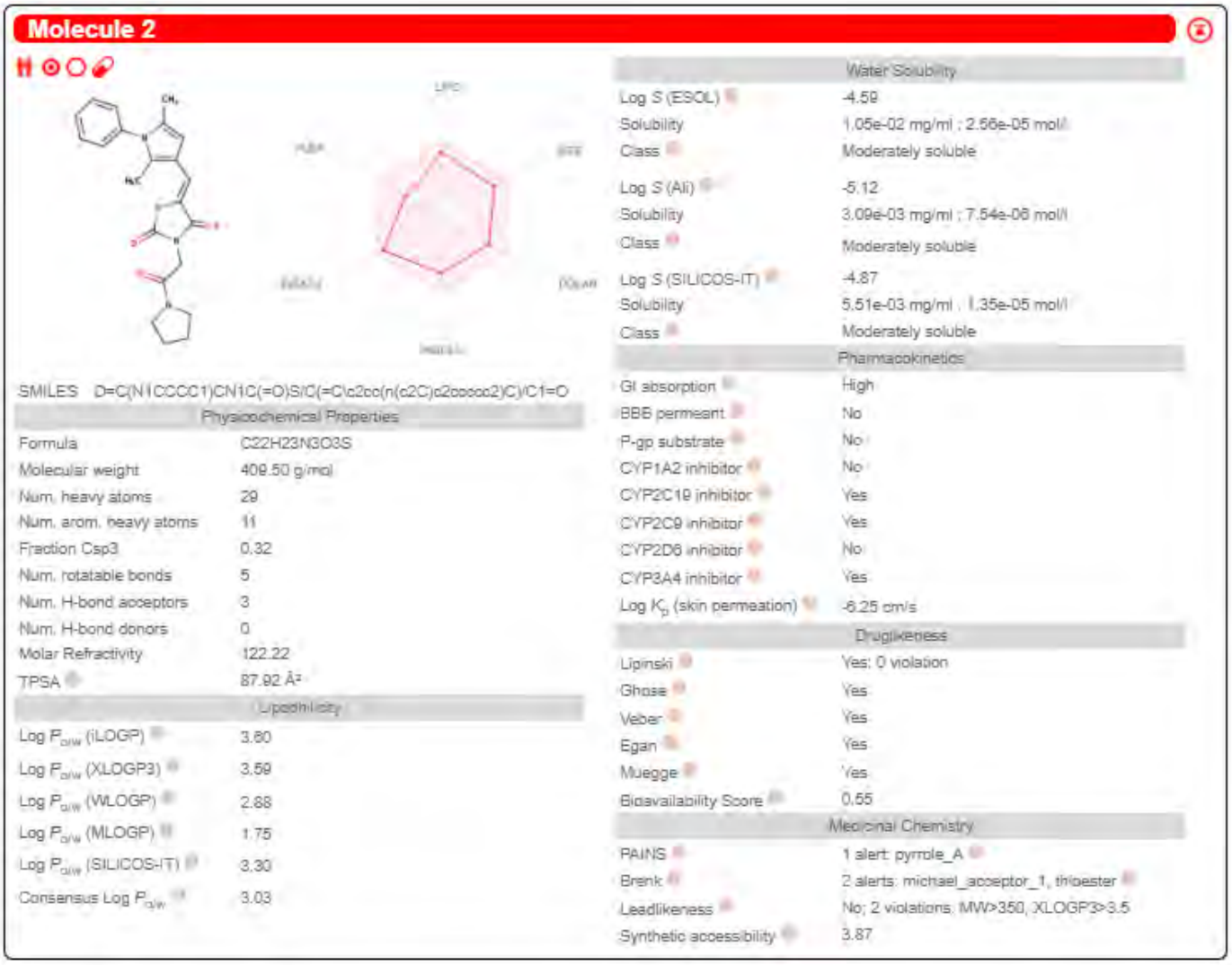

Figure B2: Detailed ADME profiling of TZDD2, generated from SwissADME: *Sci. Rep.* (2017) 7:42717.

Figure B3: Detailed ADME profiling of TZDD3, generated from SwissADME: *Sci. Rep.* (2017) 7:42717.

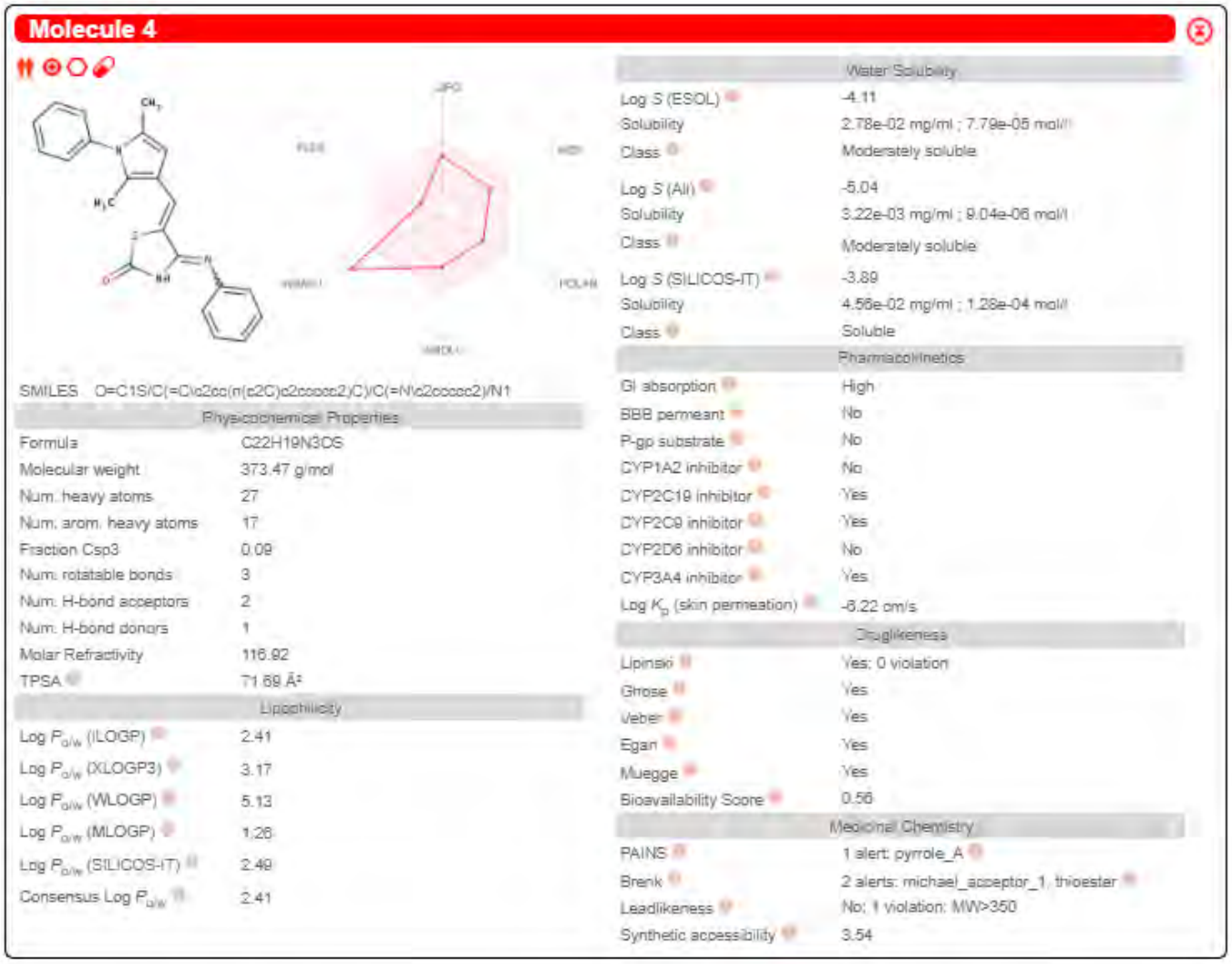

Figure B4: Detailed ADME profiling of TZDD4, generated from SwissADME: *Sci. Rep.* (2017) 7:42717.

Appendix C: In-silico determination of PPARγ activation using autodock tools.

CLUSTERING HISTOGRAM

Cluster Rank	Lowest Binding Energy	Run	Mean Binding Energy	Num in Clus	Histogram 5 10 15 20 25 30 35
1	-8.63	6	-8.63	1	#
2	-8.47	49	-8.17	5	#####
3	-8.42	48	-8.06	11	##########
4	-8.41	24	-8.37	3	###
5	-8.08	18	-8.02	3	###
6	-8.07	2	-7.66	3	###
7	-7.99	25	-7.90	3	###
8	-7.98	28	-7.63	2	##
9	-7.86	47	-7.79	2	##
10	-7.86	21	-7.74	2	##
11	-7.82	5	-7.82	1	#
12	-7.82	30	-7.82	1	#
13	-7.79	10	-7.62	2	##
14	-7.61	22	-7.61	1	#
15	-7.61	39	-7.61	1	#
16	-7.58	16	-7.38	3	###
17	-7.38	20	-7.38	1	#
18	-7.36	37	-7.36	1	#
19	-7.28	32	-7.28	1	#
20	-7.06	44	-7.06	1	#
21	-6.55	26	-6.55	1	#
22	-6.34	8	-6.34	1	#

Number of multi-member conformational clusters found = 11, out of 50 runs.

Figure C1: Cluster conformations analysis of Rosiglitazone

RMSD TABLE

Rank	Sub-Rank	Run	Binding Energy	Cluster RMSD	Reference RMSD	Grep Pattern
1	1	6	-8.63	0.00	26.19	RANKING
2	1	49	-8.47	0.00	25.03	RANKING
2	2	50	-8.24	0.92	25.26	RANKING
2	3	29	-8.21	1.90	24.25	RANKING
2	4	19	-8.19	1.88	24.10	RANKING
2	5	42	-7.76	1.81	24.94	RANKING
3	1	48	-8.42	0.00	24.72	RANKING
3	2	13	-8.40	1.03	24.87	RANKING
3	3	7	-8.38	0.76	24.18	RANKING
3	4	11	-8.27	1.77	24.78	RANKING
3	5	31	-8.14	1.51	24.66	RANKING
3	6	17	-8.13	1.26	24.69	RANKING
3	7	1	-8.02	1.83	24.06	RANKING
3	8	45	-7.85	1.68	24.45	RANKING
3	9	27	-7.79	1.94	24.44	RANKING
3	10	23	-7.72	1.99	24.32	RANKING
3	11	3	-7.60	1.72	25.36	RANKING
4	1	24	-8.41	0.00	25.38	RANKING
4	2	33	-8.39	0.85	25.34	RANKING
4	3	9	-8.30	1.67	25.32	RANKING
5	1	18	-8.08	0.00	25.76	RANKING
5	2	34	-8.01	1.64	25.38	RANKING
5	3	35	-7.95	1.97	26.03	RANKING
6	1	2	-8.07	0.00	22.86	RANKING
6	2	38	-7.68	1.53	22.71	RANKING
6	3	15	-7.23	1.29	22.45	RANKING
7	1	25	-7.99	0.00	24.10	RANKING

Figure C2: RMSD table of Rosiglitazone

INFORMATION ENTROPY ANALYSIS FOR THIS CLUSTERING

Information entropy for this clustering = 0.71 (rmstol = 2.00 Angstrom)

STATISTICAL MECHANICAL ANALYSIS

Partition function, Q =   50.66   at Temperature, T = 298.15 K
Free energy,   A ~ -2325.61 kcal/mol   at Temperature, T = 298.15 K
Internal energy,   U =   -7.81 kcal/mol   at Temperature, T = 298.15 K
Entropy,   S =   7.77 kcal/mol/K at Temperature, T = 298.15 K

Figure C3: Entropy analysis for Rosiglitazone

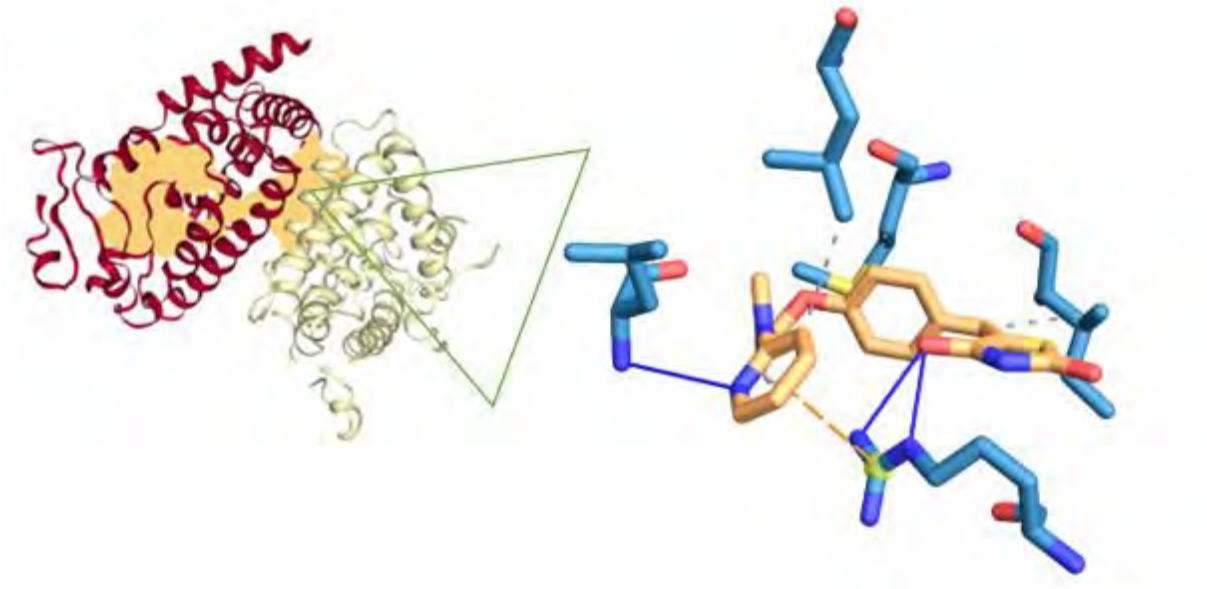

Figure C4: Rosiglitazone interacting with PPARγ (highest ranked cluster conformation analysed)

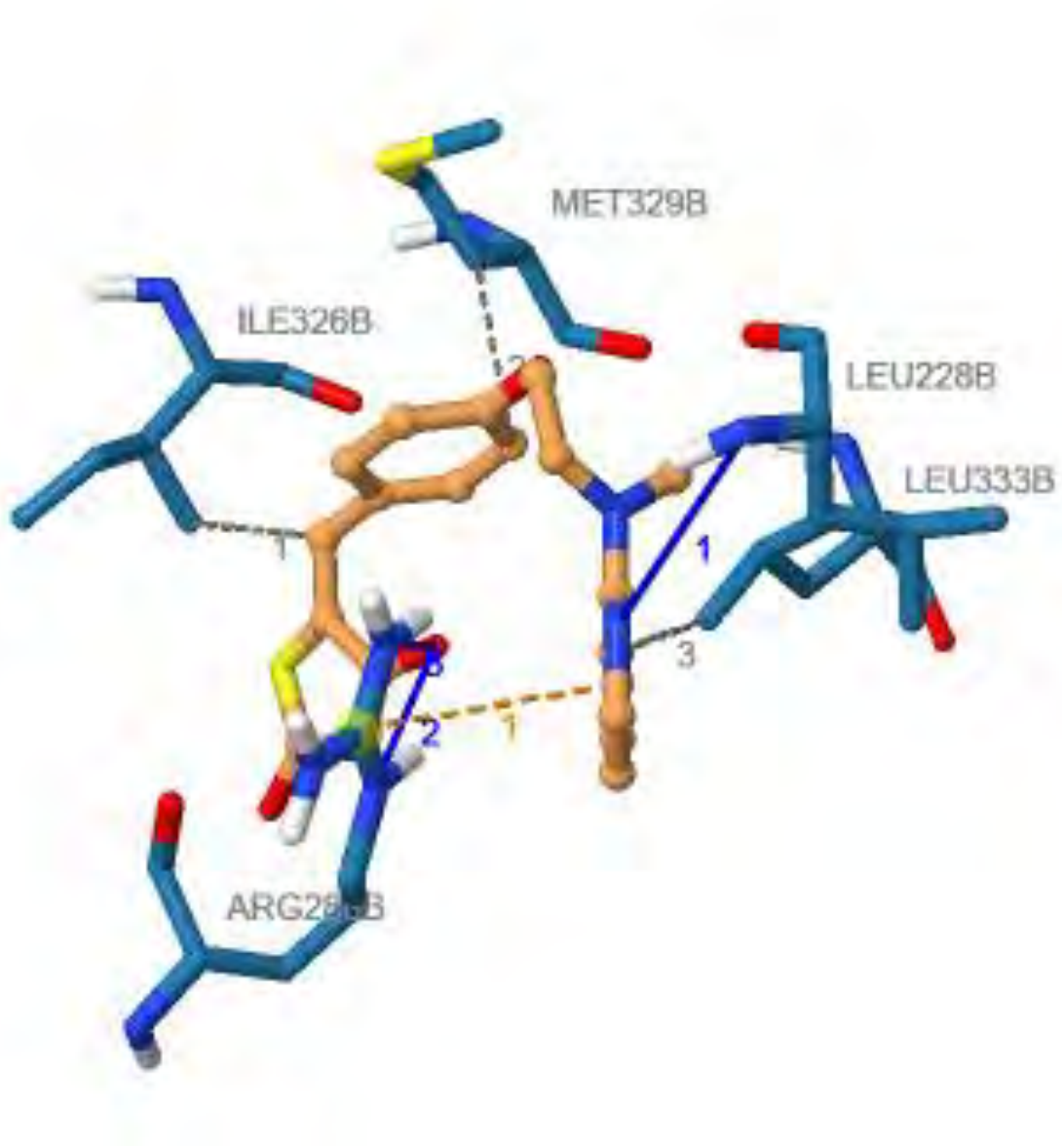

Figure C5 (i): Rosiglitazone interacting with PPARγ, showing amino acids involved.

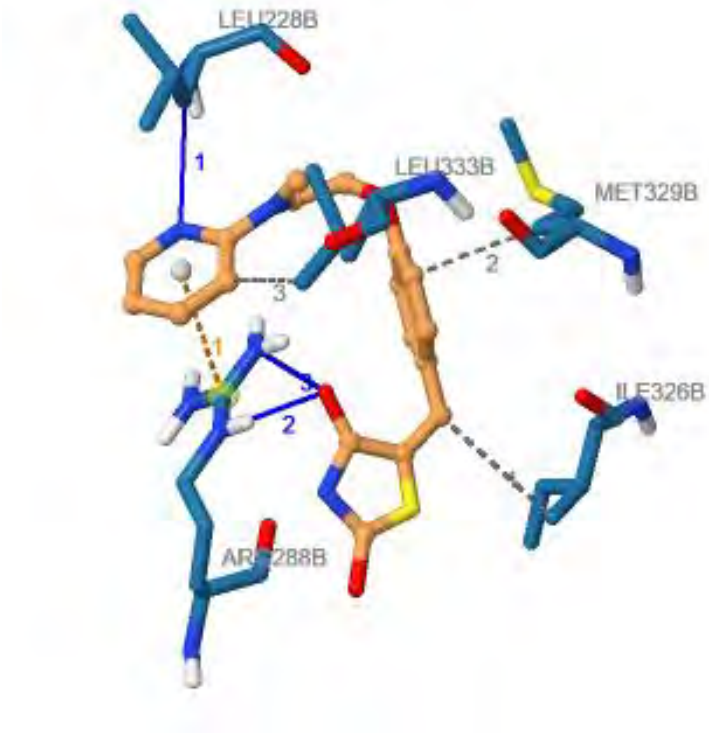

Figure C5 (ii): Rosiglitazone interacting with PPARγ, showing amino acids involved.

Hydrophobic Interactions ····

Index	Residue	AA	Distance	Ligand Atom	Protein Atom
1	326B	ILE	3.52	4874	3476
2	329B	MET	3.19	4862	3506
3	333B	LEU	3.40	4873	3540

Hydrogen Bonds —

Index	Residue	AA	Distance H-A	Distance D-A	Donor Angle	Protein donor?	Side chain	Donor Atom	Acceptor Atom
1	228B	LEU	3.07	3.86	134.40	✓	×	2701 [Nam]	4869 [Nar]
2	288B	ARG	2.09	3.01	149.29	✓	✓	3111 [Ng+]	4881 [O2]
3	288B	ARG	2.32	3.16	139.31	✓	✓	3117 [Ng+]	4881 [O2]

π-Cation Interactions ····

Index	Residue	AA	Distance	Offset	Protein charged?	Ligand Group	Ligand Atoms
1	288B	ARG	3.85	0.71	✓	Aromatic	4868, 4869, 4870, 4871, 4872, 4873

Figure C5 (iii): Rosiglitazone interacting with PPARγ, showing bonds involved.

CLUSTER ANALYSIS OF CONFORMATIONS

Number of conformations = 50

RMSD cluster analysis will be performed using the ligand atoms only (35 / 35 total atoms).

Outputting structurally similar clusters, ranked in order of increasing energy.

Number of distinct conformational clusters found = 8, out of 50 runs,
Using an rmsd-tolerance of 2.0 A

CLUSTERING HISTOGRAM

Cluster Rank	Lowest Binding Energy	Run	Mean Binding Energy	Num in Clus	Histogram 5 10 15 20 25 30 35
1	-12.02	33	-11.71	5	#####
2	-12.01	45	-11.70	22	######################
3	-11.88	44	-11.82	4	####
4	-11.57	49	-11.28	9	#########
5	-11.46	6	-11.07	2	##
6	-11.43	36	-11.37	3	###
7	-11.38	25	-11.38	1	#
8	-10.90	22	-10.87	4	####

Figure C6 (i): Cluster conformations analysis of TZDD1

RMSD TABLE

Rank	Sub-Rank	Run	Binding Energy	Cluster RMSD	Reference RMSD	Grep Pattern
1	1	33	-12.02	0.00	21.67	RANKING
1	2	14	-11.89	1.44	22.35	RANKING
1	3	41	-11.61	0.97	22.43	RANKING
1	4	48	-11.57	0.94	22.41	RANKING
1	5	4	-11.46	1.45	22.29	RANKING
2	1	45	-12.01	0.00	19.44	RANKING
2	2	35	-11.98	0.15	19.42	RANKING
2	3	16	-11.97	0.15	19.43	RANKING
2	4	10	-11.96	0.11	19.45	RANKING
2	5	47	-11.95	0.06	19.44	RANKING
2	6	23	-11.91	0.32	19.41	RANKING
2	7	38	-11.88	0.45	19.39	RANKING
2	8	32	-11.78	0.27	19.38	RANKING
2	9	20	-11.73	0.32	19.37	RANKING
2	10	46	-11.65	1.17	19.98	RANKING
2	11	12	-11.65	1.20	19.99	RANKING
2	12	50	-11.65	1.18	19.97	RANKING
2	13	31	-11.65	1.16	19.99	RANKING
2	14	2	-11.64	1.21	20.00	RANKING
2	15	17	-11.63	1.25	20.02	RANKING
2	16	1	-11.53	1.98	19.53	RANKING
2	17	11	-11.53	1.86	19.40	RANKING
2	18	7	-11.50	1.99	19.55	RANKING
2	19	34	-11.47	1.68	20.15	RANKING
2	20	43	-11.47	1.63	20.09	RANKING
2	21	30	-11.43	1.73	20.21	RANKING
2	22	21	-11.41	1.00	19.76	RANKING
3	1	44	-11.88	0.00	21.62	RANKING
3	2	39	-11.86	0.04	21.60	RANKING

Figure C6 (ii): Cluster conformations analysis showing binding energies of TZDD1

INFORMATION ENTROPY ANALYSIS FOR THIS CLUSTERING

Information entropy for this clustering = 0.43 (rmstol = 2.00 Angstrom)

STATISTICAL MECHANICAL ANALYSIS

```
Partition function, Q =    50.98            at Temperature, T = 298.15 K
Free energy,        A ~ -2329.32 kcal/mol   at Temperature, T = 298.15 K
Internal energy,    U =   -11.52 kcal/mol   at Temperature, T = 298.15 K
Entropy,            S =     7.77 kcal/mol/K at Temperature, T = 298.15 K
```

Figure C6 (iii): Cluster conformations analysis entropy of TZDD1

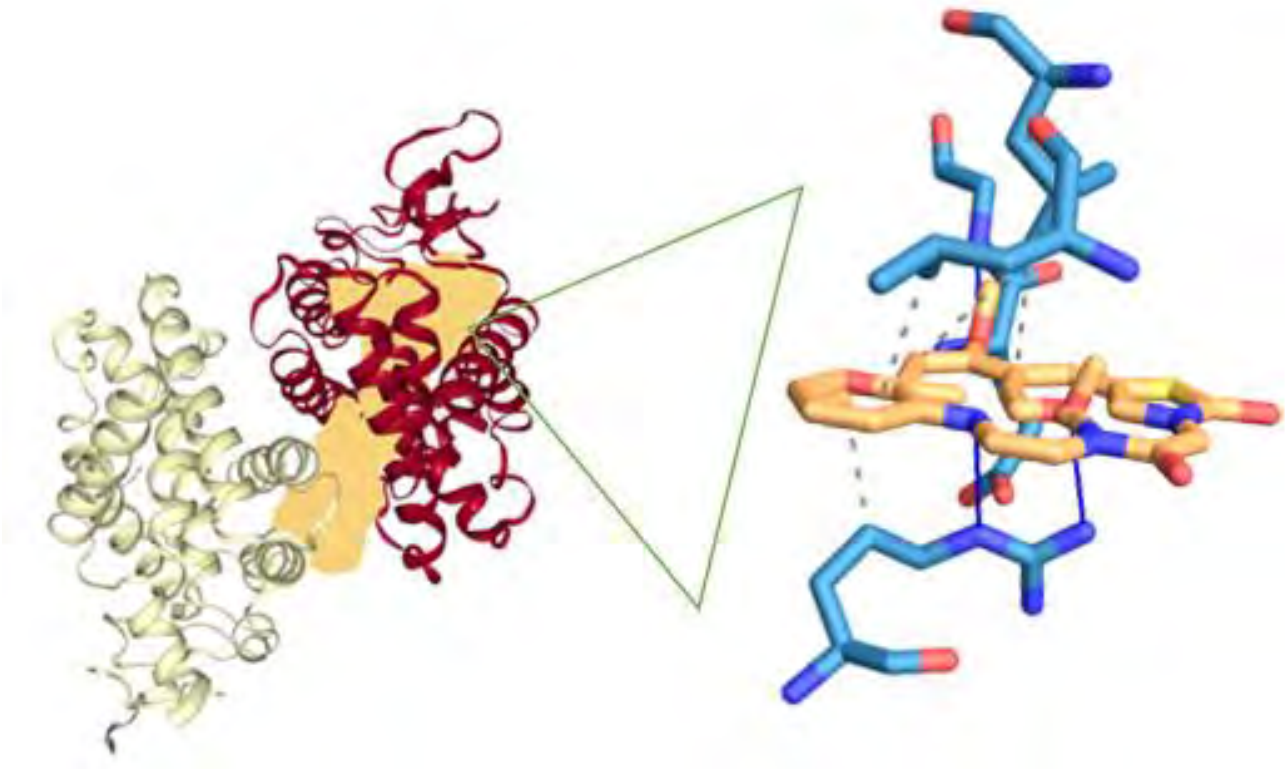

Figure C7 (i): TZDD1 interacting with PPARγ (highest ranked cluster conformation analysed)

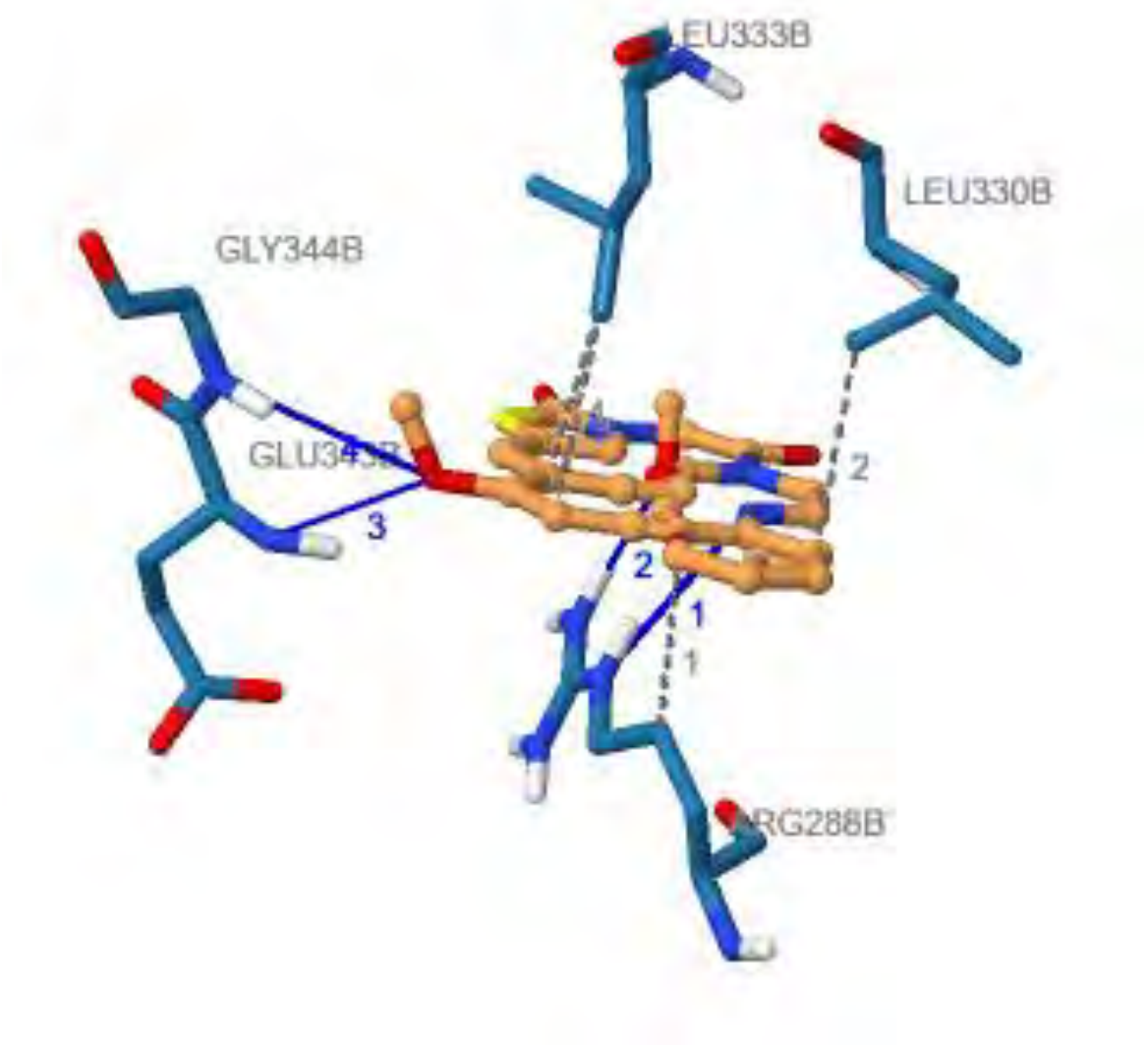

Figure C7 (ii): TZDD1 interacting with PPARγ, showing amino acids involved.

Hydrophobic Interactions ····

Index	Residue	AA	Distance	Ligand Atom	Protein Atom
1	288B	ARG	3.48	4874	3109
2	330B	LEU	3.60	4869	3517
3	333B	LEU	3.79	4882	3540
4	333B	LEU	3.01	4865	3540

Hydrogen Bonds —

Index	Residue	AA	Distance H-A	Distance D-A	Donor Angle	Protein donor?	Side chain	Donor Atom	Acceptor Atom
1	288B	ARG	2.83	3.80	159.74	✓	✓	3111 [Ng+]	4876 [N2]
2	288B	ARG	2.18	3.19	171.67	✓	✓	3117 [Ng+]	4862 [O2]
3	343B	GLU	2.15	2.99	138.40	✓	×	3623 [Nam]	4890 [O2]
4	344B	GLY	3.47	4.06	118.19	✓	×	3633 [Nam]	4890 [O2]

Figure C7 (iii): TZDD1 interacting with PPARγ, showing bonds and amino acids involved.

CLUSTER ANALYSIS OF CONFORMATIONS

Number of conformations = 50

RMSD cluster analysis will be performed using the ligand atoms only (29 / 29 total atoms).

Outputting structurally similar clusters, ranked in order of increasing energy.

Number of distinct conformational clusters found = 9, out of 50 runs,
Using an rmsd-tolerance of 2.0 A

CLUSTERING HISTOGRAM

Clus-ter Rank	Lowest Binding Energy	Run	Mean Binding Energy	Num in Clus	Histogram 5 10 15 20 25 30 35
1	-10.40	7	-10.34	29	############################
2	-10.29	6	-9.84	7	#######
3	-10.15	45	-10.15	1	#
4	-10.11	4	-10.00	3	###
5	-10.11	40	-9.96	4	####
6	-9.37	14	-9.32	2	##
7	-9.04	39	-8.91	2	##
8	-7.69	1	-7.69	1	#
9	-7.24	9	-7.24	1	#

Figure C8 (i): Cluster conformation analysis for TZDD2

RMSD TABLE

Rank	Sub-Rank	Run	Binding Energy	Cluster RMSD	Reference RMSD	Grep Pattern
1	1	7	-10.40	0.00	25.52	RANKING
1	2	33	-10.40	0.02	25.52	RANKING
1	3	18	-10.40	0.05	25.50	RANKING
1	4	31	-10.40	0.13	25.58	RANKING
1	5	23	-10.39	0.07	25.54	RANKING
1	6	37	-10.39	0.16	25.60	RANKING
1	7	41	-10.39	0.09	25.54	RANKING
1	8	29	-10.39	0.09	25.53	RANKING
1	9	36	-10.38	0.07	25.54	RANKING
1	10	11	-10.37	0.13	25.55	RANKING
1	11	3	-10.36	0.10	25.55	RANKING
1	12	20	-10.36	0.94	25.83	RANKING
1	13	2	-10.36	0.92	25.78	RANKING
1	14	49	-10.35	0.13	25.55	RANKING
1	15	24	-10.35	0.15	25.56	RANKING
1	16	16	-10.34	0.14	25.55	RANKING
1	17	5	-10.34	0.42	25.72	RANKING
1	18	8	-10.34	0.13	25.52	RANKING
1	19	28	-10.34	0.15	25.57	RANKING
1	20	46	-10.33	0.93	25.78	RANKING
1	21	22	-10.33	0.42	25.75	RANKING
1	22	48	-10.32	0.45	25.79	RANKING
1	23	21	-10.32	0.16	25.57	RANKING
1	24	26	-10.30	0.21	25.59	RANKING
1	25	27	-10.28	0.87	26.12	RANKING
1	26	12	-10.27	0.89	25.85	RANKING

Figure C8 (ii): Cluster conformation analysis showing binding energies for TZDD2

STATISTICAL MECHANICAL ANALYSIS

```
Partition function, Q =    50.85            at Temperature, T = 298.15 K
Free energy,        A ~ -2327.80 kcal/mol   at Temperature, T = 298.15 K
Internal energy,    U =   -10.00 kcal/mol   at Temperature, T = 298.15 K
Entropy,            S =     7.77 kcal/mol/K at Temperature, T = 298.15 K
```

Figure C8 (iii): Cluster conformation analysis showing energies for TZDD2

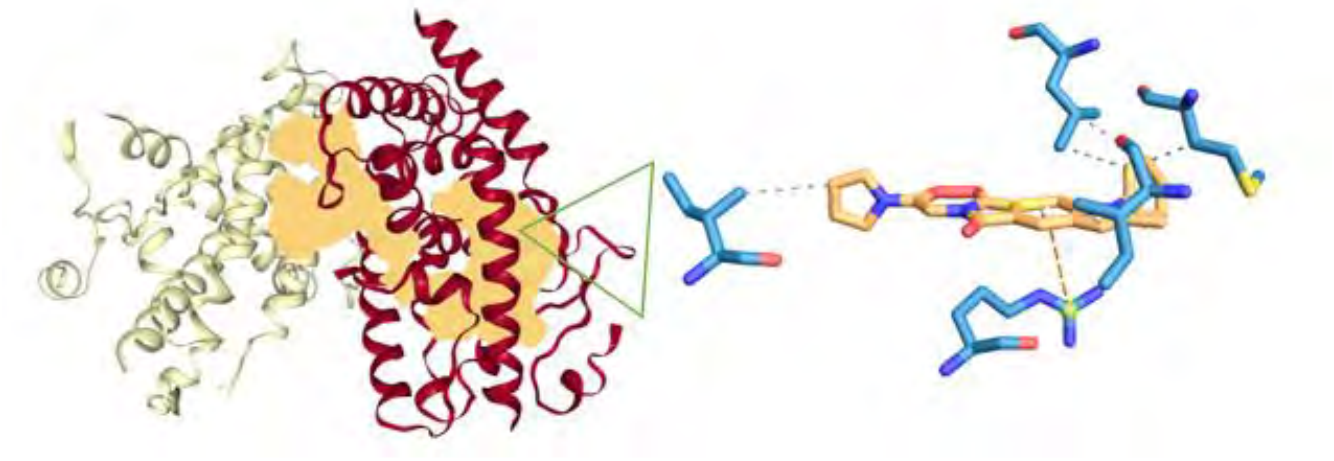

Figure C9 (i): TZDD2 interacting with PPARγ (highest ranked cluster conformation analysed)

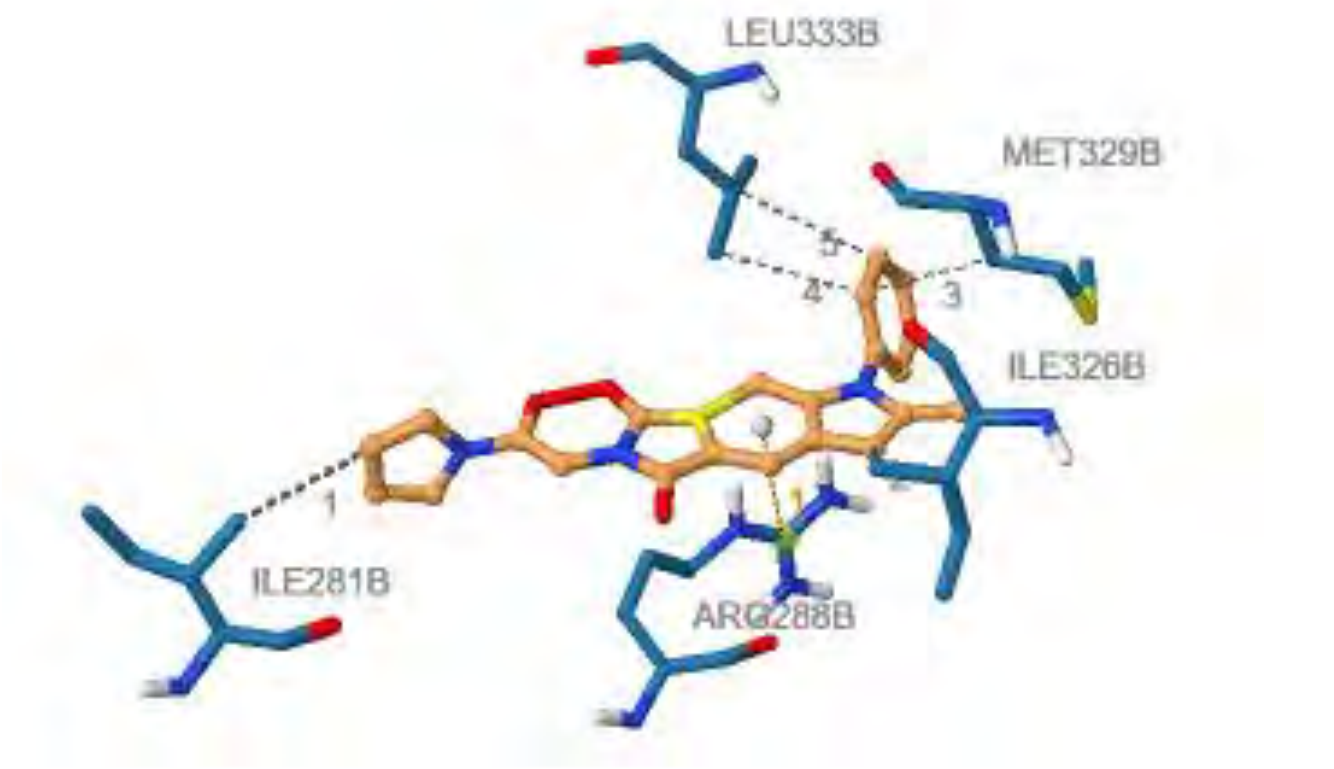

Figure C9 (ii): TZDD2 interacting with PPARγ showing amino acid interactions involved

▾ Hydrophobic Interactions ····

Index	Residue	AA	Distance	Ligand Atom	Protein Atom
1	281B	ILE	3.83	4884	3041
2	326B	ILE	3.34	4874	3476
3	329B	MET	3.31	4880	3506
4	333B	LEU	3.65	4880	3540
5	333B	LEU	3.64	4879	3539

▾ π-Cation Interactions ····

Index	Residue	AA	Distance	Offset	Protein charged?	Ligand Group	Ligand Atoms
1	288B	ARG	4.84	1.54	✔	Aromatic	4860, 4861, 4862, 4871, 4872, 4873

Figure C9 (iii): TZDD2 interacting with PPARγ showing amino acid interaction bonds involved

```
Number of distinct conformational clusters found = 8,  out of 50 runs,
Using an rmsd-tolerance of 2.0 A

        CLUSTERING HISTOGRAM
        ____________________

_____|_____________|_____|_____________|_____|
     |             |     |             |     |
Clus | Lowest      | Run | Mean        | Num | Histogram
-ter | Binding     |     | Binding     | in  |
Rank | Energy      |     | Energy      | Clus|    5    10   15   20   25   30   35
_____|_____________|_____|_____________|_____|___:____|____:____|____:____|____:____|
   1 |      -8.84  |  43 |      -8.59  |   6 |######
   2 |      -8.78  |  20 |      -8.72  |  30 |##############################
   3 |      -8.45  |   1 |      -8.39  |   4 |####
   4 |      -8.37  |  29 |      -8.28  |   4 |####
   5 |      -8.28  |   9 |      -8.28  |   1 |#
   6 |      -7.96  |  38 |      -7.96  |   1 |#
   7 |      -7.88  |  32 |      -7.87  |   3 |###
   8 |      -7.31  |  22 |      -7.31  |   1 |#
_____|_____________|_____|_____________|_____|_____________________________________
```

Figure C10 (i): Cluster conformations analysis of TZDD3

Number of multi-member conformational clusters found = 5, out of 50 runs.

RMSD TABLE

Rank	Sub-Rank	Run	Binding Energy	Cluster RMSD	Reference RMSD	Grep Pattern
1	1	43	-8.84	0.00	23.66	RANKING
1	2	7	-8.82	0.03	23.66	RANKING
1	3	11	-8.70	0.12	23.72	RANKING
1	4	27	-8.44	0.69	23.78	RANKING
1	5	46	-8.41	0.62	23.63	RANKING
1	6	33	-8.31	0.71	23.88	RANKING
2	1	20	-8.78	0.00	25.60	RANKING
2	2	12	-8.78	0.02	25.60	RANKING
2	3	28	-8.77	0.04	25.59	RANKING
2	4	44	-8.77	0.09	25.61	RANKING
2	5	13	-8.76	0.22	25.65	RANKING
2	6	18	-8.76	0.04	25.60	RANKING
2	7	39	-8.76	0.06	25.62	RANKING
2	8	24	-8.76	0.04	25.60	RANKING
2	9	2	-8.76	0.04	25.61	RANKING
2	10	37	-8.75	0.33	25.59	RANKING
2	11	6	-8.74	0.13	25.63	RANKING
2	12	30	-8.74	0.06	25.59	RANKING
2	13	42	-8.73	0.25	25.67	RANKING
2	14	25	-8.73	0.66	25.77	RANKING

Figure C10 (ii): Cluster conformations analysis of TZDD3 showing binding energies

STATISTICAL MECHANICAL ANALYSIS

```
Partition function, Q =    50.73            at Temperature, T = 298.15 K
Free energy,        A ~ -2326.34 kcal/mol   at Temperature, T = 298.15 K
Internal energy,    U =    -8.54 kcal/mol   at Temperature, T = 298.15 K
Entropy,            S =     7.77 kcal/mol/K at Temperature, T = 298.15 K
```

Figure C10 (iii): Cluster conformations analysis of TZDD3 showing energies

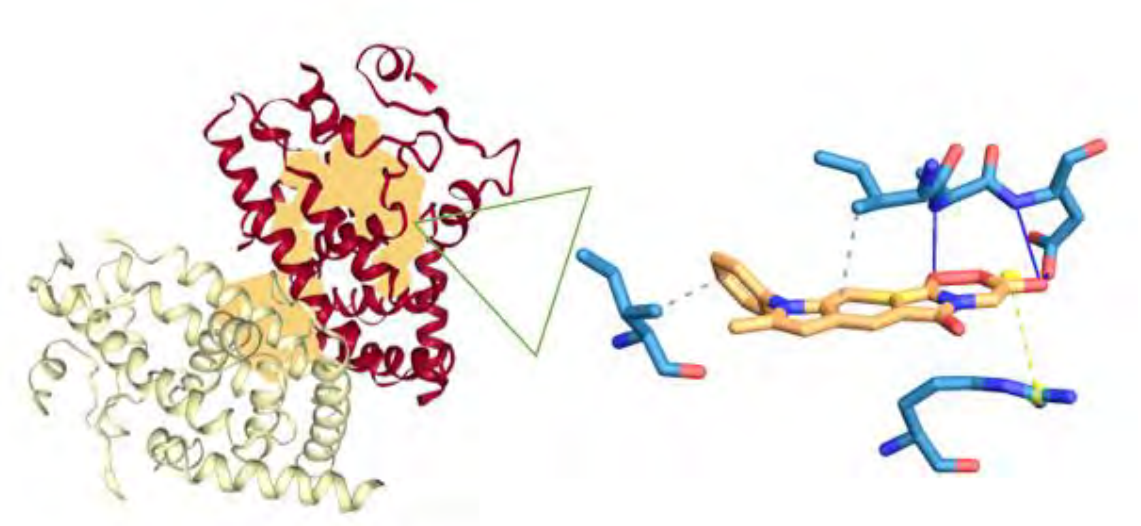

Figure C11 (i): TZDD3 interacting with PPARγ (highest ranked cluster conformation)

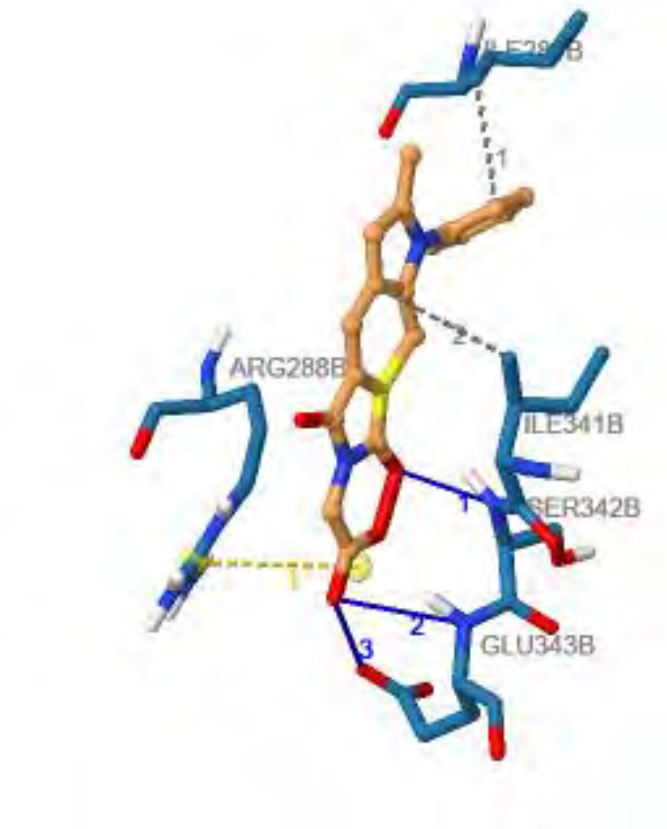

Figure C11 (ii): TZDD3 interacting with PPARγ showing amino acid interactions

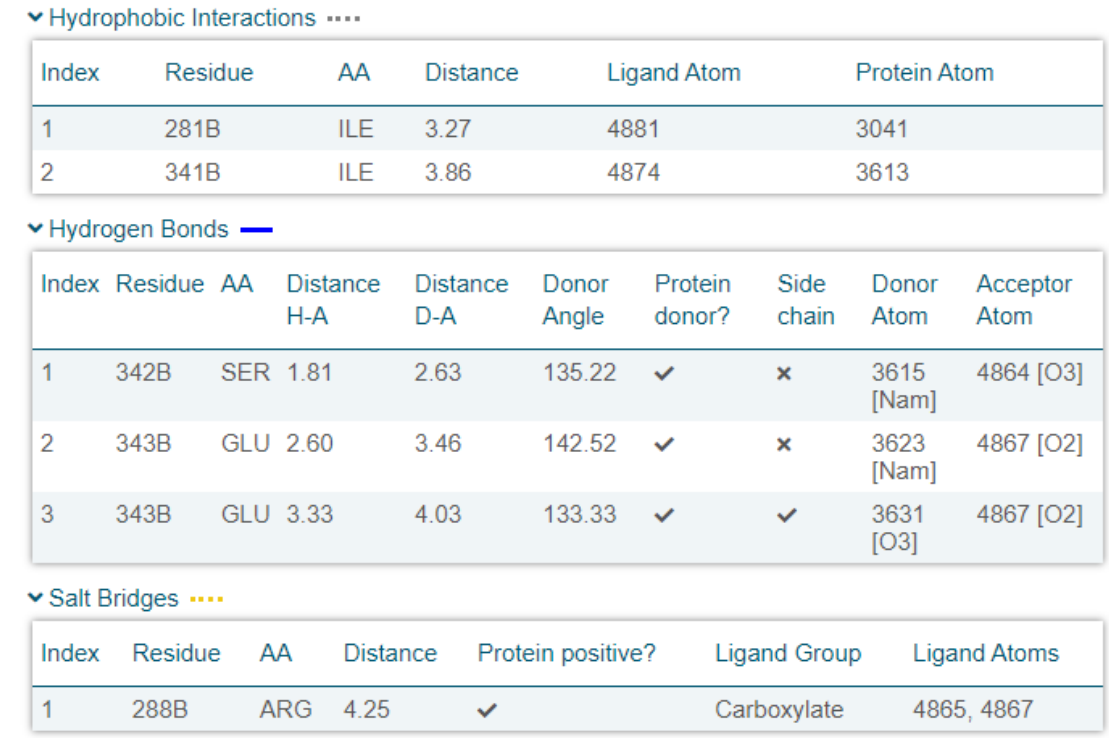

Hydrophobic Interactions ····

Index	Residue	AA	Distance	Ligand Atom	Protein Atom
1	281B	ILE	3.27	4881	3041
2	341B	ILE	3.86	4874	3613

Hydrogen Bonds —

Index	Residue	AA	Distance H-A	Distance D-A	Donor Angle	Protein donor?	Side chain	Donor Atom	Acceptor Atom
1	342B	SER	1.81	2.63	135.22	✓	×	3615 [Nam]	4864 [O3]
2	343B	GLU	2.60	3.46	142.52	✓	×	3623 [Nam]	4867 [O2]
3	343B	GLU	3.33	4.03	133.33	✓	✓	3631 [O3]	4867 [O2]

Salt Bridges ····

Index	Residue	AA	Distance	Protein positive?	Ligand Group	Ligand Atoms
1	288B	ARG	4.25	✓	Carboxylate	4865, 4867

Figure C11 (iii): TZDD3 interacting with PPARγ showing amino acid bond interactions

CLUSTER ANALYSIS OF CONFORMATIONS

Number of conformations = 50

RMSD cluster analysis will be performed using the ligand atoms only (27 / 27 total atoms).

Outputting structurally similar clusters, ranked in order of increasing energy.

Number of distinct conformational clusters found = 8, out of 50 runs,
Using an rmsd-tolerance of 2.0 A

CLUSTERING HISTOGRAM

Clus-ter Rank	Lowest Binding Energy	Run	Mean Binding Energy	Num in Clus	Histogram 5 10 15 20 25 30 35
1	-9.91	28	-9.74	14	##############
2	-9.86	19	-9.75	9	#########
3	-9.69	44	-9.66	5	#####
4	-9.58	4	-9.56	8	########
5	-9.47	25	-9.35	3	###
6	-9.47	17	-9.45	8	########
7	-9.20	32	-9.17	2	##
8	-8.95	40	-8.95	1	#

Figure C12 (i): Cluster conformations analysis of TZDD4

Number of multi-member conformational clusters found = 7, out of 50 runs.

RMSD TABLE

Rank	Sub-Rank	Run	Binding Energy	Cluster RMSD	Reference RMSD	Grep Pattern
1	1	28	-9.91	0.00	24.20	RANKING
1	2	27	-9.90	0.29	24.06	RANKING
1	3	34	-9.89	0.12	24.15	RANKING
1	4	26	-9.88	0.30	24.05	RANKING
1	5	24	-9.82	0.32	24.05	RANKING
1	6	20	-9.75	0.32	24.10	RANKING
1	7	50	-9.74	0.33	24.06	RANKING
1	8	21	-9.73	0.62	23.88	RANKING
1	9	47	-9.67	0.64	23.87	RANKING
1	10	43	-9.64	0.71	23.82	RANKING
1	11	7	-9.63	0.62	24.47	RANKING
1	12	16	-9.62	0.62	24.46	RANKING
1	13	14	-9.62	0.62	24.47	RANKING
1	14	2	-9.60	0.41	24.33	RANKING
2	1	19	-9.86	0.00	24.51	RANKING
2	2	33	-9.85	0.81	24.69	RANKING
2	3	11	-9.84	0.83	24.69	RANKING
2	4	22	-9.83	0.79	24.70	RANKING
2	5	9	-9.83	0.80	24.71	RANKING
2	6	3	-9.79	0.61	24.68	RANKING
2	7	39	-9.74	0.53	24.57	RANKING
2	8	45	-9.65	0.82	24.60	RANKING
2	9	10	-9.38	1.20	24.77	RANKING
3	1	44	-9.69	0.00	24.40	RANKING
3	2	31	-9.66	0.13	24.37	RANKING
3	3	42	-9.66	0.08	24.39	RANKING
3	4	6	-9.66	0.16	24.44	RANKING

Figure C12 (ii): Cluster conformations analysis of TZDD4 showing binding energies

STATISTICAL MECHANICAL ANALYSIS

Partition function, Q = 50.82 at Temperature, T = 298.15 K
Free energy, A ~ -2327.40 kcal/mol at Temperature, T = 298.15 K
Internal energy, U = -9.60 kcal/mol at Temperature, T = 298.15 K
Entropy, S = 7.77 kcal/mol/K at Temperature, T = 298.15 K

Figure C12 (ii): Cluster conformations analysis of TZDD4 showing energies

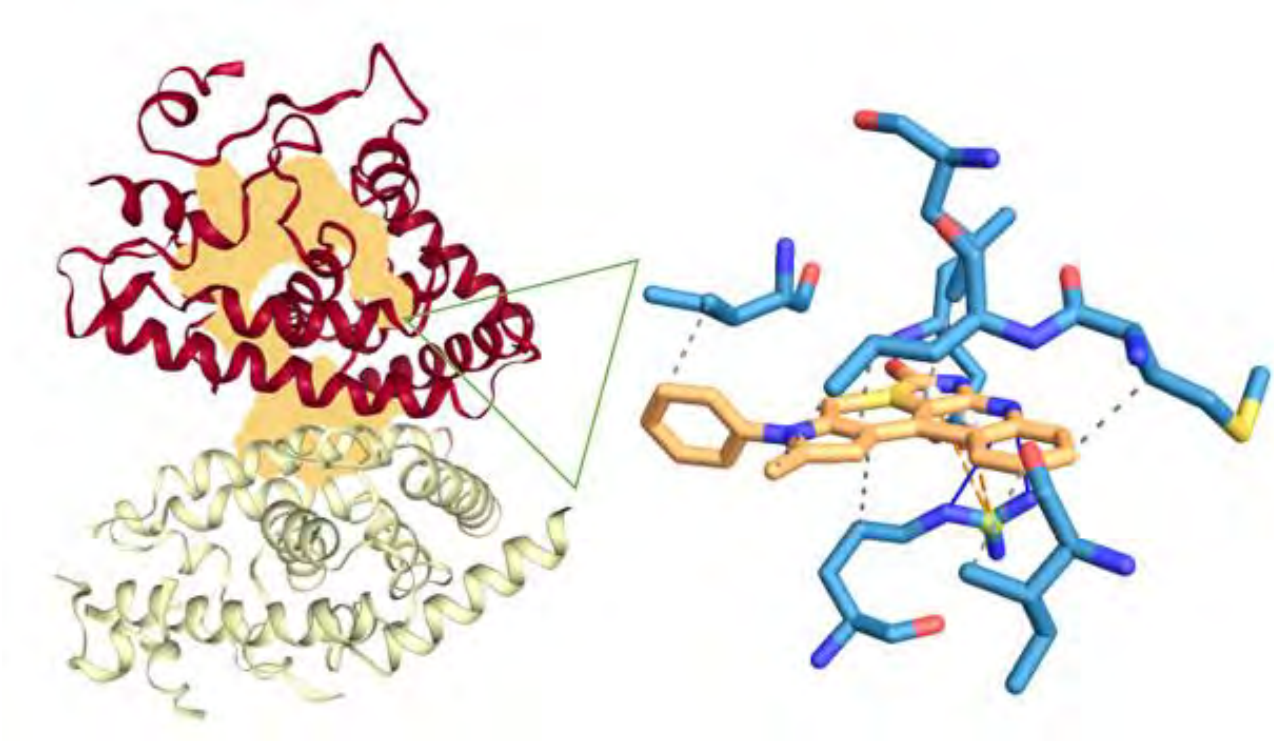

Figure C13 (i): Conformation analysis of TZDD4, interactions with PPARγ

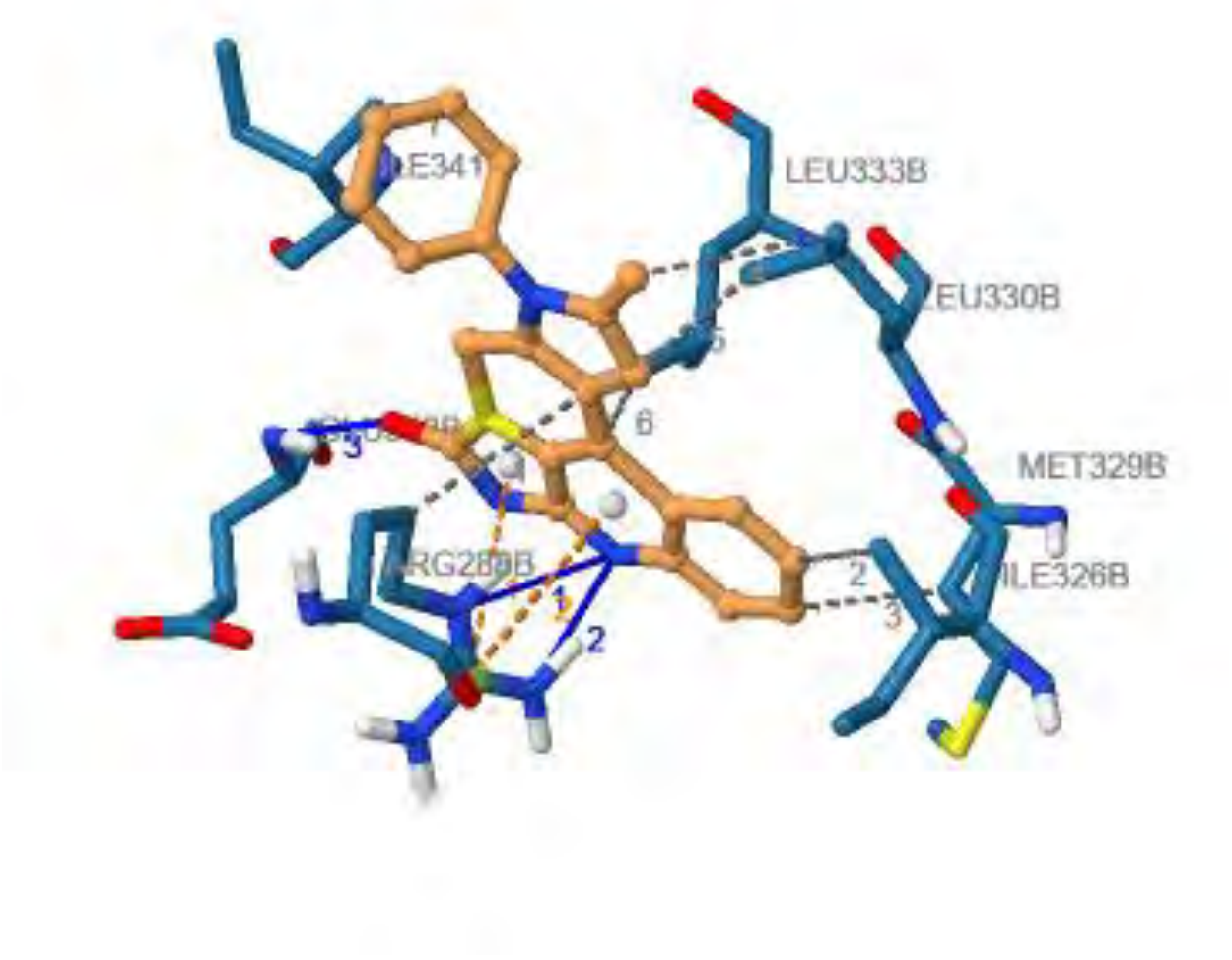

Figure C13 (ii): Conformation analysis of TZDD4, interactions with PPARγ showing amino acids

Hydrophobic Interactions ····

Index	Residue	AA	Distance	Ligand Atom	Protein Atom
1	288B	ARG	3.83	4876	3109
2	326B	ILE	3.95	4871	3476
3	329B	MET	3.35	4870	3506
4	330B	LEU	3.69	4857	3518
5	330B	LEU	3.03	4877	3517
6	333B	LEU	3.71	4874	3540
7	341B	ILE	3.71	4880	3613

Hydrogen Bonds —

Index	Residue	AA	Distance H-A	Distance D-A	Donor Angle	Protein donor?	Side chain	Donor Atom	Acceptor Atom
1	288B	ARG	2.95	3.68	128.83	✓	✓	3111 [Ng+]	4867 [Npl]
2	288B	ARG	1.94	2.90	155.71	✓	✓	3117 [Ng+]	4867 [Npl]
3	343B	GLU	1.95	2.91	156.81	✓	×	3623 [Nam]	4864 [O2]

π-Cation Interactions ····

Index	Residue	AA	Distance	Offset	Protein charged?	Ligand Group	Ligand Atoms
1	288B	ARG	3.98	1.68	✓	Aromatic	4862, 4863, 4865, 4866, 4875
2	288B	ARG	3.91	1.51	✓	Aromatic	4866, 4867, 4868, 4873, 4874, 4875

Figure C13 (iii): Conformation analysis of TZDD4, interactions with PPARγ showing amino acids and bonds of interactions

Appendix D: Standard curves used in the analysis of results

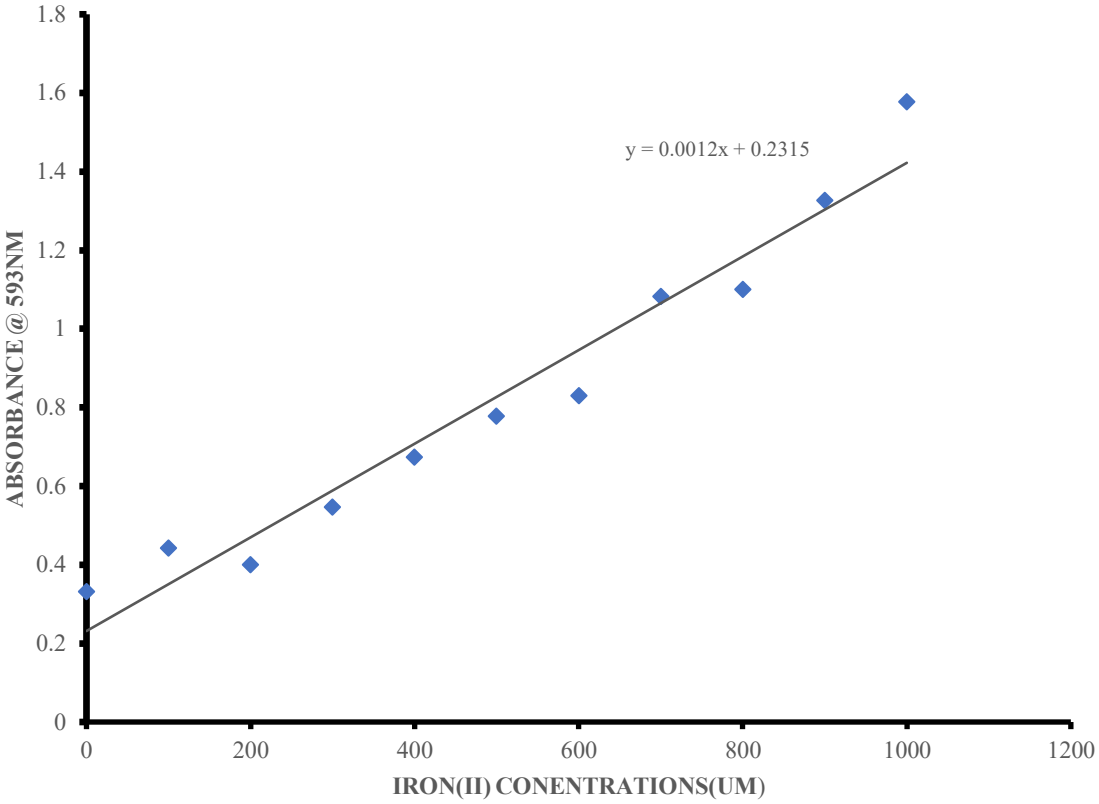

Figure D1: Standard curve of Iron (II) used to obtain the amount of Iron (II) (µM) reduced from Iron (III) by the derivatives in the FRAP activity assay as expressed by absorbance obtained.

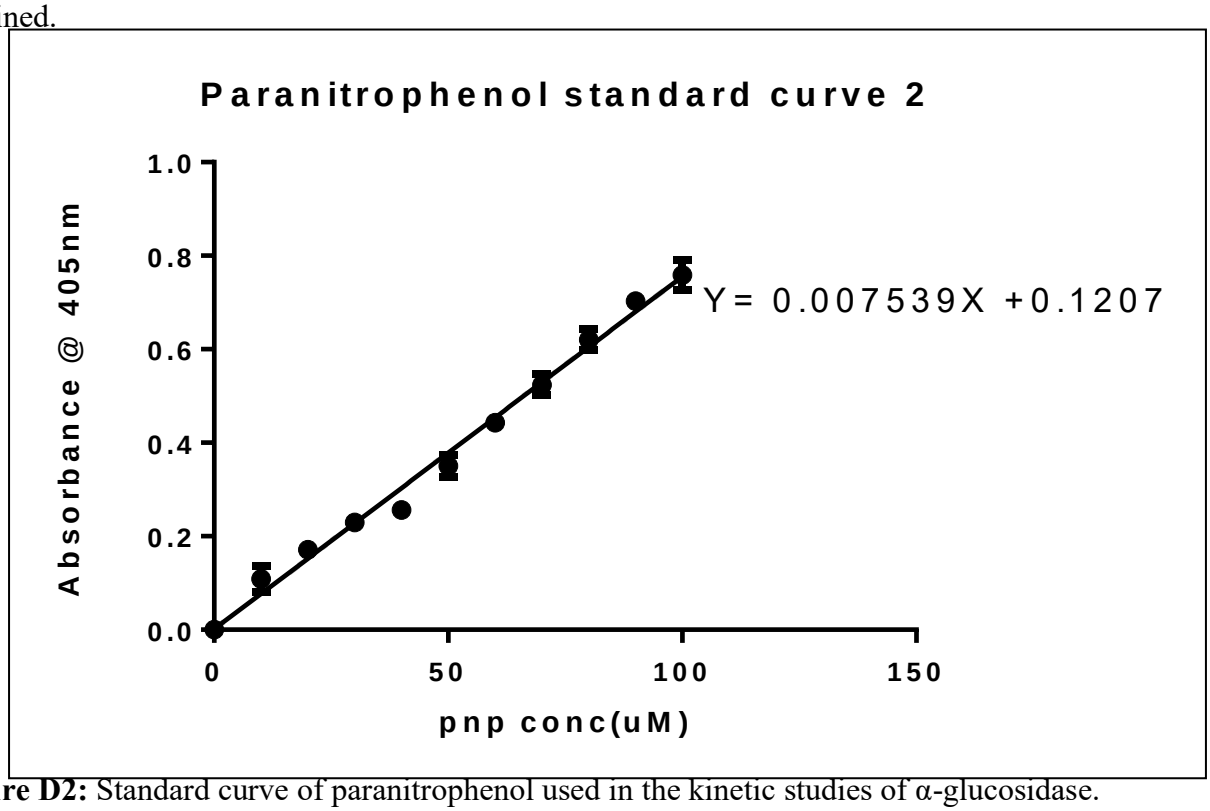

Figure D2: Standard curve of paranitrophenol used in the kinetic studies of α-glucosidase.